# PURIFICATION AND CHARACTERIZATION OF ISOFORMS OF GLUTATHIONE S-TRANSFERASE (GST) FROM *ACINETOBACTER CALCOACETICUS* Y1

**CHEE CHIN SOON**

**FACULTY OF SCIENCE**
**UNIVERSITY OF MALAYA**
**KUALA LUMPUR**

**2014**

# PURIFICATION AND CHARACTERIZATION OF ISOFORMS OF GLUTATHIONE S-TRANSFERASE (GST) FROM *ACINETOBACTER CALCOACETICUS* Y1

**CHEE CHIN SOON**

**DISSERTATION SUBMITTED IN FULFILLMENT OF THE REQUIREMENTS FOR THE DEGREE OF MASTER OF SCIENCE**

**INSTITUTE OF BIOLOGICAL SCIENCES**
**FACULTY OF SCIENCE**
**UNIVERSITY OF MALAYA**
**KUALA LUMPUR**

**2014**

# Acknowledgement

I am heartily thankful to my supervisors, Dr. Zazali Alias and Prof. Dr. Irene Tan Kit Ping, whose encouragement, guidance and support from the early and final stage of my study and enabled me to develop an understanding of the subject.

I would like to offer my regards and blessing to master student, Tanusya Murali, Kithalakshimi Vignesvaran, Pang Wai Mei, Tan Yong Hao, Vennobaahshini Venu and PhD student, Siti Nasuha Hamzha that support me in any aspect during the completion of my project.

I would also like to thank to Institute of Biological Sciences, Biochemistry laboratory, Virology laboratory and Medical biotechnology laboratory for giving me the permission to use the laboratory equipment. Assistance provided by Miss Rosfizah, Miss Zanariah, and Mr. Izuwan were greatly appreciated.

Most importantly were the love and patience from my family. They had shown constant of support, concern and strength to me all these years. I would like to express my heart-felt gratitude to my family.

Last but not least, my special thanks to Institute of Graduate Studies, University of Malaya that helped me in term of financial assistant to make my research successful.

# Abstract

Bacteria were isolated from chemically-contaminated soil and the isolates were screened for glutathione S-transferase (GST) expression by spraying with monochlorobimane. The isolate with the most promising GST activity was later identified as *Acinetobacter calcoacticus* Y1 based on its 16S rRNA gene sequence.

By using affinity chromatography, *A. calcoaceticus* Y1 putative GST (AcGST) was successfully purified and expressed GST subunit with molecular weight estimated at 23 kDa when analysed on sodium dodecyl sulphate polyacrylamide gel electrophoresis (SDS-PAGE). The purified protein was then further analysed by using two-dimensional electrophoresis where two putative GST isozymes were identified and designated as AcGST-1 and AcGST-2. Upon isoelectric focusing, AcGST-1 and AcGST-2 were found to be in pI values of 4.5 and 6.2 respectively.

AcGST-1 and AcGST-2 were purified by using carboxylmethyl (CM) and diethylaminoethyl (DEAE) ion exchange chromatography respectively. AcGST-1 was reactive towards ethacrynic acid (EA) (24.99 ± 1.24 µmol/min/mg), hydrogen peroxide (3.93 ± 0.32 µmol/min/mg), 1-Chloro-2,4-dinitrobenzene (CDNB) (0.61 ± 0.12 µmol/min/mg), 2,4-heptadienal (0.11 ± 0.03 µmol/min/mg), trans-2-octenal (0.08 ± 0.02 µmol/min/mg), and hexadienal (0.04 ± 0.003 µmol/min/mg) whereas AcGST-2 was reactive towards EA (15.87 ± 2.54 µmol/min/mg ), CDNB (0.54 ± 0.13 µmol/min/mg), 2,4-heptadienal (0.08 ± 0.01 µmol/min/mg), and trans-2-octenal (0.09 ± 0.01 µmol/min/mg). The substrate specificities of both putative GST isozymes were different and therefore suggesting they were of two existing homodimers.

For AcGST-1, the $V_{max}$ for EA and GSH were estimated as 3.74 ± 1.40 µmol/min and 1.46 ± 0.02 µmol/min, $K_m$ for EA and GSH were estimated as 0.28 ± 0.02 mM and

0.01 ± 0.0003 mM. Whereas for AcGST-2, the $V_{max}$ for EA and GSH were estimated as 8.41 ± 1.08 μmol/min and 1.35 ± 0.01 μmol/min, $K_m$ for EA and GSH were estimated as 0.28 ± 0.002 mM and 0.02 ± 0.003 mM.

From thin layer chromatography to determine the reactivity of both putative GST isozymes towards Isoproturon, Fenoxaprop-ethyl, Propoxur and Clodinafop-propargyl, only AcGST-2 showed conjugation activity towards Isoproturon, a pesticide. Disc diffusion test indicated that Bromophos, Malathione, DDT, Propoxur, Permethin, Chlorpyrifos, Fenitrothion did not affect the propagation of *A. calcoaecticus* Y1 but hydrogen peroxide inhibited the propagation of *A. calcoaceticus* Y1. Based on our result, zone of inhibition at 25 % of hydrogen peroxide was smaller compared with 50 % of hydrogen peroxide suggesting some degree of tolerance of *A. calcoaceticus* Y1 towards hydrogen peroxide.

# Abstrak

Bakteria telah diasingkan daripada tanah yang dicemar oleh bahan kimia dan asingan bakteria ini telah disaring untuk penghasilan glutathione S-transferase (GST) dengan menyebarkan monoklorobin. Asingan bakteria yang menghasilkan aktiviti GST yang paling tinggi kemudian telah dikenal pasti sebagai *Acinetobacter calcoacticus* Y1 daripada jujukan gen 16s rRNA nya.

Dengan menggunakan kromatografi, affiniti, *A. calcoaceticus* Y1 GST yang diduga telah berjaya ditulenkan dan didapati menghasilkan subunit GST dengan berat molekul dianggar sebanyak 23 kDa apabila dianalisa dengan menggunakan *sodium dodecyl sulphate polyacrylamide gel electrophoresis* (SDS-PAGE). Protein-protein yang ditulenkan kemudian dianalisa dengan kromatografi dua dimensi di mana dua GST isozim berjaya dikenal pasti dan direka sebagai AcGST-1 dan AcGST-2. Apabila dianalisa dengan "isoelectric focusing", AcGST-1 dan AcGST-2 didapati mempunyai nilai pI 4.5 and 6.2 masing-masing.

AcGST-1 dan AcGST-2 telah ditulenkan dengan menggunakan kaboksilmetil (CM) and dietilaminoetill (DEAE) kromatografi penukaran ion. AcGST-1 reaktif terhadap *ethacrynic acid* (EA) (24.99 ± 1.24 µmol/min/mg), hidrogen peroxida (3.93 ± 0.32 µmol/min/mg), *1-Chloro-2,4-dinitrobenzene* (CDNB) (0.61 ± 0.12 µmol/min/mg), *2,4-heptadienal* (0.11 ± 0.03 µmol/min/mg), *trans-2-octenal* (0.08 ± 0.02 µmol/min/mg), dan *hexadienal* (0.04 ± 0.003 µmol/min/mg) manakala AcGST-2 reakftif terhadap EA (15.87 ± 2.54 µmol/min/mg), CDNB (0.54 ± 0.13 µmol/min/mg), *2,4-heptadienal* (0.08 ± 0.01 µmol/min/mg), dan *trans-2-octenal* (0.09 ± 0.01 µmol/min/mg). Aktiviti kekhususan subsutrate kedua-dua GST isozim yang diduga adalah berlainan, maka dicadangkan bahawa kewujudan dua *homodimer* yang berbeza.

Untuk AcGST-1, $V_{max}$ untuk EA dan GSH telah dianggarkan sebagai 3.74 ± 1.40 μmol/min dan 1.46 ± 0.02 μmol/min, $K_m$ untuk EA dan GSH telah dianggarkan sebagai 0.28 ± 0.02 mM dan 0.008 ± 0.0003 mM. Manakala untuk AcGST-2, $V_{max}$ untuk EA dan GSH telah dianggarkan sebagai 8.41 ± 1.08 μmol/min dan 1.35 ± 0.06 μmol/min, $K_m$ untuk EA dan GSH telah dianggarkan sebagai 0.28 ± 0.01 mM dan 0.02 ± 0.003 mM.

Daripada analisa kromatografi lapisan nipis untuk menentukan kereaktifan kedua-dua GST isozim yang diduga terhadap *Isoproturon*, *Fenoxaprop-ethyl*, *Propoxur* dan *Clodinafop-propargyl*, didapati AcGST-2 sahaja yang bergabung dengan *Isoproturon*, sejenis racun perosak. Ujian penyebaran cakera menunjukkan *Bromophos*, *Malathione*, *DDT*, *Propoxur*, *Permethin*, *Chlorpyrifos*, *Fenitrothion* tidak menjejaskan penggandaan sel *A. calcoaceticus* Y1 tetapi hidrogen peroxida akan menhalang kehidupan *A.calcoaceticus* Y1. Berdasarkan keputusan kami, zon perencatan pada 25 % hidrogen peroxida adalah lebih kecil daripada zon perencatan pada 50 % hidrogen peroxida mencadangkan tahap ketoleran *A. calcoaceticus* Y1 terhadap hidrogen peroxida.

# Contents


| Contents | Pages |
|---|---|
| **Acknowledgement** | i |
| **Abstract** | ii |
| **Abstrak** | iv |
| **Table of contents** | vi |
| **List of figures** | x |
| **List of tables** | xiv |
| **List of formulas** | xv |
| **List of abbreviations** | xvi |

## CHAPTERS

| | |
|---|---|
| **1.0 Introduction** | 1 |
| 1.1 Objectives | 2 |
| **2.0 Literature review** | |
| 2.1 Glutathione S-transferase | |
| 2.1.1 Introduction | 3 |
| 2.1.2 Functional role of GSTs | 4 |
| 2.1.3 Families of GSTs | |
| 2.1.3.1 Cytosolic GSTs | 15 |
| 2.1.3.2 Mitochondrial GSTs | 28 |
| 2.1.3.3 Microsomal GSTs | 29 |
| 2.1.3.4 Bacteria fosfomycin-resistance protein | 31 |
| 2.1.4 Potential application of GSTs | 34 |


`

**3.0 Materials**

3.1 Apparatuses 36

3.2 Equipment 37

3.2 Chemicals 38

**4.0 Methodology**

4.1.1 Bacteria isolation 42

4.1.2 Screening of GSTs 42

4.1.3 Bacteria identification 43

4.1.4 Extraction of proteins from cells 44

4.1.5 Purification of putative GSTs by using affinity chromatography 44

4.1.6 Putative GST isozymes separation by using ion exchange chromatography and chromatofocusing 45

4.1.7 Molecular weight determination by using Sodium Dodecyl Sulfate-Polyacrylamide Gel Electrophoresis (SDS-PAGE) 45

4.1.8 Two-dimensional electrophoresis for putative GST isozymes determination 48

4.1.9 An assays to determine substrate specificity of putative GST isozymes 49

4.2.0 Kinetic properties of AcGST-1 and AcGST-2 50

4.2.1 N-terminal sequencing of AcGST-1 and AcGST-2 51

4.2.2 MALDI-TOF analysis 52

4.2.3 Reactivity of purified putative GST isozymes towards pesticides by thin Layer Chromatography (TLC) analysis 53

4.2.4 Disc diffusion test 54

**5.0 Results**

5.1.1 Bacteria identification from 16S rRNA gene sequence 55

5.1.2 Screening of bacteria GSTs by using monochlorobimane 59

5.1.3 SDS-PAGE of purified putative cytosolic GSTs 61

5.1.4 Two-dimensional electrophoresis to determine number of putative GST isozymes 62

5.1.5 Isoelectric focusing separates putative GST isozymes based on pI value 63

5.1.6 Putative GST isozymes separated by using Ion-exchange chromatography 64

5.1.7 Substrate specificity test for AcGST-1 and AcGST-2 66

5.1.8 Kinetic properties of AcGST-1 and AcGST-2 67

5.1.9 N-terminal sequencing of AcGST-1 and AcGST-2 68

5.2.0 MALDI-TOF analysis of AcGST-1 and AcGST-2 69

5.2.1 Reactivity of purified putative GST isozymes towards pesticides by Thin Layer Chromatography (TLC) analysis 71

5.2.2 Disc diffusion test towards pesticides and hydrogen peroxide 73

**6.0 Discussion** 75

**7.0 Conclusion** 88

**8.0 References** 91

**9.0 Appendices**

9.1 Appendix A 105

9.2 Appendix B 106

9.3 Appendix C 108

9.4 Appendix D 108

9.5 Appendix E 109

# List of figures


| Figures | Pages |
|---|---|
| Figure 1: GST monomer and dimer | 4 |
| Figure 2: Phase 1 and Phase 2 detoxification pathways | 5 |
| Figure 3: Example of GSTs catalysed reactions. | 6 |
| Figure 4: Structure of some eicosanoids | 10 |
| Figure 5: Biosynthesis of $PGE_2$, $PGF_{2\alpha}$ and $PGD_2$ | 11 |
| Figure 6: Conversion of $PGE_2$ to $PGE_1$ and $PGA_2$ | 12 |
| Figure 7: The formation of $LTA_4$ from arachidonic acid and conversion of $LTA_4$ to $LTC_4$ and LTB | 13 |
| Figure 8: Structure of Beta class GST | 18 |
| Figure 9: Secondary structure predictions with comparative crystal data for Zeta class GST | 20 |
| Figure 10: Metabolism of dichloromethane by methylotrophic bacteria | 21 |
| Figure 11: N-terminal amino acid sequences of strain DM 11 strain DM2 and strain DM 4 | 23 |
| Figure 12: Bacterial Theta class GST, Insect Theta class GST and Human Pi class GST. | 23 |
| Figure 13: The conversion pathway from maleyacetoacetate to fumarylacetoacetate | 24 |
| Figure 14: The pathways for catabolism of naphthalene via gentisate and tyrosine via homogentisate | 25 |

Figure 15: Pathway for degradation of PCP to 2,4-dichloro-3-hydroxy-cis,cis-muconic semialdehyde (DCHMS) in *S. chlorophenolica* RA-2 26

Figure 16: The glutathione-dependent peroxidase reaction catalysed by mPGES1 and the glutathione conjugation reaction catalysed by LTC4S 30

Figure 17: Side view ribbon representation of the currently available structures from MAPEG family 31

Figure 18: Proposed reaction of modification of fosfomycin 32

Figure 19: Mechanism of reaction of FosX 34

Figure 20: The amplicon of 16S rRNA targeted gene of *Acinetobacter calcoaceticus* Y1 56

Figure 21: Partial sequence of 16S rRNA amplicon 57

Figure 22: Top 10 hits using NCBI Nucleotide blast 57

Figure 23: Phylogenetic tree-neighbour joining (unrooted tree) 58

Figure 24: No fluorescence colonies can be seen after spraying with monochlorobimane and view under 365nm wavelength UV light for non-GSTs producing bacteria 59

Figure 25: No fluorescence colonies can be seen without spraying with monochlorobimane after viewing under 365nm wavelength UV light for *Acinetobacter calcoaceticus* Y1 59

Figure 26: Fluorescence colonies can be seen after spraying with monochlorobimane and view under 365nm wavelength UV light for *Acinetobacter calcoaceticus* Y1 60

Figure 27: SDS-PAGE of purified putative GSTs from *Acinetobacter calcoaceticus* Y1 61

Figure 28: Two-dimensional electrophoresis of purified putative GSTs from *Acinetobacter calcoaceticus* Y1 62

Figure 29: Isoelectric-focusing (IEF) of purified protein sample 63

Figure 30: SDS-PAGE of AcGST-1 purified from CM Sepharose fast flow column 64

Figure 31: SDS-PAGE of AcGST-2 purified from DEAE Sepharose fast flow column 65

Figure 32: N-terminal sequence of AcGST-1 until 5th amino acids 68

Figure 33: N-terminal sequence of AcGST-2 until 9th amino acids 68

Figure 34: Top 10 hits of AcGST-1 excised from ion-exchange chromatography 69

Figure 35: Top 10 hits of AcGST-2 excised from two-dimensional electrophoresis 70

Figure 36: Top 10 hits of AcGST-2 excised from ion-exchange chromatograph 70

Figure 37: No conjugation can be viewed between AcGST-1 towards Isoproturon, Fenoxaprop-ethyl, Prospoxur and Clodinafop-propargyl 71

Figure 38: Conjugation happened between AcGST-2 with Isoproturon while AcGST-2 did not conjugate with Fenaxaprop-ethyl, Propoxur and Clodinafop-propargyl 72

Figure 39: Susceptibility of *Acinetobacter calcoaceticus* Y1 towards 1 mg/ml pesticides and 50 % of hydrogen peroxide 73

Figure 40: Susceptibility of *Acinetobacter calcoaceticus* Y1 towards 0.5 mg/ml pesticides and 25 % of hydrogen peroxide 74

Figure 41: Schematic illustrations of five common aggregation mechanisms 80

Figure 42: Crystal structure of Pi class GST during EA binding 81

Figure 43: Proposed catalytic mechanism of glutathione peroxidase 83

# List of tables


| Tables | Pages |
|---|---|
| Table 1: Involvement of human GST isozymes in leukotriene and prostaglandin metabolism | 13 |
| Table 2: Volume of solution used in preparing 4 % stacking gel and 12 % resolving gel | 46 |
| Table 3: Volume of solution to prepare 2 ml of 1× SDS sample buffer | 46 |
| Table 4: Vorum silver stain method | 47 |
| Table 5: Preparation of colloidal brilliant blue CBB G-250 | 48 |
| Table 6: Composition of mixture for TLC | 53 |
| Table 7: Substrate specificity of AcGST-1 and AcGST-2 from *Acinetobacter calcoaceticus* Y1 | 66 |
| Table 8: $V_{max}$ and $K_m$ of AcGST-1 and AcGST-2 | 67 |
| Table 9: List of putative glutathione transferases of *Acinetobacter calcoaceticus* (strain PHEA-2) | 86 |

# List of formulas

| Formulas | Pages |
|---|---|
| $\frac{1}{V} = \frac{1}{Vmax} + \frac{Km}{Vmax}\frac{1}{[S]}$ | 83 |
| $\frac{[S]}{V} = \frac{[S]}{Vmax} + \frac{Km}{Vmax}$ | 84 |
| $V = -Km\frac{V}{[S]} + Vmax$ | 84 |

# List of abbreviations

| | |
|---|---|
| ACN | Acetonitrile |
| AcGST | *Acinetobacter calcoaceticus* GST |
| Ala | Alanine |
| APS | Ammonium persulphate |
| Arg | Arginine |
| Asp | Aspartate |
| AtGSTZ | *Arabidopsis thaliana* GST zeta |
| ASK1 | Apoptosis signal-regulating kinase 1 |
| ATP | Adenosine triphosphate |
| BxGST | *Burkholderia xenovorans* GST |
| Bp | Base-pair |
| BSP | Sulfobromophthalein |
| CDNB | 1-chloro-2,4-dinitrobenzene |
| CBB | Colloidal brilliant blue |
| CHAPS | 3-[(3-cholamidopropyl)-dimethylammonio]-1-propane sulfonate |
| CHCA | α-cyano-4-hydroxycinnamic acid |
| cGST | Cytosolic GST |
| COX | Cyclooxygenase |
| CM | Carboxylmethyl |
| Cys | Cysteine |
| DCHMS | 2,4-dichloro-3-hydroxy-cis,cis-muconic semialdehyde |
| DCNB | 1,2-Dichloro-4-nitrobenzene |
| DCM | Dichloromethane |
| DDT | Dichlorodiphenyltrichloroethane |
| DEAE | Diethylaminoethanol |

| | |
|---|---|
| DNA | Deoxyribonucleic acid |
| DNICs | Dinitrosyl dithiol iron-complexes |
| DNDGIC | Dinitrosy-diglutathionyll-dithiol iron-complexes |
| EA | Ethacrynic acid |
| EB | Equilibration buffer |
| ESeOH | Selenic acid |
| ESeSG | Selenenyl sulfide adduct |
| EcGST | *Escherichia coli* GST |
| EDTA | Ethylenediaminetetraacetic acid |
| EFAs | Essential fatty acids |
| FAH | Fumarylacetoacetate hydrolase |
| FLAP | 5-lipoxygenase-activating protein |
| FosA | Fosfomycin A |
| FosB | Fosfomycin B |
| FosC | Fosfomycin C |
| FosX | Fosfomycin X |
| Glu | Glutamate |
| Gln | Glutatamine |
| GSSG | Glutathione reductase |
| GST | Glutathione S-transferase |
| GSTπ | GST pi |
| GSTA | GST alpha |
| GSTM | GST mu |
| GSTP | GST pi |
| GSTZ | GST zeta |
| GSH | Glutathione tripeptide |

| | |
|---|---|
| G- site | Glutathione tripeptide binding site |
| hGSTP | Human GST pi |
| hGSTK1 | Human GST kappa-1 |
| HCCA | 2-hydroxychromene-2 carboxylate isomerases |
| HDO | Homogentisate-1,2-deoygenase |
| His | Histidine |
| H-site | Substrate binding site |
| HPETs | Hydroperoxyeicosatetraenoic acids |
| HT-1 | Hereditary tyrosinemia type 1 |
| IEF | Isoelectric focusing |
| ITC | Isothiocyanates |
| JNK | C-jun N-terminal kinase |
| kDa | Kilo Dalton |
| $K_m$ | Substrate concentration at half of the enzyme velocity |
| LOX | Lipoxygenase |
| LPO | Lipid peroxidation |
| LT | Leukotrienes |
| MAAI | Maleylacetoacetate isomerase |
| mGST | Mitochondrial GST |
| MALDI-TOF | Matrix-assisted laser desorption/ionization-time of flight |
| MAP | Mitogen-activated protein |
| MAPEG | Membrane-associated proteins in eicosanoid and glutathione metabolism |
| MCB | Monochlorobimane |
| $Mn^{2+}$ | Manganese ion +2 |
| MPAG | Microsomal glutathione S-transferase |

| | |
|---|---|
| mPGES-1 | Microsomal prostaglandin E synthase-1 |
| MPI | Maleyl pyruvate isomerase |
| NaCl | Sodium chloride |
| NADH | Nicotinamide adenine dinucleotide |
| NADPH | Nicotinamide adenine dinucleotide phosphate |
| NBC | p-nitrobenzyl chloride |
| NCBI | National centre for biotechnology information |
| NEM | N-ethylmaleimide |
| NO | Nitric oxide |
| OaGST | *Ochrobactrum anthropic* GST |
| OvGST | *Onchocerca volvulus* GST |
| PBO | Trans-4-phenyl-3-butene-2-one |
| PCP | Pentachlorophenol |
| PCR | Polymerase chain reaction |
| PG | Prostaglandins |
| Phe | Phenylalanine |
| PmGST | *Proteus mirabilis* GST |
| PMNs | Polymorphonuclear cells |
| PTU | Phenylthiourea |
| PMSF | Phenylmethylsulfonyl fluoride |
| PVDF | Polyvinylidene fluoride membrane |
| rGSTK | Rat GST kappa |
| ROS | Reactive oxygen species |
| rRNA | Ribosomal ribonucleic acid |
| [S] | Substrate concentration |
| SDS | Sodium Dodecyl Sulphate |

| | |
|---|---|
| SDS-PAGE | Sodium Dodecyl Sulphate-Polyacrylamide Gel Electrophoresis |
| *S. chlorophenolica* | *Sphingomonas chlorophenolica* |
| SeGST | *Synechococcus elongatus* PCC 6301 GST |
| Ser | Serine |
| TCHQ | Tetrachlorohydroquinone |
| TeGST | *Thermosynechococcus elongatus* BP-1 GST |
| TEMED | Tetramethylethylenediamine |
| TFA | Trifluroacetic acid |
| Trp | Tryptophan |
| Tris HCL | Tris hydrochloride |
| TLC | Thin layer chromatography |
| TX | Thromboxanes |
| UDP-NAG | Uridine diphospho-N-acetylglucosamine |
| [V] | Velocity |
| $V_{max}$ | Maximum initial rate of enzyme |
| 15d-PGJ2 | 15-deoxy-Δ12,14-prostaglandin J2 |
| 4-HNE | 4-hydroxynonenal |
| 5-HETE | 5S-hydroxyl-eicosatetraenoic acid |
| 5-HPETE | 5-hydroperoxyeicosatetraenoic acid |
| 3D | Three dimension |

# 1.0 Introduction

Bacterial glutathione S-transferases (GSTs) are enzymes that play a key role in cellular detoxification. They are implicated in a variety of processes such as the biodegradation of xenobiotics, protection against chemical and oxidative stresses and resistance to antimicrobial drugs. GSTs were divided into different classes based on the sequence similarity, immunologic properties and substrate and inhibitor specificity (Udomsinprasert *et al.,* 2004). GST isozymes belonging to the same class had 70-80% identity in their primary structure, whereas GST belonging to different classes had less than 30% sequence identity (Mignogna *et al.,* 1993). Bacterial GSTs appeared to be structurally, kinetically and immunologically different from mammalian GSTs (Dainelli *et al.,* 2002). Currently, there is no delineating information on bacterial GSTs compared to mammalians and insects GSTs.

GSTs are widely distributed in aerobic bacteria but not detected in anaerobic bacteria. There are several GSTs producing aerobic bacteria have been reported such as *Ochrobactrum anthropi*, *Pseudomonas* sp., *Serratia marcescens*, *Proteus mirabilis*, *Escherichia coli*, and *Xanthomonas campestris*. N-terminal amino acid sequence of these bacteria were likely similar (68% identity) and some amino acid such as tyrosine, serine, histidine, leucine and glycine were highly conserved among bacteria GSTs (Favaloro *et al.,* 1998). The N-terminal region comprises part of the active site where residues interact with GSH and it is evolutionary conserved.

In bacteria, 4 cytosolic GSTs have been identified: beta, chi, theta and zeta. Beta class GSTs were purified and characterized in *P. mirabilis* (Di ilio *et al.,* 1988), *E. coli* (Lizuka *et al.,* 1989) and *Burkholderia xenovorans* (Bartels *et al.,* 1999). They are able to conjugate 1-chloro-2,4-dinitrobenzene (CDNB) and bind to GSH affinity matrix. All beta class GSTs have a cysteine residue at the GSH binding site. Dichloromethane (DCM)

dehalogenases produced by facultative *Methylophilus* sp. represents the theta class GSTs. They possess high amino acid sequence similarity with mammalian theta class GSTs and characterized by their unique conjugating activity towards DCM with zero CDNB conjugating activity and incapability to bind GSH affinity matrix. Tetrachlorohydroquinone (TCHQ) dehalogenase was reported by Anandarajah *et al.* (2000) to belong to the zeta class. This enzyme is characterized by the distinctive motif of GSH binding site including two serine and a cysteine residues. TCHQ dehalogenase involves in the biodegradation of pentachlorophenol and isomerase activity. A novel class of cytosolic GSTs, Chi class was purified and characterized from cyanobacteria *Thermosynechoccus elongatus* BP-1 (Wiktelius & Stenberg, 2007). Chi class GSTs lack of cysteines in the GSH binding site suggesting different evolutionary pathway for the cyanobacterial GSTs from the beta class GSTs.

Membrane-associated proteins involved in ecosanoid and glutathione metabolism (MAPEG) member is identified in certain bacteria: *E. coli*, *Vibrio cholerae* and *Synechocystis* sp. They show GSTs activity towards CDNB, however, to date, no information about their physiological role in bacteria is available. Fosfomycin resistance protein is found exclusively in bacteria.

## 1.1 Objectives

The objectives of this study are listed out as below:

- To screen and identify the GST-expressing bacteria isolated from chemically contaminated soil
- To purify the GST isoforms from proteome of GST-expressing bacteria
- To characterize the GST isoforms from GST-expressing bacteria

# 2.0 Literature review

## 2.1 Glutathione S-transferase

### 2.1.1 Introduction

Glutathione S-transferases (GSTs; EC 2. 5. 1. 18) are a group of enzymes that use glutathione tripeptide (GSH) to transform a wide range of carcinogenic compounds, therapeutic drugs and products of oxidative stress. GSTs are widely distributed in nature and can be found in prokaryotes and eukaryotes from single cellular organisms to multicellular organisms. In prokaryotes, GST activity was very low or undetectable, but it seemed to be very important in the processes involving the biodegradation of xenobiotics, including antibiotics, although other roles of this enzyme had not yet well defined (Favaloro *et al.*, 1998). According to Piccolomini *et al.* (1989), in the bacterial strains investigated, GST concentration ranged from as low as 0.002% of total cytosolic proteins for *Pseudomonas aeruginosa* ATCC 27853 to 0.060% for *Proteus mirabilis* AF 2924. These values are much lower than those (2-5%) found in mammalian tissues. GSTs had been most extensively studied in man, rat and mouse, in which multiple isoforms composed of two subunits were present (Piccolomini *et al.*, 1989). The dimer could be a homodimer or heterodimer. In order to form an active enzyme, two monomers must bind together to form a cleft for GSH and substrates binding. Most GST classes show a high degree of polymorphism. Each subunit had about 199–244 amino acids in length and 22–29 kDa and contained a catalytically independent active site consisted of a GSH-binding site (‘G-site’) in the amino-terminal domain and a hydrophobic substrate binding site (‘H-site’) in the carboxyl-terminal domain (Laborde, 2010).

Figure 1: GST monomer and dimer

(Source: http://enzymefunction.org/about/bridging-projects/gst-superfamily)

2.1.2 Functional roles of GSTs

All cells including mammalian and non-mammalian are vulnerable and potentially exposed to toxic compounds from the environment. Production of enzymes with specified biochemical pathways to deal with these toxic compounds is the one way to sustain life and survive on earth. The detoxification process of GSTs included two major phases; phase one was catalysed by the cytochrome P-450 system and phase two by enzymes catalysing the conjugation of the toxic compound or xenobiotic to an endogenous substrate, namely glutathione (GSH) (Favaloro *et.al.,* 1998). GSTs are involved in the phase two detoxification process. In phase two detoxification, the activated hydrophobic xenobiotic (electrophilic or nucleophilic compounds) is conjugated with GSH catalysed by GSTs. GSH is a tripeptide made up of cysteine, glycine and glutamate that functions as an antioxidant compound. Adding GSH to the toxic compounds modify its polarity to become more water-soluble and this process facilitate its transportation out of the cells. GSTs had been implicated in a variety of resistance phenomena involving cancer chemotherapy agents, insecticides, herbicides and microbial antibiotics (Sheehan *et al.,* 2001). Other natural GST substrates include steroids,

leukotrienes, anthocyanines, and organic isothiocyanates. GSTs had the capacity to bind lipophilic compounds that act as ligands but not as substrates (Vuilleumier, 1997). Human GSTs play an important role in protection against toxic chemicals, pesticides, herbicides, carcinogens, drugs, and many other harmful pathogens in the body. In plants, GSTs protect the plants against pesticides, herbicides, insects, pathogens, and other chemical compounds that are harmful to their survival. Bacterial GSTs had been implicated in the microbial biodegradation and detoxification of xenobiotics (Dhar *et al.*, 2003). From their studies, Alias & Clark (2007) proposed that a primary role of the GSTs was to minimize the effect of the products oxygen toxicity, such as peroxides, alkenals and hydroalkenals.

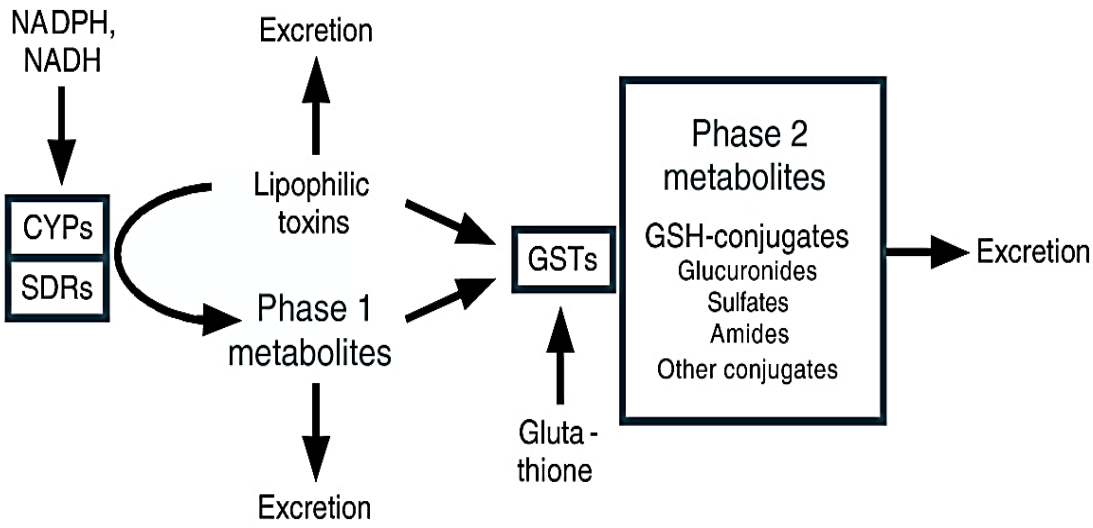


Figure 2: Phase 1 and Phase 2 detoxification pathways.

(Source: http://genomebiology.com/2007/8/7/r132/figure/f3?highres=y)

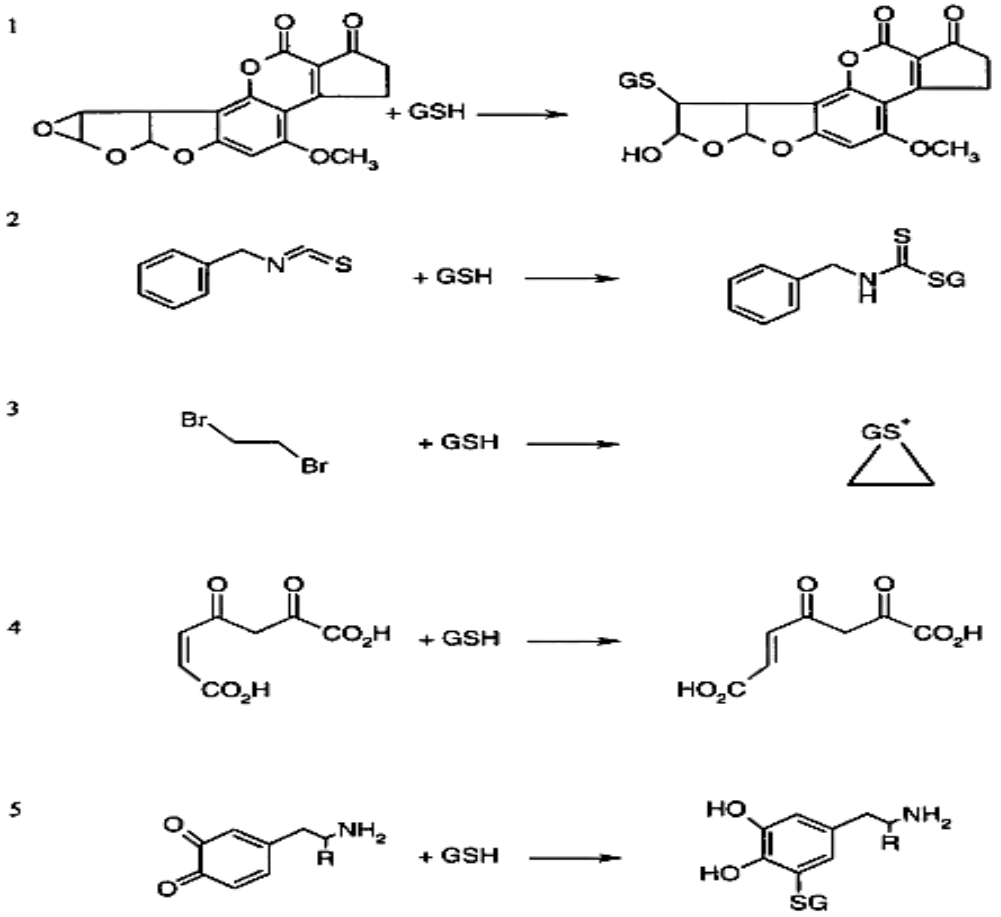


Figure 3: Example of GSTs catalysed reactions. (1) Aflatoxin $B_1$-8,9-epoxide (2) benzylisothiocyanate (3) dibromoehtane (4) maleyacetoacetate (5) *o*-quinone

(Source: Sherratt *et al.*, 2001)

Besides acting as housekeeper enzyme involves in detoxification and degradation of xenobiotics, recent studies had suggested that GSTs also acted as mediators in signalling pathways involved in cells proliferation and cells death. GSTs are found to metabolize endogenous substances that are important in signalling pathways. For example, the prostaglandin 15-deoxy-Δ12,14-prostaglandin J2 (15d-PGJ2) was metabolized by GSTs and these compounds were known to influence the activity of transcription factors and protein kinases involved in stress response, proliferation, differentiation, or apoptosis (Pajaud *et al.*, 2012). The endogenous lipid peroxidation product 4-hydroxynonenal (4-HNE) believed to act as an intracellular signalling molecule (Dwivedi *et al.*, 2007). 4-HNE is at the highest concentration during oxidative stress in

animal cells. A moderately high concentration of 4-HNE could induce apoptosis, differentiation, and affected activation of adenylate cyclase, JNK, protein kinase C, and caspase 3, however, a low concentration of 4-HNE could induce cell proliferation (Pajaud *et al.,* 2012). Intracellular concentrations of HNE were regulated by glutathione S-transferases, GSH and a protein called RLIP76 that catalysed the ATP-dependent transport HNE out of cells (Mattson, 2009). Furthermore, several studies had revealed that GSTs bound to mitogen activated protein kinases such as apoptosis signal-regulating kinase 1 (ASK1) which involved in activation of c-jun N-terminal kinase (JNK) in response to various oxidative stress, endoplasmic reticulum stress and calcium influx. JNK is responsible for phosphorylation of c-jun (name of a gene and protein) on Ser-63 and Ser-73 within its transcriptional domain. Other functions of GSTs such as the S-glutathionylation of proteins and the ability to be a nitric oxide (NO) carrier had also been described (Brune, 2003).

S-glutathionylation is a protein post-translational modification by conjugating GSH to the cysteine residues. S-glutathionyl protein involves in oxidative stress, nitrosative stress, preventing irreversible binding of thiol proteins and controls the cells signalling pathways by modulating the function of proteins. Cysteine side chains of proteins were being increasingly appreciated as the site of major post-translational modifications that exert profound degrees of protein regulation (Dulce *et al.,* 2010). According to Townsend *et al.* (2008), GST Pi (π) potentiated S-glutathionylation reactions following oxidative and nitrosative stress in vitro and in vivo. S-glutathionylation on Cys47 and Cys101 auto-regulates GSTπ that breaks ligand binding interactions with c-jun NH2 terminal kinase (JNK) and causes GSTπ to form aggregates. S-glutathionylation results in the formation of an intermolecular disulfide bond between two GST subunits. GSH-dependent reduction of the disulphide will restore the reduced active-site thiol.

Nitric oxide (NO) is an important signalling molecule in both physiological and cytotoxic processes. At physiological level, dinitrosyl dithiol iron-complexes (DNICs) play a vital role as NO carrier to pro-long its half-life. Dinitrosy-diglutathionyll-dithiol iron-complexes (DNDGIC)) comprise of NO, iron and two glutathiones. On the other hand, at cytotoxic concentrations, such as during chronic inflammation, these complexes, by sequestrating NO, could prevent its cytotoxic effect (Pajaud *et al.,* 2012). From previous studies, GSTA1-1, GSTM1-1 and GSTP1-1 were able to bind DNDGIC in vitro.

Apart from metabolizing xenobiotic and mediating the signalling pathways, GSTs also play an important role in eicosanoid biosynthesis. Specific isoforms of GST were involved in the biosynthesis of eicosanoids by reducing hydroperoxides, endoperoxides, and formation of peptide leukotrienes (Anuradha *et al.,* 2000). Microsomal glutathione S-transferase (MPAG), a newly designed membrane associated protein involved in eicosanoid and glutathione metabolism (Sherratt *et al.,* 2001). Eicosanoid is a signalling molecule derived from a twenty carbon essential fatty acids (EFAs), arachidonic acid. Eicosanoid consists of the prostaglandins (PG), thromboxanes (TX), leukotrienes (LT) and lipoxins (LX). PG has five different forms: $PGD_2$, $PGE_1$, $PGE_2$, $PGF_{2\alpha}$ and $PGH_2$ which function to dilate arterioles and capillaries to decrease the blood pressure, relax vascular smooth muscle, open the bronchi of the lungs, enhance blood flow through the kidneys, increase urinary volume as well as the excretion of sodium ions, and cause contraction of gut muscle in humans. TX can occur as active form ($TXA_1$ and $TXA_2$) and inactive form ($TXB_2$ and $TXA_2$) which is actually modified prostaglandins. TX functions as blood vessels constrictors, cyclic AMP suppressers, and promotion of platelet aggregation. LT exists as $LTEB_4$, $LTEC_4$, $LTED_4$ and $LTED_4$. These 4 forms of LT are synthesized in monocytes and alveolar macrophages, basophils, eosinophils, mast cells and epithelial cells. LT involves in several immune-mediated inflammatory reactions of anaphylaxis and are constituents of substances originally called "slow-reacting substance

of anaphylaxis." This substances cause smooth muscle contraction, affecting vascular permeability, and are strong attractants of polymorphonuclear leukocytes. There are two forms of LX: $LXA_4$ and $LXB_4$. Both $LXA_4$ and $LXB_4$ are synthesized from platelets, endothelial cells, mucosal epithelial cells and other leukocytes via interactions with PMNs. They have a high affinity towards LX A4 receptor to stimulate chemotaxis of polymorphonuclear cells (PMNs) and calcium mobilization. There are two main pathways involve in the biosynthesis of eicosanoid. The PG and TX are synthesized from the cyclic pathway while the LT are from the linear pathway which involves cyclooxygenase (COX) enzyme and lipoxygenase (LOX) enzyme.

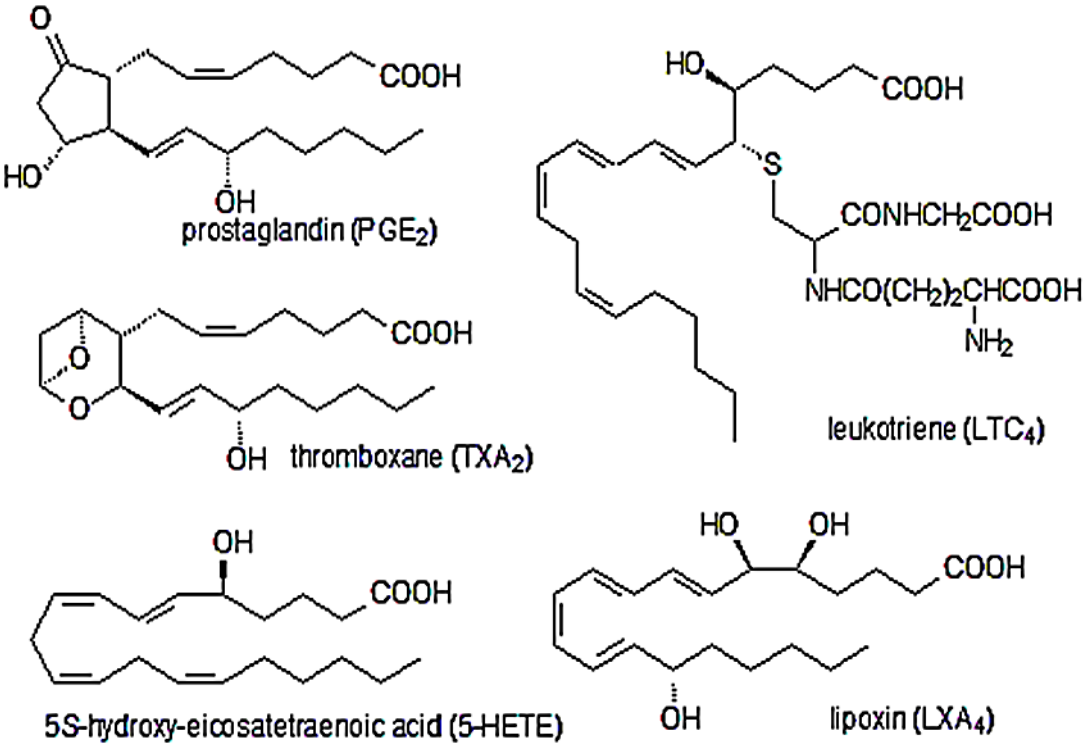


Figure 4: Structure of some eicosanoids

(Source: http://lipidlibrary.aocs.org/lipids/eicintro/index.html)

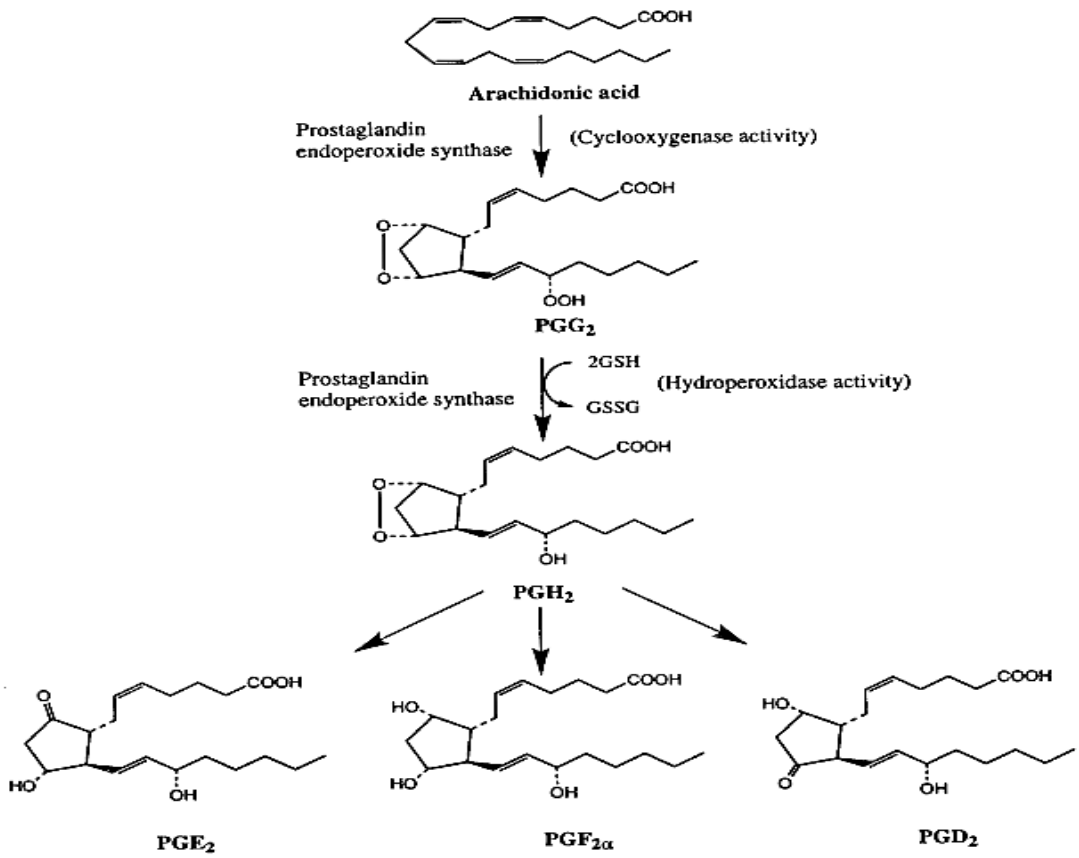


Figure 5: Biosynthesis of $PGE_2$, $PGF_{2\alpha}$ and $PGD_2$.

(Source: Wang & Ballatori, 1998)

Biosynthesis of prostaglandin has two control points. The starting materials of prostaglandin biosynthesis is membrane phospholipid (Phosphatidylinositol). The second control point is where the enzyme plays an important role in converting the arachidonic acid to $PGG_2$. Prostaglandin endoperoxidase synthase converts arachidonic acid to $PGH_2$. Prostaglandin endoperoxidase synthase has two catalytic activities: cyclooxygenase activity and hydroperoxidase activity. Cyclooxygenase add two molecules of oxygen to arachidonic acid to form $PGG_2$ while hydroperoxidase convert the hydroperoxy group of $PGG_2$ to hydroxyl group lead to formation of $PGH_2$. $PGH_2$ is a useful intermediate product for subsequent formation of $PGF_2$, $PGF_{2\alpha}$ and $PGD_2$. According to Wang & Ballatori (1998), $PGD_2$, $PGE_2$ and $PGF_{2\alpha}$ were formed from $PGH_2$ by various rat GSH S-transferase isozymes. Class Alpha GST catalysed production of $PGF_{2\alpha}$ and class Sigma

were known as GSH-dependent $PGD_2$ synthase that catalysed the formation of $PGD_2$ (Sherratt *et al.*, 2001).

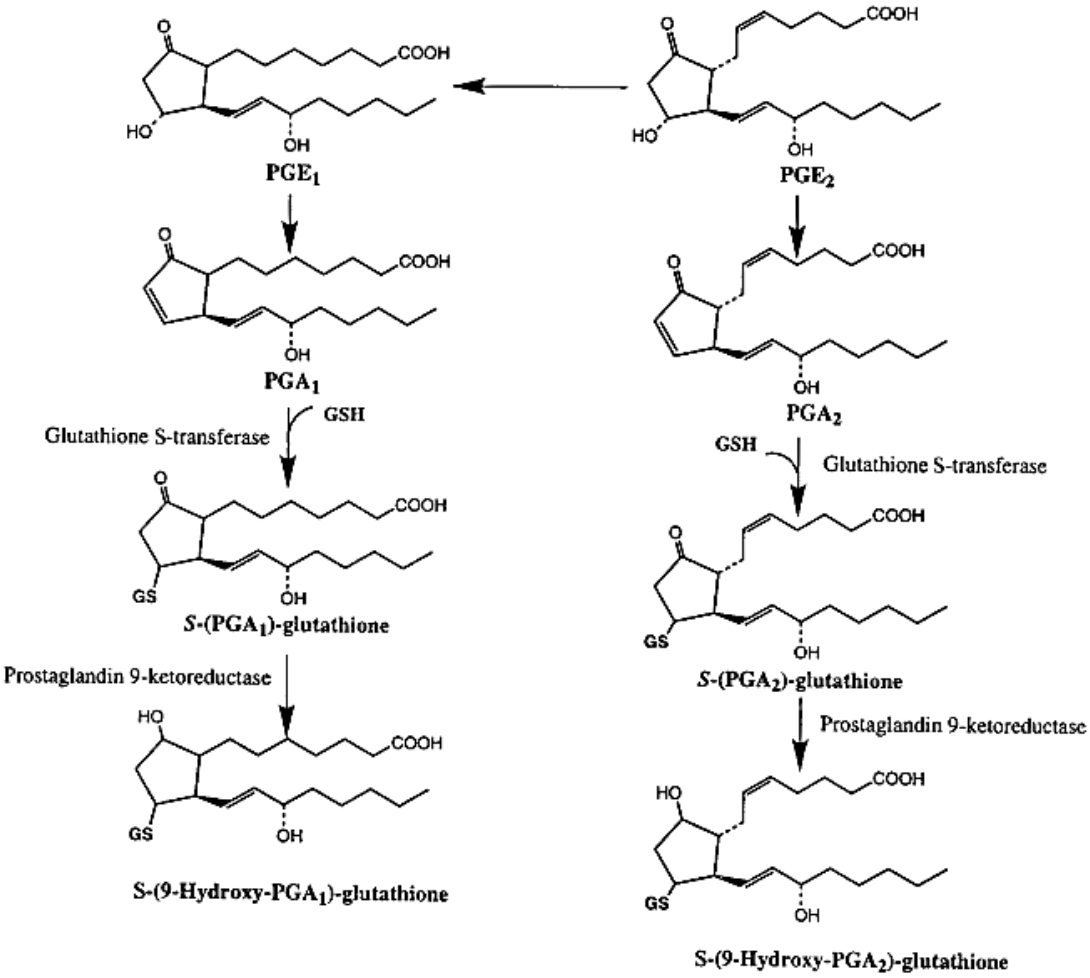


Figure 6: Conversion of $PGE_2$ to $PGE_1$ and $PGA_2$.

(Source: Wang & Ballatori, 1998)

$PGE_2$ and $PGE_1$ are dehydrated to $PGA_2$ and to $PGA_1$. Both $PGA_1$ and $PGA_2$ were potentially toxic and GSH could conjugate with both to form S-(PGA)-GSH derivatives (Wang & Ballatori, 1988). $PGA_1$ and $PGA_2$ can cause haematology toxicity such as anaemia and thrombocytopenia. Certain vertebrate alpha-, mu-, and pi-class GSTs were found to enhance $PGA_2$ conjugation with glutathione, suggesting that the overexpression of GST could modulate the cytotoxic effects of cyclopentenone prostaglandins (Whalen *et al.*, 2010).

| Superfamily | Isozymes | Biosynthesis involving isomerisation, reduction or non-catalytic binding | Conjugation reactions with GSH |
|---|---|---|---|
| **Soluble** | GSTA1-1 | $PGH_2$->$PGE_2$;$PGH_2$->$PGF_{2\alpha}$ | Conjugation of $PGA_2$ and $PGJ_2$ |
| | GSTA2-2 | $PGH_2$->$PGD_2$;$PGH_2$->$PGF_{2\alpha}$ | - |
| | GSTM1-1 | - | Conjugation of $PGA_2$ and $PGJ_2$ |
| | GSTP1-1 | - | Conjugation of $PGA_2$ and $PGJ_2$ |
| | GSTS1-1 | $PGH_2$->$PGD_2$ | - |
| **MAPEG** | MGST-I-like 1 | $PGH_2$->$PGE_2$ | - |
| | MGST-II | Reduction of 5-HPETE | $LTA_4$->$LTC_4$ |
| | MGST-III | Reduction of 5-HPETE | $LTA_4$->$LTC_4$ |
| | LTC4S | - | $LTA_4$->$LTC_4$ |
| | FLAP | Binding of arachidonic acid | - |

Table 1: Involvement of human GST isozymes in leukotriene and prostaglandin metabolism. (Source: Sherratt *et al.*, 2001)

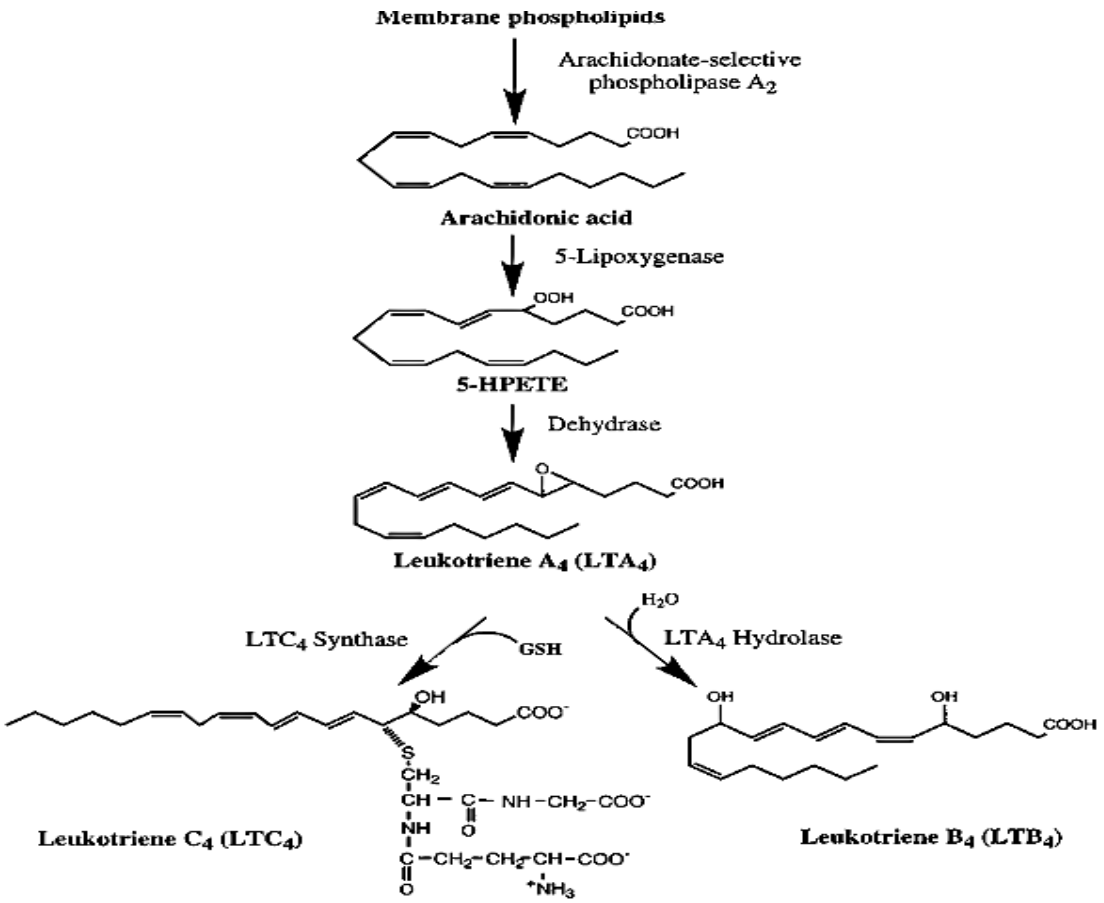


Figure 7: The formation of $LTA_4$ from arachidonic acid and conversion of $LTA_4$ to $LTC_4$ and $LTB_4$.

(Source: Wang & Ballatori, 1988)

Biosynthesis initiates with the metabolizing of arachidonic acid to hydroperoxyeicosatetraenoic acids (HPETs). This reaction is catalysed by 5-lipoxygenase and 5-lipoxygenase-activating protein (FLAP). Calcium and ATP were required for maximal activity of these enzymes (Samuelsson *et al.*, 1989). $LTA_4$ can be metabolized in different two routes. $LTB_4$ is synthesized from $LTA_4$ catalysed by the enzyme $LTA_4$ hydrolase.

The second pathway involves the conjugation of GSH to $LTA_4$ catalysed by the membrane-bound $LTC_4$ synthase enzyme. $LTC_4$ synthase was a unique membrane-bound enzyme that catalysed the committed step in the biosynthesis of all of the peptidoleukotrienes (Nicholson *et al.*, 1992). This enzyme was encoded by the $LTC_{4s}$ gene and kind of related to microsomal GSTs. $LTC_4$ synthase was enzymatically active as a multimer composed of low molecular mass subunits (Nicholson *et al.*, 1992). $LTC_4$ synthase is very unique as it committed in the biosynthesis of $LTC_4$ instead of conjugation with xenobiotics. According to Welsch *et al.* (1994), $LTC_4$ synthase showed no homology to other glutathione S-transferases, however, $LTC_4$ was found to be most similar to 5-lipoxygenase activating protein (31% identity, 53% similarity).

### 2.1.3 Families of GSTs

#### 2.1.3.1 Cytosolic GSTs

GSTs are widely distributed in nature and found in prokaryotes and eukaryotes. GSTs are divided into four major families of proteins: cytosolic GST (cGST), mitochondrial GST (mGST), microsomal GST and bacteria fosfomycin-resistant protein (Allocati *et al.,* 2008). In mammals, at least seven classes of GSTs (Alpha, Mu, Pi, Zeta, Sigma, Theta and Omega) had been grouped into the cGST family on the basis of sequence similarity, immunologic properties and substrate-inhibitor specificity (Di illio *et al.,* 1988). These GSTs are known to protect organisms from oxidative stress, possess peroxidase activity, isomerase activity and involve in drug resistant. Apart from mammals, the theta class of GST was also presented in plants, fishes, birds, insects, yeasts and fungi (Vuilleumier, 1997). Four additional classes of GSTs had been discovered in bacteria, insects and plants namely Beta, Phi, Tau and Delta (Sherratt *et al.,* 2001). Due to peculiar structure and immunology properties of *Proteus mirabilis* GSTs, it had now being identified as the prototype of a new GST class, i.e. “beta class” following the guidelines adopted for mammalian GSTs it was now referred as PmGSTB1-1 (Di ilio *et al.,* 1988). The Pi and Mu classes of GSTs played a regulatory role in the mitogen-activated protein (MAP) kinase pathway that participated in cellular survival and death signals via protein-protein interactions with c-Jun N-terminal kinase 1 (JNK1) and ASK1 (apoptosis signal-regulating kinase) (Townsend *et al.,* 2003). According to Bader & Leisinger (1994), dichloromethane dehalogenase from *Methylobacterium* sp. was closely related to eukaryotic class theta GST than to a number of bacterial GSTs. Recent bioinformatics analysis had split cGSTs into 2 different major groups: S/C-type and Y-type based on the sequence similarity and structure of active site. Beta, Omega, Pi, Tau, Theta and Zeta belong to the S/C-type while Alpha, Mu, Pi and Sigma belong to the Y-type.

All cGSTs are comprised of two subunits and water-soluble. Soluble GST was a dimer hydrophobic protein of 50-kDa with isoelectric point of 4-5 (Dixon *et al.,* 2002). Phi, tau, theta and zeta classes of GST were dimeric protein and possessed a serine residue in their active sites (Mohsenzadeh *et al.,* 2011). The N-terminal domain (domain I) adopted α/β topology and provided the GSH-binding site (G-site) while the C-terminal domain (domain II) was an all-α-helical structure and provided the structural element for recognition of a broad range of hydrophobic co-substrate (H-site) (Skopelitou *et al.,* 2012). The H-site lied adjacent to the G-site and defined the substrate specificity of the enzyme (Skopelitou *et al.,* 2012). Much more is known for mammalian GSTs compared to bacterial GSTs. Bacterial GSTs appeared to be structurally, kinetically and immunologically different from mammalian GST (Dainelli *et al.,* 2002). No conclusive decision to adhere whether bacterial GSTs should be grouped into the mammalian classes of GST. Bacterial GSTs did not cross-reacted with antisera from mammals and plants. Moreover, they showed low cross-reactivity among themselves as well (Favaloro *et al.,* 1998). The plausible reason for the low cross-reactivity is because GST isozymes belonging to the same class showed greater than 60% sequence similarity in their primary structure, whereas GSTs belonging to different classes had less than 30% sequence identity (Dainelli *et al.,* 2002).

In bacteria, four different classes of cGSTs had been identified: beta, chi, theta and zeta (Allocati *et al.,* 2008). Beta class was purified and characterized in *Escherichia coli* B. (Lizuka *et al.,* 1989), *Rhizosphere* sp. (Zablotowicz *et al.,* 1995), and *Pseudomonas* sp. (Jung *et al.,* 1996). The Beta class of GST is first reported in *P. mirabillis.* According to Di Illio *et al.* (1988), three forms of GSTs (GST-6.0, GST-6.4 and GST-7.3) had been characterized in *P. mirabillis.* GST-7.3 cross-reacted with the antisera raised against GST-6.0. However, none of the antisera raise against a number of human, rats and mouse GSTs cross-react with the bacterial enzymes suggesting structural

differences between them and the mammalian GSTs. Western blot analysis indicated that a GST antigenically identical to Pm-GST-6.0 was presented in *Enterobacter cloacae* CIP 6085, *E. coli* ATCC 25422 and *Proteus vulgaris* ATCC 8427, but absented in *E. coli* ATCC 25922, *Klebsiella oxytoca* CIP 666, *K. oxytoca* AF 101 and *Serratia marcescens* CIP 6755 (Picollomini *et al.,* 1989). Further analysis of amino acid sequence showed that the enzyme subunit was composed of 203 amino acid residues corresponding to a molecular mass of 22856 Da and comparison of this sequence with other known primary structures of the corresponding enzyme from different sources showed a low level of identity (17-26%) (Mignogna *et al.,* 1993). Beta class GST able to conjugate 1-chloro-2,4-dinitrobenzene (CDNB) and bind to the GSH–affinity matrix. All beta class GST were characterized by the present of a cysteine residue at the GSH site (Rossjohn *et al.,* 1998)

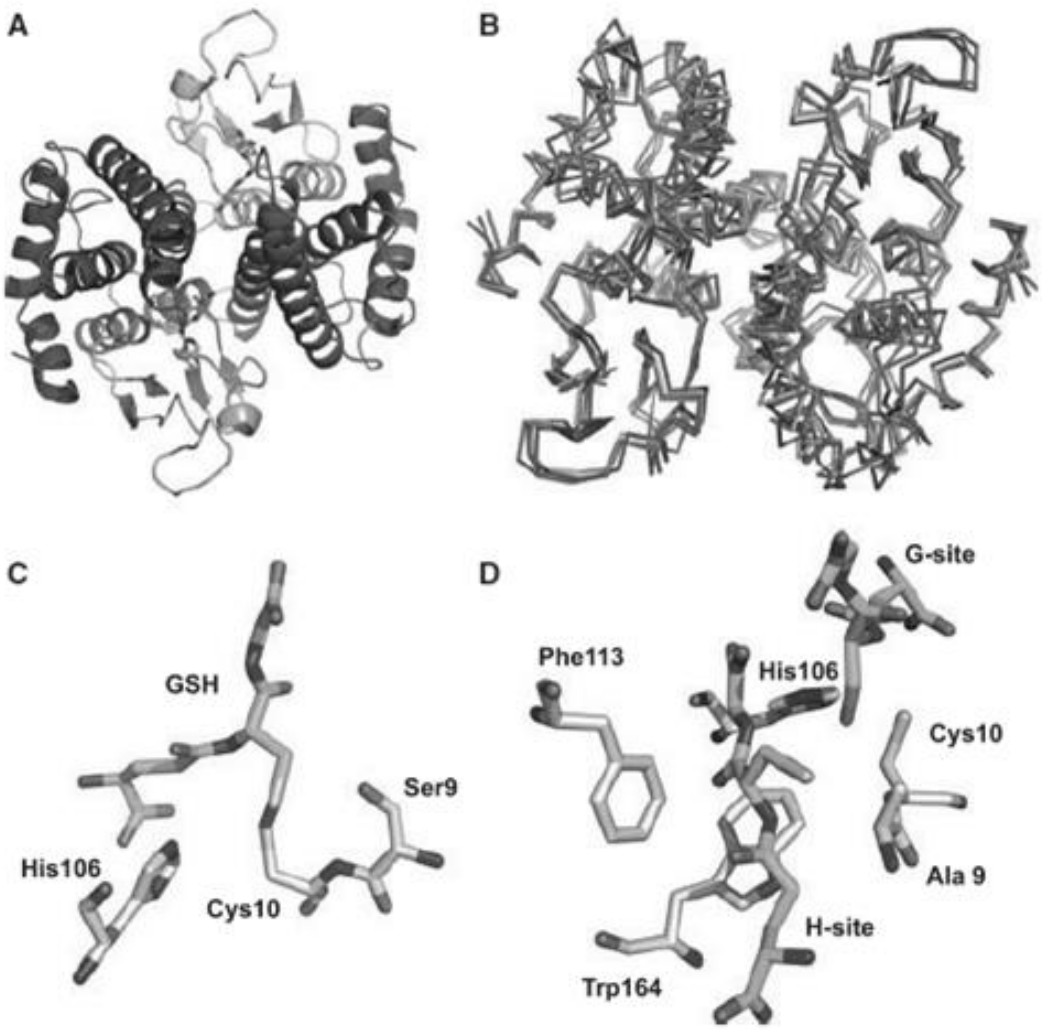


Figure 8: Structure of Beta class GST. (A) Structure of OaGST shown the two fold symmetry axis. (B) Overlay of four different beta class GSTs dimers shown as Cα races: OaGST (red), BxGST (green), EcGST (magenta) and PmGST (cyan). (C) GSH binding site in PmGST. (D) BxGST in complex with two GSH molecules.

(Source: Allocati *et al.,* 2008)

A novel class of GST, Chi class has been proposed recently. Chi class GST is first described in two species of cyanobacteria: thermophile *Thermosynechococcus elongatus* BP-1 and *Synechococcus elongatus* PCC 6301. Cyanobacteria are photosynthetic bacteria which obtain energy from photosynthesis. Cyanobacteria had high content of GSH in their cytosol (Fahey *et al.,* 1987) which indicate the presence of GSH-utilizing enzymes. Chi class GST is smaller compared to other classes of GST. The thermophilic

cyanobacterium *T. elongatus* BP-1 contained one single gene with GST annotation, encoding a protein of only 186 amino acids as opposed to most cytosolic GSTs containing 200–250 amino acids (Wiktelius & Stenberg, 2007). The lack of the two cysteine residues and the low sequence identity between the cyanobacterial enzymes with other bacterial representatives excluded the incorporation of the former into the Beta class GST (Wektelius & Stenberg, 2007). There are different expression level of GST for *T. elongatus* BP-1 (TeGST) and *S. elongatus* PCC 6301 (SeGST) due to the lower stability of the latter. Different catalytic properties between the two GSTs are observed. Cibacron Blue (typical GSTs inhibitor) is generally a strong inhibitor of GSTs, and here the effect is more pronounced for TeGST, displaying a 7-fold lower IC50 value than for SeGST. For substrate specificity test, SeGST are more efficient compared with TeGST. The Chi class GST able to conjugate isothiocyanates (ITC). ITC is part of the chemical defence of the plants in response to injury or stress to inhibit growing of pathogen. ITC shows antimicrobial activity towards certain bacteria species. The plants themselves produce GSTs against ITC to prevent harming or killing by ITC. According to Skipsey *et al.* (1997), 2 $\mu$mol $min^{-1}mg^{-1}$ of GST activity towards ITC had been recorded from soy bean. Chi class display higher sequence similarity with Zeta class GST compared to Beta class.

```
                10        20        30        40        50        60        70        80        90       10C
        ....|....|....|....|....|....|....|....|....|....|....|....|....|....|....|....|....|....|....|
TeGST   ---------------------MLKLYGGAKSR-ASIVRWYLEELGIPYEF---VLIDLQAGEQHQ------PEFLKLNPMGKVPVIVDGDVVLWESG-A
JPred   ----------------------EEE--------HHHHHHHHHH-----EE---EEE--------------HHHH--------EEEE---EEEHHHH-H

SeGST   ---------------------MLKLYGSARTR-ASLVAWYLEELGQPYES---VAVDMAAGEHRQ------PTFLSLNPFGKVPALVDDAFTLWESG-A
JPred   -----------------------EEE-------HHHHHHHHHH-----EE---EEE--------------HHHHH-------EEEE----EEHHHH-H

AtGST Z ---------------MANSGEEKLKLYSYWRSSCAHRVRIALALKGLDYEY---IPVNLLKGDQFD------SDFKKINPMGTVPALVDGDVVINDSF-A
JPred   ----------------------EEEEE------HHHHHHHHHH-----EE---EEE--------------HHHH--------EEEE----EEHHHH-H
1E6B    -----------------------EEEE-TT-HHHHHHHHHHHHTT---EE---EE--TTTTGGG-------HHHHHH-TT--SSEEEETTEEEESHH-H

                110       120       130       140       150       160       170       180       190       20C
        ....|....|....|....|....|....|....|....|....|....|....|....|....|....|....|....|....|....|....|
TeGST   ILLYLAQVHGE----LPKDAAAAAQVYQWVLFANSTLTQA-----------MFPAETRDRQ--LPPLLKGIE--------TALMGQS----YILGKDFS
JPred   HHHHHHHH-----------HHHHHHHHHHHHHHH----H------------HHHHHHHHHH--HHHHHHHHH--------HHH---------E----HH

SeGST   ILLYLAEKFG-----ELQTPQDRAIAAQWVLFANATLGPG-----------LFVEANRAKE--APRLLGSLN--------TLLSQRE----YLVSDRLS
JPred   HHHHHHHH-----------HHHHHHHHHHHHHHH-----------------HHHHHHHHH--HHHHHHHHH--------HHH---------E----HH

AtGST Z IIMYLDEKYPEPP-LLPRDLHKRAVNYQAMSIVLSGIQPHQN------LAVIRYIEEKINVEEKTAWVNNAITK-GFTALEKLLVNCAG--KHATGDEIY
JPred   HHHHHHHH----------HHHHHHHHHHHHHHHH---HHHH------HHHHHH-------HHHHHHHHHHHHH-HHHHHHHHHH-------EE----HH
1E6B    HHHHHHHHS-SS--SS-S-HHHHHHHHHHHHHHHHTT-----------------------------HHHHH-HHHHHHHHHTTS-S--SBTTBSS--

                210       220       230       240       250       260       270
        ....|....|....|....|....|....|....|....|....|....|....|....|....|....|..
TeGST   VADVALGSMLAYLQMLF-QVDLSPYPAVADYVARLQQ-RPAFQKGLMGARA-------------------------
JPred   HHHHHHHHHHHHHHHH---------HHHHHHHHHHH---HHHHHHHHH----------------------------

SeGST   VSDVAVGSYLAYVPMFFPDFDLSPYPAVQDYIRRLTQ-RPAYQQ-SIGRR--------------------------
JPred   HHHHHHHHHHHHHHHH---------HHHHHHHHHHH---HHHHH-HH-----------------------------

AtGST Z LADLFLAPQIHGAINRF-QINMEPYPTLAKCYESYNE-LPAFQNALPEKQPDAPSSTI------------------
JPred   HHHHHHHHHHHHHHHH--------HHHHHHHHHHHH--HHHHHHH-----------------------------
1E6B    HHHHHHHHHHHHHHHHH-----TT-HHHHHHHHHHTT--HHHHHHSGGGSTTS-----------------------
```

Figure 9: Secondary structure predictions with comparative crystal data for Zeta class GST. The results show the same secondary structure pattern as found in the cytosolic GSTs, indicating that cyanobacterial GSTs belong to this GST family.

(Source: Wiktelius & Stenberg, 2007)

Theta class GST is represented by dichloromethane (DCM) dehalogenase produced by facultative methylotrophic bacteria. Halogenated organic compounds are manufactured in large scale and are type of pollutants that cause environmental pollution. Apart from man-made, an abundance of haloorganic compounds was also produced naturally (Fetzner, 1998). DCM dehalogenase/Glutathione S-transferase is a GSH-dependent enzyme that allows bacteria to grow on DCM utilize carbon as an energy source. The dechlorination of dichloromethane (DCM) by facultative methylotrophic bacteria is catalysed by inducible glutathione S-transferase to form chloride and S-chloromethylglutathione. This unstable intermediate was hydrolysed to glutathione, chloride, and formaldehyde, which was a central metabolite of methylotrophic growth (Allocati *et al.*, 2008). Mammalian DCM dehalogenases were close relative of bacterial DCM dehalogenase (25% protein sequences identity) (Vuilleumier *et al.*, 2002). DNA polymerase I, an enzyme known for its DNA repairing activity, was required for the growth of Methylobacterium in DCM due to formation of DNA adducts (Kayser & Vuilleumier, 2001).

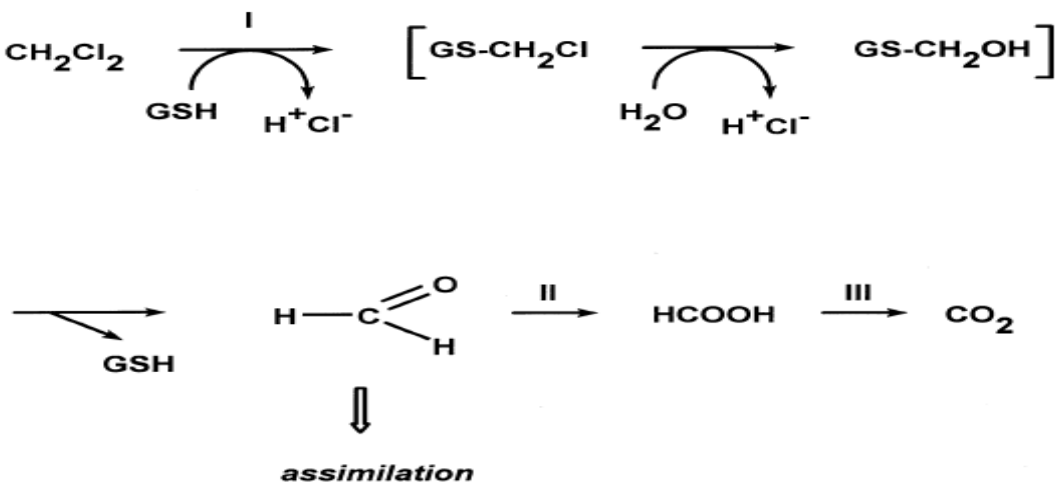


Figure 10: Metabolism of dichloromethane by methylotrophic bacteria. (I) Dichloromethane dehalogenase; (II) formaldehyde dehydrogenase; (III) formate dehydrogenase.

(Source: Allocate *et al.*, 2008)

There were two type of DCM dehalogenases - group A dehalogenases, which yielded low catalytic activity and upon induction by DCM constitute, there are about 20% and 50% of total suspended protein for batch and chemostat cultures respectively while group B dehalogenases, which were almost six times more active than group A dehalogenases and reached significantly lower percentage of total suspended protein, only 9% and 20% for batch and chemostat cultures respectively (Emanuelsson & Osuna, 2009). Bacterial dehalogenase show numbers of distinct feature compared to other GSTs. First, glutathione conjugates generated in the initial stage of degradation are unstable and subsequently hydrolysed to glutathione, formaldehyde and hydrochloric acid. Second, the substrate range of DCM dehalogenases are essentially restricted to halomethanes and typical model GST substrates such as chlorinated compounds, peroxides or epoxides are not turned over by these enzymes. Lastly, DCM dehalogenases do not retain on glutathione-derivative chromatography support used in affinity purification of GST enzymes (Vuilleumier *et al.*, 1997a). Dehalogenases from *Hyphomicrobium* sp. strain DM2 and *Methylobacterium dichloromethanicum* DM4 belong to type A dehalogenase while *Methylophilus* sp. strain DM11 belong to type B dehalogenase. Two forms of DCM dehalogenases derived from *M. dichloromethanicum* DM4 and *Methylophilus* sp. strain DM11 had 56% sequence identity and well-characterized (Copley, 1998). The DM2 and DM4 enzymes are significant different in affinity towards glutathione due to the glutathione binding residue at position 27. DM11 has higher affinity towards glutathione but low affinity towards DCM due to the nature of residue at position 18. The N-terminal amino acid sequence of DM11 dehalogenase are determined and compared with the sequence of the DM 2 and DM4 enzymes. There were no direct homology was observed between the N termini, with the exception of the histidine residue in position 9; the amino acid pair L-R was observed in both sequences (positions 4 and 5 in DM 11 and 14 and 15 in DM 4) (Scholtz *et al.*, 1988).

| | |
|---|---|
| Position: | 1 5 10 15 |
| DM11: | ?-T-K-L-R-Y-L-H-H-P-A-S-Q-P-P |
| DM2 and DM4: | M-S-P-N-P-T-N-I-H-T-G-K-T-L-R |

Figure 11: N-terminal amino acid sequences of strain DM ll and strain DM 2 and strain DM 4.

(Source: Scholtz *et al.*, 1988)

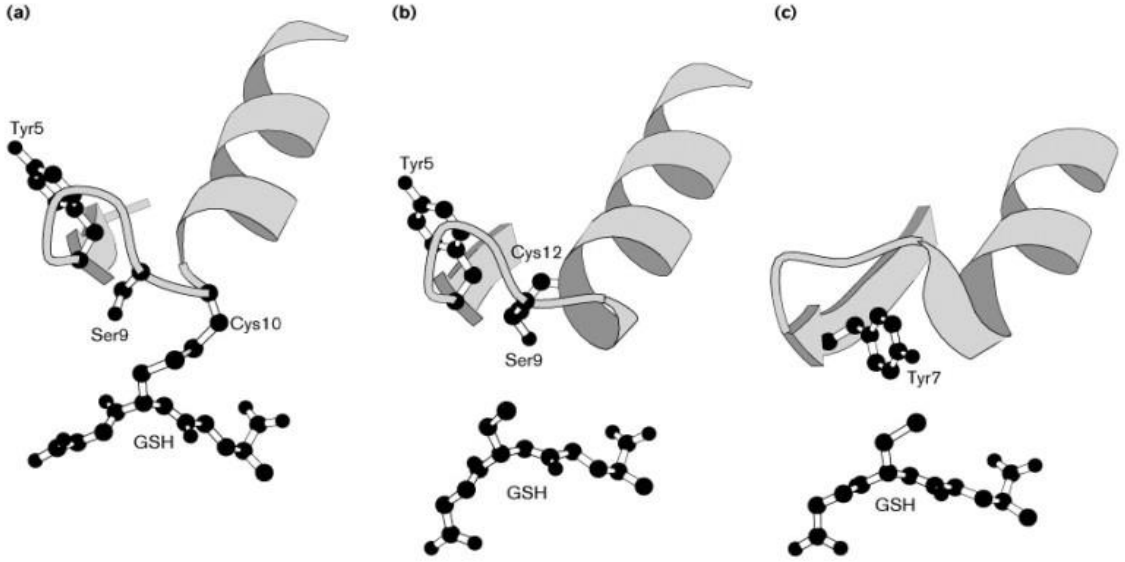


Figure 12: A) Bacterial Theta class GST B) Insect Theta class GST C) Human Pi class GST.

(Source: Rossjohn *et al.*, 1998)

Zeta class GST (GSTZ) is a novel class of GST discovered recently and there is a poor understanding about GSTZ. Zeta class unlike other classes of GST because of its poor conjugating activity towards standard GST substrates. Zeta class is more known for its isomerase and dehalogenase activities. MAAI from *Aspergillus nidulans*, GSTZ1 from *Homo sapiens* and AtGSTZ1 from *Arabidopsis thaliana* catalyse GSH-dependent isomerization of maleylacetoacetate to fumarylacetoacetate in the homogentisate pathway. On the other hands, NagL from the prokaryotic *Ralstonia* sp. strain U2 converted maleylpyruvate to fumarylpyruvate in the gentisate pathway (Fang *et al.*, 2011).

The glutathione-dependent isomerization of maleylacetoacetate by GSTZ/ maleylacetoacetate isomerase (MAAI) was imperative in catabolism of phenylalanine and tyrosine to fumarate and acetoacetate (Board *et al.*, 2005). In human, deficiency of GSTZ/ MAAI will cause severe illnesses such as hereditary tyrosinemia type 1 (HT-1).

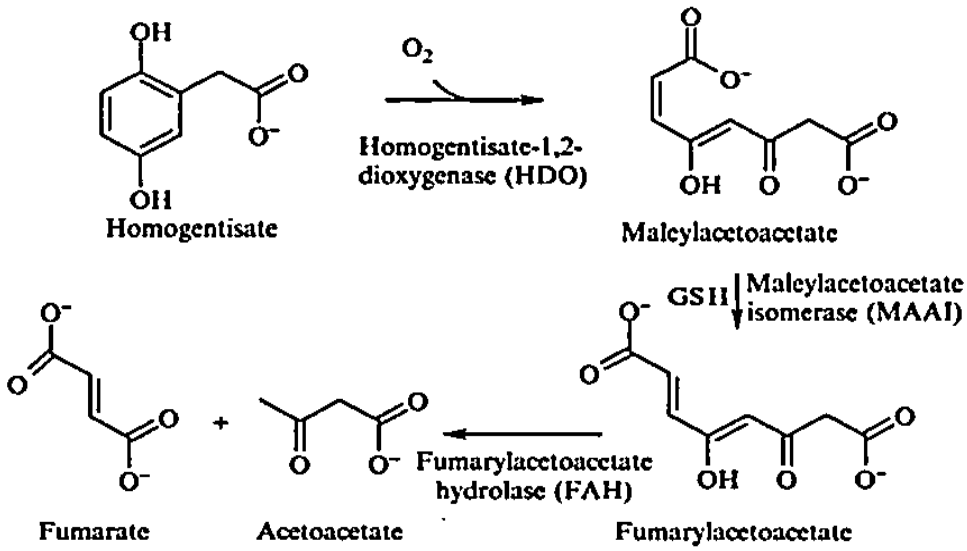


Figure 13: The conversion pathway from maleyacetoacetate to fumarylacetoacetate (Source: Edwards & Cixon, 2005).

Maleyl pyruvate isomerase (MPI), a bacterial GST, was derived from the naphthalene via gentisate degradation pathway that enabled the *Ralstonia* sp. to use polyaromatic hydrocarbons as a sole carbon source (Marsh *et al.,* 2008). In details, MPI and NagL from the prokaryotic *Ralstonia* sp. strain U2 involved in the conversion of maleylpyruvate to fumarylpyruvate in the gentisate pathway, (Fang *et al.,* 2011).

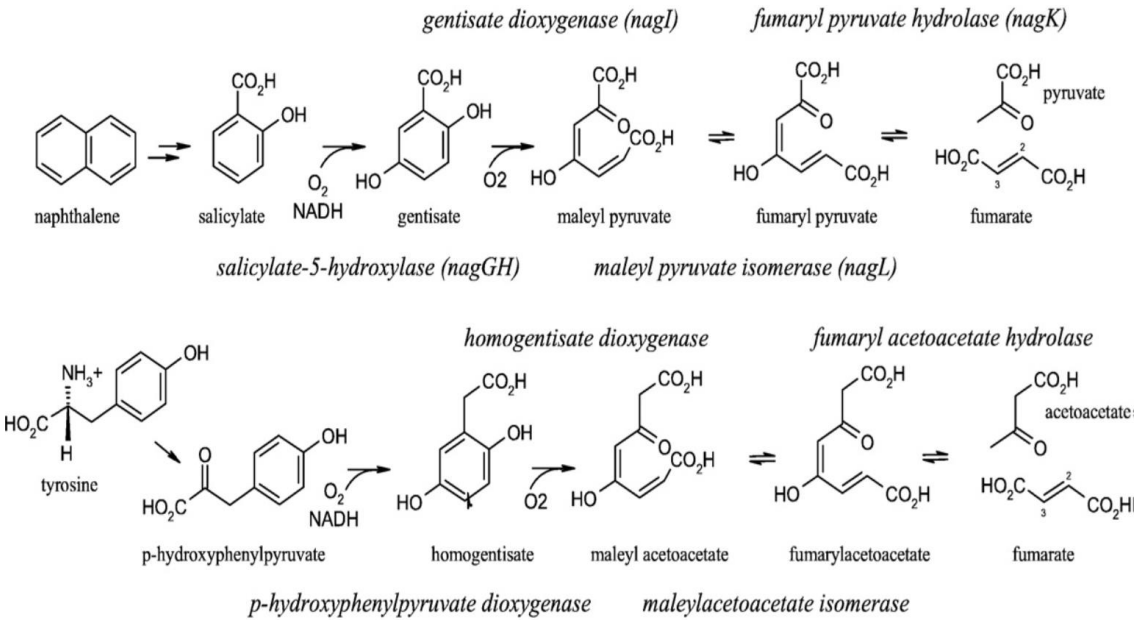


Figure 14: The pathways for catabolism of naphthalene via gentisate and tyrosine via homogentisate.

(Source: Marsh *et al.,* 2008).

Unlike many other GSTs, the reaction catalysed by MPI was an isomerisation of an aromatic ring breakdown product, and glutathione was a true cofactor rather than a substrate in the reaction (Marsh *et al.,* 2008). There are 40 % sequence similarity between MPI and MAAI in which both of the enzymes involve in the catabolism of phenylalanine and tyrosine. The fold of MPI enzyme was similar to the other zeta class members where the N-terminal domain was comprised of four-stranded β-sheet flanked on the outside by two short α-helices and on the inside by two longer α-helices, and was connected to the C-terminal domain by a linker region (Marsh *et al.,* 2008). Asp102 (previously mistaken for Glu102) and Gln64 in the G-site had been shown in the crystal structure to directly

interact with the α-amino group of the glutamyl moiety of glutathione (Fang *et al.*, 2011). Mutation in Gln64 residue produces an inactive enzyme. This proved that Gln64 play a critical role in conjugation with GSH. The mutation of the fully conserved Arg176 residue in GSTZ to alanine resulted in an 8-fold decrease in catalytic efficiency and a decrease in substrate affinity (Fang *et al.*, 2011). Arg176 has been proven to play a crucial role in orientating the substrates.

According to Anandarajah *et al.* (2000), Tetrachlorohydroquinone (TCHQ) dehalogenase belonged to the zeta class GST on the basis of multiple sequence alignments. This enzyme was characterized, in the GSH site, by the distinctive motif of zeta class enzymes including two serine and a cysteine residues (Allocati *et al.*, 2008). TCHQ dehalogenase was found in *Sphingomonas chlorophenolica* RA-2, a soil microorganism that could grow on pentachlorophenol (PCP) as a sole carbon source (McCarthy *et al.*, 1997). PCP is an organochlorine compound that widely used as pesticide and wood preservative. PCP can cause a harmful effect on kidney, lung, blood, nervous system and immune system on short term exposure.

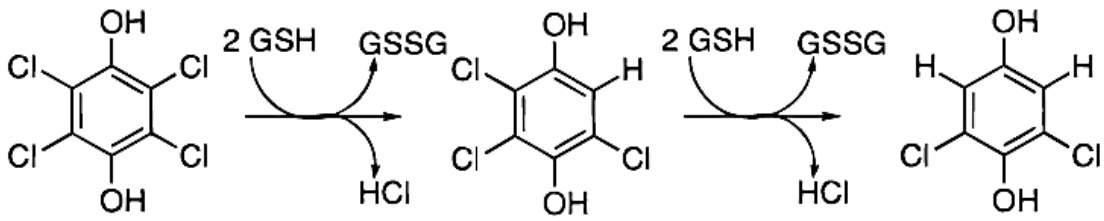


Figure 15: Pathway for degradation of PCP to 2,4-dichloro-3-hydroxy-cis,cis-muconic semialdehyde (DCHMS) in *S. chlorophenolica* RA-2.

(Source: McCarthy *et al.*, 1996)

Biodegradation of PCP starts with removal of halogen substituents from the aromatic rings. TCHQ dehalogenase utilizes two GSH molecules to reductively dechlorinate TCHQ to trichlorohydroquinone and then dichlorohydroquinone. Removal of halogen substituents can be replaced by either hydroxyl group or hydrogen atom. The intermediates produced indicating another problem arises due to the toxicity of the intermediates. Both TCHQ and DCHQ had been shown to cause single-stranded breaks in DNA, predominantly through the formation of reactive oxygen species (McCarthy *et al.,* 1997).

TCHQ dehalogenase appeared to be related maleylacetoacetate (MAA) isomerase catalysed the glutathione-dependent conversion of a cis double bond in MAA to the trans configuration during the catabolism of phenylalanine and tyrosine in mammals and some bacteria and fungi (Anandarajah *et al.,* 2000). Although the overall sequence identity between TCHQ dehalogenase and MAA isomerase was low, the active site was highly conserved and the catalytic site contained a cysteine residue (Allocati *et al.,* 2008). Another interesting finding revealed that TCHQ dehalogenase contained neither metal ion nor organic cofactors that ruled out mechanisms involving indirect transferred of reducing equivalents between TCHQ and GSH. This suggested that the reducing electrons must be transferred by some type of covalent interaction with either glutathione or an enzymes thiol (McCarthy *et al.,* 1996). Recently, GSTZ was found to metabolize dichloroacetic acid and other α-halo acids, including dichloroacetic acid (Tong *et al.,* 1998).

2.1.3.2 Mitochondrial GSTs

The mitochondrial GSTs are known as kappa class of GST identified from mammals such as human and rat. Kappa GST was a 26.5 kDa protein that was initially isolated from the rat liver mitochondrial matrix and classified as a theta GST (Harris *et al.,* 1991). The determination of the three-dimensional structure of the kappa GST from rat (rGSTK1-1) conjugated with glutathione (GSH) showed a different folding topology from that of the other GST classes (Petit *et al.,* 2009). There was an evidence showed that this sequence lacked of the SNAIL/TRAIL motif found in all other GST classes (Pemble *et al.,* 1996). According to Robinson *et al.* (2004), sequence analyses, homology modelling and secondary structure predictions showed that human GSTK1 was closely resemble to bacterial HCCA (2-hydroxychromene-2 carboxylate) isomerases and a predicted C-terminal domain structure that was almost identical to that of bacterial disulphide-bond forming DsbA oxidoreductase. Although kappa class GST showed an activity towards aryl halides, such as 1-chloro-2,4-dinitrobenzene, and could reduce cumene hydroperoxide and (S)-15-hydroperoxy-5,8,11,13-eicosatetraenoic acid, this activity remained quite low when compared with that of other soluble GSTs (Petit *et al.,* 2009).

The mitochondria was an important cellular site where reactive oxygen species (ROS) were produced during respiration-coupled oxidative metabolism (Raza *et al.,* 2002). Kappa class GST was reported participating in energetic and lipid metabolism in the mitochondria (Sun *et al.,* 2012). It was proven that GSH content inside mitochondrial was pulled from cytoplasm. Mitochondrial GSH conjugates with ROS to GST in order to minimize the oxidative stress. The process of kappa class GST targeting mitochondria was unclear, it had been reported to associate with the Hsp60 chaperone (Robinson, *et al.,* 2004). hGSTK1 had identified as a key regulator for the multimerization of adiponectin,

which was an adipocyte-derived hormone, in both human and rodent (Liu *et al.,* 2008). Kappa class GST might possess a glutathione-independent reaction in adipose tissue.

There were some evidences proved that Kappa GST showed most similarity with HCCA isomerase. Firstly, both enzymes were predicted to form a mixed protein of four strands and ten (hGSTK1) or nine (HCCA isomerase) helices in aβαβαxββα motif with essentially identical C-terminal domains. Secondly, both enzymes required much higher concentrations of glutathione for maximal activity. Thirdly, both enzymes showed a pH optimum of ~9 (Robinson *et al.,* 2004).

2.1.3.4 Microsomal GSTs

Microsomal GSTs also known as membrane-associated proteins in eicosanoid and glutathione metabolism (MAPEG). Members of MAPEG family are grouped according to enzymatic activities, sequence motifs, and structural properties. The family consisted of six human proteins including 5-lipoxygenase-activating protein (FLAP), leukotriene $C_4$ ($LTC_4$) synthase, microsomal glutathione S-transferase 1 (MGST1), MGST2, MGST3, and MGST1-like 1 (MGST1-L1) (Jakobsson *et al.,* 2000). Recently, crystallographic studies on different MAPEG members clearly demonstrated that they were arranged into trimmers (Molina *et al.,* 2008). MAPEG members were identified in several bacteria such as *E. coli*, *Vibrio cholerae* and *Synechocystis* sp. (Allocati *et al.,* 2008). MAPEG family can be subdivided into four subgroups. The first subfamily consists of the members FLAP, $LTC_4$ synthase, and MGST2 and the second subfamily consists of MGST3 together with the members found in plants and fungi. The third and fourth subfamilies were composed of the proteins identified in bacteria (*E. coli* and *V. cholerae*) and MGST1 and MGST1-L1, respectively (Jakobsson *et al.,* 2000). MAPEG family members were currently known

to involve in the protection against oxidative stress, xenobiotic detoxification, and the production of arachidonic acid-derived mediators (Molina *et al.*, 2008).

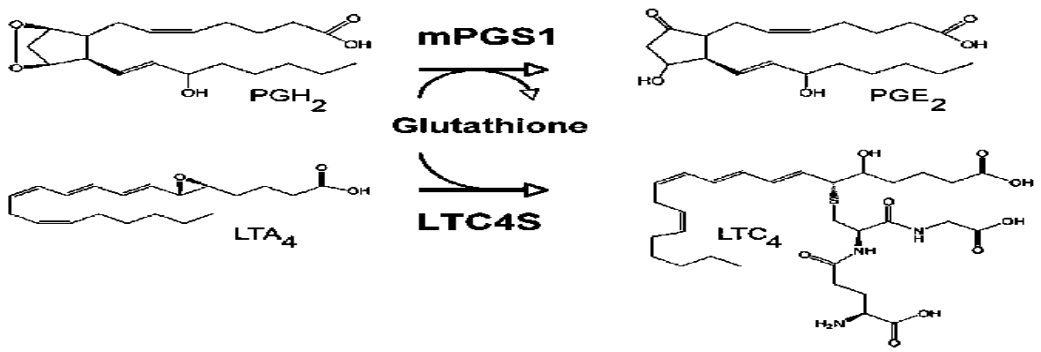


Figure 16: The glutathione-dependent peroxidase reaction catalysed by microsomal prostaglandin E synthase-1 (mPGES-1) and the glutathione conjugation reaction catalysed by LTC4S.

(Source: Molina *et al.*, 2008)

Microsomal glutathione S-transferase 1 (MGST1) isolated from the rat liver had a molecular weight of 14 kDa and a very restricted substrate specificity compared to the wider range of substrates which could be conjugated with glutathione by the cytosolic GSTs (Morgenstern & De Pierre, 1983). Among the many substrates for this enzyme were 1-chloro-2,4-dinitrobenzene (CDNB) and various polyhalogenated unsaturated hydrocarbons (Jakobsson *et al.*, 2000). MGST1 also catalysed a glutathione-dependent reduction of organic hydroperoxides, fatty acid hydroperoxides and phospholipid hyroperoxides (Morgenstern & De Pierre, 1983). Hydroperoxidase activity is detrimental against lipid peroxidation during oxidative stress. MGST1 was activated after covalent modification by reactive electrophiles such as N-ethylmaleimide (NEM)), oxidative stress and NADPH generating system (Rinaldi *et al.*, 2004).

Both MGST2 and MGST3 were reported to catalyse the glutathione-dependent reduction of 5-hydroperoxyeicosatetraenoic acid (5-HPETE) to 5-hydroxyeicosatetraenoic acid (Jakobsson *et al.,* 1997). MGST2 uses 1-chloro-2,4-dinitrobenzene (CDNB) as a common GST substrate while MGST3 do not conjugate with CDNB. These enzymes clearly catalysed both glutathione S-transferase and glutathione peroxide activities (Jakobsson *et al.,* 2000). Detoxification properties of both MGST2 and MGST3 may protect against harmful metabolites under oxidative stress.

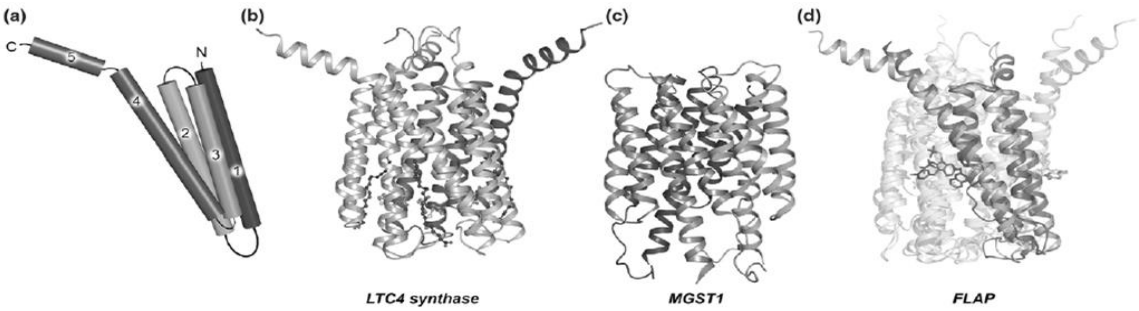

Figure 17: Side view ribbon representation of the currently available structures from MAPEG family. (Source: Molina *et al.,* 2008)

2.1.3.5 Bacterial fosfomycin-resistance proteins

The last family of GST is the bacterial fosfomycin-resistance proteins that only exists in bacteria. Fosfomycin ([1R,2S]-[1,2-epoxypropyl]-phosphonic acid) was a bactericidal broad-spectrum antibiotic effective against both Gram-negative and Gram-positive bacteria (Allocati *et al.,* 2008). Fosfomycin inhibits the UDP-NAG enolpyruvyl transferase enzyme which blocks the transferring of enolpyruvate from phosphoenolpyruvate to uridine diphospho-N-acetylglucosamine. Inhibition of synthesis of peptidoglycan will diminish the bacterial cell wall synthesis. Resistant to fosfomycin was exerted by three mechanisms. The first mechanism was to decrease the uptake of L-α-glycerophosphate or glucose-6-phosphate. Second mechanism involved mutation or

overexpression of UDP-N-acetylglucosamine enolypyruvyl transferase which could differentiate phosphoenolpyruvate acid and fosfomycin (Venkateswaran & Wu, 1972). Third mechanism increased the translation of a plasmid-encoded resistant to fosfomycin protein was exerted by a gene located in transposon (Arca *et al.,* 1990.). Plasmid-encoded genes encoded a 140 amino acids polypeptide with GST activity (Vuilleumier, 1997).

GST catalysed the formation of an adduct between fosfomycin and glutathione in which a formation of covalent bond between the sulfhydryl residue of the cysteine in glutathione and the C-1 of fosfomycin resulted in opening of the epoxide ring of the fosfomycin (Arca *et al.,* 1988).

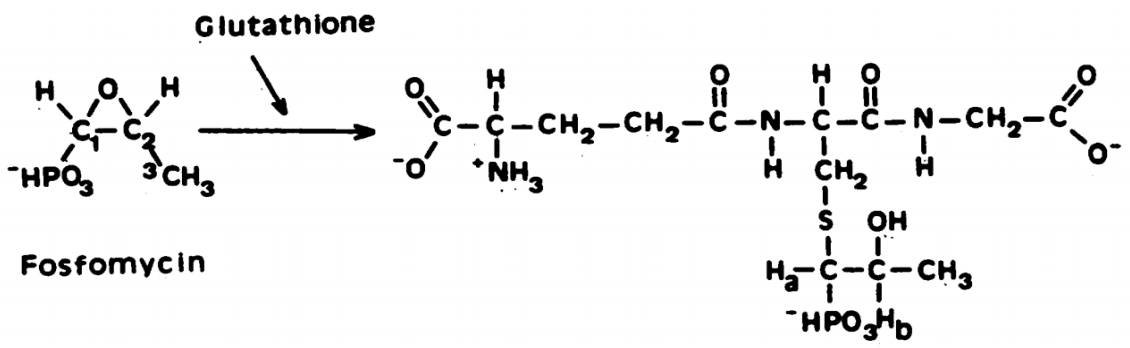


Figure 18: Proposed reaction of modification of fosfomycin.

(Source: Arca *et al.,* 1988)

FosA, FosB and FosX represented three mechanistically distinct classes of enzyme that conferring resistant to fosfomycin by adding GSH, l-cysteine or a hydroxyl group, respectively, to the oxirane ring of the antibiotic, and inactivating it (Allocati *et al.,* 2008).

FosA was first identified from *Serratia marcescens* isolated from hospitalized patients and its ability to transfer antibiotic resistance to *E. coli* by conjugation was examined (Mendoza *et al.,* 1980). FosA was purified and characterized. FosA do not bind to GSH affinity matrix and there is no conjugation between FosA and CDNB are observed.

FosA was a homodimer made up of 16kDa subunits and its maximal activity was dependent on the addition of the $Mn^{2+}$ cation (Arca *et al.,* 1990). Each subunit from the homodimer contained a mononuclear $Mn^{2+}$ centre that interacting strongly with fosfomycin and this enzyme required a monovalent cation $K^{+}$ for optimal catalytic activity (Bernat *et al.,* 1997). 3D structure of FosA showed similarity to members of vicinal oxygen chelate superfamily and consisted of paired βαβββ motifs that formed a cupped-shaped cavity in the metal ion-binding site (Allocati *et al.,* 2008).

FosB was originally identified in fosfomycin-resistant *Staphylococcus* strains and the expressing gene located in plasmids (Allocati *et al.,* 2008). FosB was detected in *Bacillus subtilis* and encoded by *Bacillus subtilis* fosfomycin-resistant gene. FosB was a metallothiol transferase related to the FosA class of $Mn^{2+}$-dependent glutathione transferase but with a preference for $Mg^{2+}$ and L-cysteine as cofactors (Bryan *et al.,* 2001). *B. subtilis* was a typical Gram-positive bacteria lacking of glutathione while L-Cysteine and coenzyme A sulfhydryl (CoASH) were two abundant thiols in gram-positive bacteria (Fahey *et al.,* 1978).

FosX was activated by divalent cation Mn(II) and did not require a monovalent cation for optimal activity (Fillgrove *et al.,* 2003). It was found in several microorganisms and it had been well characterized in *Mesorhizobium loti* and *Listeria monocytogenes* (Allocati *et al.,* 2008). FosX from *L. monocytogenes* is more effective against fosfomycin compared with FosX from *M. loti.* The structure of FosX from *L. monocytogenes* and FosX from *M. loti* closely resemble to each other.

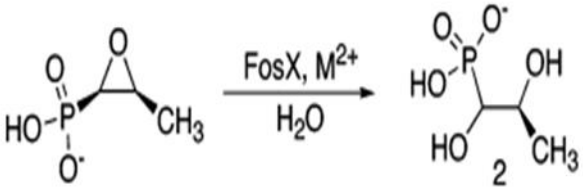


Figure 19: Mechanism of reaction of FosX.

(Fillgrove *et al.*, 2003)

FosC was a newly discovered fosfomycin-resistance protein from *Pseudomonas syringae.* FosC gene encoded a 19kDa protein and displayed sequence similarities to GSTs (Garcia *et al.,* 1995). ATP is a core co-substrate for FosC in inactivation of fosfomycin and could be reversed by alkaline phosphatase. To date, no relationship between FosC and the other fosfomycin resistance proteins were known (Allocati *et al.,* 2008).

2.1.4 Potential application of GSTs

Bacteria are widely distributed in nature from extreme to moderate environment and even the places once we thought cannot support life. Bacteria survive in extreme environments such as in extreme heat or in extreme cold and even under radioactive exposure. This microscopic size bacteria can survive and propagate under these hazardous and toxic compounds contaminated environment, in other way, they can use this compounds as building blocks or energy sources to support life. Families of bacteria GST have played an undeniable role in the survival and endurance of bacteria. Some GSTs, such as the bacterial DCMD, lignin b-etherase, and reductive dehalogenase enzymes which had already been well-characterized, catalysed reactions that yielded products which could be useful for bacteria growth (Vuilleumier, 1997). Another type of GSTs can

conjugate with xenobiotic in the presence of GSH and reduce the toxicity of the xenobiotic for bacteria survival.

Such promising results conclude that bacterial GSTs have high potential applications in different fields. The first application described was the use of GSTs in detoxification of chemical compounds from bacteria (Vuilleumier, 1997). Bacterial GSTs have shown a very promising result in degradation of xenobiotics which were once considered non-degradable. For example, the Beta class of GST from *P. mirabilis* can degrade DCM and use it as a carbon source where DCM was once considered un-degradable. Hence, in the field of bioremediation, the detoxification property of GSTs were used to clean up the environmentally contaminated site (Allocati *et al.,* 2008). Another potential application is the use of GSTs as biosensors. Biosensors function as a detection system to detect contaminated environment, and this method is inexpensive, easy to handle and has high sensitivity. GSTs also play a vital role in medical field. For instance, cytosolic GSTs are used to diagnosis and monitor the course of cancer. For example: GSTP1-1 levels will increase in patients with gastric cancer.

# 3.0 Materials

## 3.1 Apparatuses

CM Sepharose fast flow column (GE Healthcare)

DEAE Sepharose fast flow column (GE Healthcare)

Filter paper (Advantec)

Fume hood

IEF gels (Invitrogen)

Incubator (RS Biotech)

Isoelectric focusing (IEF) apparatuses (Invitrogen)

Laminar hood (Sastec)

Loop

Magnetic stirrer (Heidolph)

Methacrylate cuvette (Fisher Scientific)

Mono P™ 5/200GL column (GE Healthcare)

Multipipettor (Eppendorf)

pI 3-10 IPG strips (GE Healthcare)

Polyvinylidene fluoride (PVDF) membrane (Bio-rad)

Protein concentrator (Invitrogen)

Silica gel (Merck)

Sodium dodecyl sulphate-polyacrylamide gel electrophoresis (SDS-PAGE) apparatuses (Bio-rad)

Tricorn™ 5/20 column (GE Healthcare)

Western blotting apparatuses (Bio-rad)

## 3.2 Equipments

-20 ºC freezer (Denka)

-40 ºC freezer (Medfrez)

4 ºC refrigerator (Protech)

4800 Plus Proteomics Analyzer (ABI)

80 Ti ultracentrifuge machine (Benchmark)

Agar plates (Thermo Fisher Scientific)

Akta purifier (GE Healthcare)

C1000™ thermal cycler (Bio-rad)

Centrifuge machine (Eppendorf)

Freeze dryer (Labconco)

JA 7.5 centrifuge machine (Benchmark)

Laboratory digital weigh scale (METTLER TOLEDO)

Microwave oven (Pensonic)

Mili Q ultrapure water purification system (Milipore)

Multiphor II electrophoresis system (GE Healthcare)

Orbital shaker (Protech)

pH meter (METTLER TOLEDO)

494 Procise Protein Sequencing System (Applied Biosystems)

Sonicator (Powersonic 603)

Spectrophotometer (Jasco)

Thermal cell mixing block (Bioer)

Visible light gel viewer (HS)

Vortex mixer (Labnet)

Water bath (Memmert)

Water bath incubator (Wisebath)

Water distiller (Favorit)

3730xl DNA analyser (Applied Biosystems)

## 3.2 Chemicals

30 % Acrylamide/Bis (Bio-rad)

1-Chloro-2,4-dinitrobenzene (Sigma-aldrich)

2,4-heptadineal (Sigma-aldrich)

0.5 M Tris HCl, pH 6.8 (Bio-rad)

1.5 M Tris HCl, pH 8.8 (Bio-rad)

M13/pUC sequencing primer (Thermo Scientific)

Acetic acid (Systerm)

Acetone (System)

Acetonitrile (Systerm)

Acetylacetone (Systerm)

Agarose (Promega)

Ammonium acetate (Sigma-aldrich)

Ammonium bicarbonate (Sigma-aldrich)

Ammonium persulphate (APS) (Systerm)

BenchMark$^{TM}$ protein standard (Invitrogen)

Beta-mercaptoethanol (Merck)

BigDye Terminator cycle sequencing kit (Applied Biosystems)

Bis Tris (Sigma-aldrich)

Bromophenol blue (Bio-rad)

Bromophos (Sigma-aldrich)

Butan-ol (Systerm)

Carrier ampholytes (Invitrogen)

Colloidal coomasie blue CBB G-250 (Sigma-aldrich)

CHAPS (Invitrogen)

Chlorpyrifos (Sigma-aldrich)

Clodinafop-propargyl (Sigma-aldrich)

Coomasie brilliant blue R-250 (Sigma-aldrich)

Cumene hydroperoxide (Sigma-aldrich)

deoxyribonucleoside triphosphates (Promega)

Dichlorodiphenyltrichloroethane (DDT) (Sigma-aldrich)

Dichloromethane (DCM) (Sigma-aldrich)

Distilled water

Ethacrynic acid (EA) (Sigma-aldrich)

Ethanol (Systerm)

Ethylenediaminetetraacetic acid (EDTA) (Sigma-aldrich)

Fenitrothion (Sigma-aldrich),

Fenoxapop-ethyl (Sigma-aldrich)

Formaldehyde (Systerm)

Glutathione reductase (Sigma-aldrich)

Glycerol (Systerm)

Glycine (Bio-rad)

GSH (Sigma-aldrich)

GSH-agarose (Sigma-aldrich)

Hexadienal (Sigma-aldrich)

Hydrogen peroxide (Sigma-aldrich)

Iodoacetamide (Merck)

Isoproturon (Sigma-aldrich)

Lysozyme (Sigma-aldrich)

Magnesium chloride (Sigma-aldrich)

Malathione (Sigma-aldrich)

Methanol (Systerm)

Mili Q water

Monochlorobimane (MCB) (Sigma-aldrich)

Nicotinamide adenine dinucleotide phosphate (NADPH) (Sigma-aldrich)

Ninhydrin (Sigma-aldrich)

Nutrient agar (Oxoid)

Nutrient broth (Oxoid)

Permethin (Sigma-aldrich)

Phenylmethylsulfonyl fluoride (PMSF) (Sigma-aldrich)

Phenylthiourea (Sigma-aldrich)

p-nitrobenzyl chloride (NBC) (Sigma-aldrich)

Polybuffer 74 (GE Healthcare)

Potassium chloride (Sigma-aldrich)

Propoxur (Sigma-aldrich)

PureLink® PCR Purification Kit (Invitrogen)

SERVA$^{TM}$ IEF marker (Invitrogen)

Sodium carbonate (Systerm)

Sodium chloride (NaCl) (Systerm)

Sodium dihydrogen phosphate (Systerm)

Sodium Dodecyl Sulphate (SDS) (Sigma-aldrich)

Sodium Thiosulphate (Systerm)

Solution A (1$^{st}$ Base)

Solution B (1st Base)

Silver nitrate (Systerm)

Sterilized glycerol (Systerm)

Sulfobromophthalein (BSP) (Sigma-aldrich)

Taq DNA polymerase (Promega)

Tetramethylethylenediamine (TEMED) (Bio-rad)

Thiourea (Sigma-aldrich)

Trans-4-phenyl-3-butene-2-one (PBO) (Sigma-aldrich)

Trans-2-octenal (Sigma-aldrich),

Tris (Bio-rad)

Tris-buffer (Promega)

Trifluoroacetic acid (Merck)

Trypsin (Sigma-aldrich)

Urea (Invitrogen)

# 4.0 Methodology

4.1.1 Bacteria isolation

Soil was first collected from a chemical dump site located beside Block E, Faculty of Science, University of Malaya in july, 2011 (GPS coordinate: 3.122155, 101.6555788). A total of 1 g of soil was placed in a sterilized vial containing 10 ml of distilled water. The vial was shaken vigorously and left to stand overnight (18 hours) at 37 ºC in a water bath. The next day, loopfuls of the soil culture were streaked across the surface of nutrient agar plates which were then incubated at 37 ºC for 18 hours. Single colonies were picked randomly and spread on a new nutrient agar and repeated for three times to purify the isolates. The next day, single colonies were picked and grown on new nutrient agar plates. Ten bacteria isolates were purified from the soil and incubated for 18 hours at 37 ºC respectively in order to allow the bacteria cells to grow well for the following steps.

4.1.2 Screening for GSTs

Ten bacteria isolates were screened for production of GSTs by using monochlorobimane (MCB) (Eklund *et al*., 2002). MCB was first dissolved in acetonitrile at a concentration of 1 mg/ml (40 mM). The reagent was then sprayed from a distance of about ten centimetres over each nutrient agar plate containing bacteria colonies. For GST-producing bacteria isolate, fluorescence colonies could be seen under 365 nm UV light. Three bacteria isolates were discovered to be able to produce fluorescence under 365 nm UV light.

These three bacterial isolates were subjected to 1-chloro-2,4-dinitrobenzene (CDNB) activity assay in order to detect the bacteria isolate with the most promising GST activity. A single colony was picked and cultured in a flask containing 100 mL of sterilized nutrient broth for 18 hours at 37 ºC. Bacteria culture was pelleted at 5000 rpm

for 20 minutes in 4 ºC and suspended in 1 mL of 25 mM sodium phosphate buffer (pH 7.4). Suspended cells were sonicated for 10 minutes in 4 ºC by using sonicator and centrifuged at 45000 rpm for 30 minutes in 4 ºC. Supernatant was collected and used for subsequent screening protocol. Screening for GST activity was described in section 4.1.9

4.1.3 Bacteria identification

The bacteria isolate with the highest GST activity was identified from its 16S rRNA gene sequence. A single colony was touched with a sterile 10 µl-pipette tip and dipped into a tube containing 100 µl of solution A (1$^{st}$ Base). The mixture was vortexed and incubated at 95 ºC for 10 minutes in a water bath. After the heat treatment, 100 µl of solution B (1$^{st}$ Base) was added to the sample in tube A and mixed. The mixture was centrifuged for 5 minutes at 8000×g and the supernatant containing genomic DNA proceeded to PCR amplification. For PCR amplification, M13/pUC sequencing primer (5' GTAAAACGACGGCCAGGT 3') and a reverse primer (5' AAACAGCTATGACGGGTTG 3') was used to amplify enough amplicons for further sequencing. PCR was performed with 5 µl (3 ng) of template DNA in a total reaction volume of 50 µl consisting of 10 mM Tris-HCl (pH 8.8), 50 mM potassium chloride, 1.5 mM magnesium chloride, 0.8 mM deoxyribonucleoside triphosphates (0.2 mM each), 1 M (each) primer, 1 U of Taq DNA polymerase, and 50 µl of a mineral oil overlay. The PCR program consisted of an initial denaturation at 94°C for 2 min, followed by 35 cycles of denaturation (94°C for 1 min), annealing (62°C for 1 min), and extension (72°C for 1 min), with a final extension step at 72°C for 7 min. A C1000$^{TM}$ thermal cycler was used for PCR. Aliquot of PCR products were electrophoretically separated in 2.5% (w/v) agarose gels. Fifteen ng PCR products were cleaned up using PureLink® PCR Purification Kit and sequenced on C1000$^{TM}$ thermal cycler with a BigDye Terminator cycle sequencing kit. The cycle sequencing profile consisted of a 96°C denaturation step

for 10 s followed by an anneal/extension step starting at 65°C and decreasing 1°C every six cycles until a touchdown temperature of 55°C was reached, for a total of 66 cycles. Ethanol/ethylenediaminetetraacetic acid (EDTA) precipitation method was applied to clean up unincorporated dye terminators. Sequences were determined by electrophoresis with 3730xl DNA analyser and analysed using ABI PRISM® DNA Sequencing Analysis Software. 16S rRNA species barcoding was carried out by a service-provider, 1st base laboratories Sdn. Bhd.

### 4.1.4 Extraction of proteins from cells

A single colony was picked and grown in nutrient broth (Oxoid) for 18 hours at 37 ºC. On the next day, 5 mL of the broth was pipetted into a flask containing 200 mL of nutrient broth. A total of 20 flasks were inoculated to generate 4 L cell culture. Bacterial culture was allowed to grow for 18 hours at 37 ºC inside the incubator again. The next day, 4 L of bacterial culture was combined and pelleted by centrifugation at 5000 rpm for 20 minutes in 4 ºC. Cell pellet was then suspended in 5 mL of 25 mM of sodium phosphate buffer (pH 7.4) containing 1 mM EDTA, 0.1 mM dichlorodiphenyltrichloroethane (DDT), 0.1 mM phenylthiourea (PTU) and 0.1 mM phenylmethylsulfonyl fluoride (PMSF) (Favaloro *et al.*, 1998). Suspended cells were disrupted by sonication and centrifuged at 45000 rpm for 30 minutes in 4 ºC. The supernatant was collected and proceeded to GSTs purification step on the same day to retain maximal GST activity.

### 4.1.5 Purification of putative GSTs by using affinity chromatography

Tricorn™ 5/20 column was first packed with GSH-agarose matrix. The GSH-agarose column was then connected to AKTA Purifier™ and equilibrated with eluting buffer (25 mM sodium phosphate buffer, pH 7.4) for five times column volume before applying the supernatant into the column. The column was exhaustively washed with

eluting buffer to prevent any protein contamination. The enzymes were eventually eluted with eluting buffer containing 10 mM of GSH and stored in -20 ºC.

4.1.6 Putative GST isozymes separation by using ion exchange chromatography and chromatofocusing

At the beginning, GSH-agarose column was packed as described above and connected to AKTA Purifier$^{TM}$. The column was pre-equilibrated with buffer A (25 mM sodium phosphate buffer, pH 6) before applying the supernatant and washed with five times column volume of buffer A after applying supernatant to prevent proteins contamination. The column was then connected to carboxylmethyl (CM) or diethylaminoethyl (DEAE) Sepharose fast flow column and equilibrated the column with buffer A again. The enzymes were eluted with buffer A containing 10 mM of GSH in pH 6 and only the "flow-through" was collected.

Mono P$^{TM}$ 5/200GL column was connected to AKTA Purifier$^{TM}$ and equilibrated with buffer B (0.03 M bis Tris, pH 7.1) until the column was at the same pH as buffer B. Elution buffer C (polybuffer 74, pH 4) was injected into the column. Once a pre-gradient volume was eluted before the pH gradient begins (3 ml), fraction with enzymatic activity from affinity chromatography was applied into the column. Buffer C was continuously pumped with a flow rate 1 ml/min for 46 minutes to create a pH gradient. Fraction with enzymatic activity was collected and freeze-fried.

4.1.7 Molecular weight determination by using Sodium Dodecyl Sulfate-Polyacrylamide Gel Electrophoresis (SDS-PAGE)

SDS-PAGE was performed according toLaemmli's method (Laemmli, 1970). The 4 % stacking gel, 9 % resolving gel and 12 % resolving gel were prepared as shown in Table 2. The 12 % resolving solution or 9 % resolving solution was pipetted into the

space between the glass plates and allowed to polymerize before pipetting the 4 % stacking solution onto the gel. 1×SDS sample buffer was prepared as shown in Table 3.

Table 2: Volume of solution used in preparing 4 % stacking gel and 12 % resolving gel

| **Solutions** | **Stacking gel 4%** | **Resolving gel 9%** | **Resolving gel 12%** |
|---|---|---|---|
| 30 % Acrylamide/Bis | 1.3 mL | 2.4 mL | 4 mL |
| 0.5 M Tris HCl, pH 6.8 | 2.5 mL | - | - |
| 1.5 M Tris HCl, pH 8.8 | - | 2 mL | 2.5 mL |
| 10 % (w/v) SDS | 0.1 mL | 80 µl | 0.1 mL |
| Distilled water | 6.1 mL | 3.4 mL | 4 mL |
| TEMED | 10 µl | 8 µl | 5 µl |
| 10 % (w/v) APS | 50 µl | 80 µl | 50 µl |
| Total | 10 mL | 10 mL | 10 mL |

Table 3: Volume of solution to prepare 2 ml of 1× SDS sample buffer.

| **Solutions** | **Volume** |
|---|---|
| 62.5 mM Tris HCl, pH6.8 | 0.3 mL |
| 20 % (v/v) Glycerol | 0.4 mL |
| 2 % (w/v) SDS | 0.4 mL |
| 5 % (v/v) Beta-mercaptoethanol | 0.1 mL |
| 0.5% (w/v) Bromophenol blue | 0.1 mL |
| Distilled water | 0.8 mL |
| Total | 2 mL |

The purified protein was concentrated by using protein concentrator (Invitrogen) or acetone precipitation. 10 µl of concentrated sample was added into a micro-centrifuge tube contained 10 µl of SDS sample buffer and boiled for 5 minutes at 90 ºC. Samples were now ready to run on 9 % or 12 % polyacrylamide gel in the presence of 0.1% (w/v) SDS. BenchMark$^{TM}$ (Invitrogen) was used as a molecular size marker. The gel was stained using the Vorum silver stain method (Mortz *et al.*, 2001) or colloidal coomasie

blue CBB G-250 staining method (Neuhoff *et al.*, 1985). The protocol for silver staining and colloidal coomasie blue CBB G-250 staining are shown in Table 4 and 5 respectively

Table 4: Vorum silver stain method

| **Reaction** | **Solution** | **Volume** | **Time** |
|---|---|---|---|
| Fixating | Methanol | 200 mL | More than 2 hours or overnight |
| | Acetic acid | 48 mL | |
| | Formaldehyde | 190 µL | |
| | Distilled water | Top up to 400 mL | |
| Washing | Ethanol (100%) | 140 mL | 3 × 20 minutes |
| | Distilled water | Top up to 400 mL | |
| Sensitizing | Sodium Thiosulphate | 0.1 g | 3 minutes |
| | Distilled water | Top up to 400 mL | |
| Washing | Distilled water | | 3 × 5 minutes |
| Silver reaction | Silver nitrate | 0.8 µL | 20 minutes |
| | Formaldehyde | 288 µL | |
| | Distilled water | Top up to 400 mL | |
| Washing | Distilled water | | 3 × 10 seconds |
| Developing | Sodium carbonate | 48 g | 3 – 5 minutes |
| | Formaldehyde | 378 µL | |
| | Sensitizing solution | 16 ml | |
| | Distilled water | Top up to 800 mL | |
| Stopping | Methanol | 200 mL | 5 minutes |
| | Acetic acid | 48 ml | |
| | Distilled water | Top up to 400 mL | |

Table 5: Preparation of colloidal brilliant blue CBB G-250

| Chemical | Amount |
|---|---|
| 5 % (w/v) Coomaise brilliant blue G-250 | 1 g |
| Phosphoric acid | 11.8 ml |
| Ammonium sulfate | 100 g |
| Distilled water | Top up to 1 L |

4.1.8 Two-dimensional electrophoresis for putative GST isozymes determination

Rehydration buffer for first dimension electrophoresis was prepared with 8 M urea, 2 % (w/v) CHAPS, 0.15 % (w/v) DTT, 2 % (v/v) ampholytes (pH 3-10), 30 mM thiourea and traces of bromophenol blue. Twenty µl of concentrated sample are mixed with 105 µl of rehydration buffer and applied to a 7 cm, pH 3–10 IPG strip. The IPG strip was left overnight for at least 18 hours. Isoelectric focusing was performed by using Multiphor II Electrophoresis System. Equilibration buffer (EB) was prepared with 0.34 ml of 1.5 M Tris-HCl (pH 8.8), 3.6 g of urea, 3.5 ml of glycerol, 0.2 g of sodium dodecyl sulfate (SDS) and top up with deionized water until the total of 10 ml. EB was evenly poured into two new centrifuge tubes, EB 1 and EB 2 which were 5 each. EB 1 was added with 12.5 mg of DDT and EB 2 was added with 0.2 g of iodoacetamide. The proteins inside IPG strip was subsequently reduced with DDT in EB 1 and alkylated with iodoacetamide in EB 2. Second dimension electrophoresis was by placing the IPG strip on the 12 % resolving gel and run at 120 V. Gel was stained with silver stain method or colloidal coomasie brilliant blue CBB G-250 stain method as mentioned in section 4.1.7.

4.1.9 An assays to determine substrate specificity of putative GST isozymes

Enzymatic assays with 1-Chloro-2,4-dinitrobenzene (CDNB), ethacrynic acid (EA), sulfobromophthalein (BSP), p-nitrobenzyl chloride (NBC) and trans-4-phenyl-3-butene-2-one (PBO) were determined at pH 6.5 (Habig *et al*., 1974). The enzymatic assay was conducted in a 3 ml cuvette of 0.1 M sodium phosphate buffer pH 6.5 (Buffer D) containing 0.2 mM of substrates, 1 mM of GSH and 100 µl of purified protein sample except EA where 0.2 mM of substrate and 0.3 mM of GSH were added. Changes of absorbance for CDNB, EA, BSP, NBC and PBO were measured at 340 nm, 270 nm, 330 nm, 310 nm, and 290 nm respectively. Activity with 1, 2-dichloro-4-nitrobenzene (DCNB) at 344 nm was determined in a 3 ml cuvette of 0.1 M Tris-buffer at pH 9 (Buffer E) containing 4 mM of GSH, 0.4 mM of DCNB and 100 µl of purified protein sample (Motoyama & Dauterman, 1977).

Determination of glutathione peroxidase activity was performed by modifying the method described by Wendel (1981). The reaction mixture comprised of 0.2 M of sodium phosphate buffer pH 7 (Buffer F), 0.2 mM of GSH, 0.04 mM of NADPH, 0.1 µmol/min of glutathione reductase and 0.2 mM of hydrogen peroxide or cumene hydroperoxide and 100 µL of purified protein sample. Changes of absorbance were recorded at 366 nm.

Enzymatic activity to dichloromethane (DCM) was determined as described by Sherratt *et al.* (1997). 4 vials each containing 93 mM of Tris HCl buffer pH 8 (Buffer G), 0.2 mM of GSH, 0.1 mM of DCM and 100 µl of purified protein sample were prepared. 1.5 ml of the solution was withdrawn after 5, 10, 15 and 20 minutes from each of the 4 vials. The reactions were stopped by adding trifluoroacetic acid to a final concentration of 20 % (v/v). The mixtures were then added with equal volume of solution containing 2 M of ammonium acetate, 0.05 M of acetic acid and 0.02 M of acetylacetone. The reactions were completed at 42 ºC for 30 minutes before measuring the absorbance at 412 nm.

Changes of absorbance for trans-2-octenal was measured at 225 nm while hexadienal and 2, 4-heptadineal were measured at 280 nm (Brophy *et al.,* 1989). The enzymatic assay was conducted in a 3 ml cuvette of 0.09 mM sodium phosphate buffer pH 6.5 containing 0.2 mM of substrates, 1 mM of GSH and 100 µl of purified protein sample.

Protein content of putative GST isozymes were determined according to Bradford (1976).

4.2.0 Kinetic properties of AcGST-1 and AcGST-2

The kinetic parameters, $V_{max}$ and $K_m$ for ethacrynic acid (EA) were determined using a EA range from 0.03 to 0.5 mM and a fixed GSH concentration of 0.3 mM. The apparent $V_{max}$ and $K_m$ values for GSH were also calculated using a GSH range from 0.03 to 0.5 mM and a fixed EA concentration of 0.2 mM. To determine $V_{max}$ and $K_m$ value of AcGST-1 and AcGST-2 for EA, a 3 ml cuvette containing 0.1 M sodium phosphate buffer pH 6.5, 0.3 mM of GSH, 100 µl of purified protein and EA concentration range from 0.03 to 0.5 mM (0.03 mM, 0.05 mM, 0.08 mM, 0.2 mM, 0.33 mM and 0.5 mM) was prepared. On the other hand, in order to determine the $V_{max}$ and $K_m$ value of AcGST-1 and AcGST-2 for GSH, 3 ml cuvette of 0.1 M sodium phosphate buffer pH 6.5, 0.2 mM of EA, 100 µl of purified protein and GSH concentration range from 0.03 mM to 0.5 mM (0.03 mM, 0.05 mM, 0.08 mM, 0.20 mM, 0.33 mM and 0.50 mM) was prepared. Changes of absorbance were read at 270 nm wavelength.

### 4.2.1 N-terminal sequencing of AcGST-1 and AcGST-2

One L of transfer buffer was prepared using 5.8 g of Tris, 2.9 g of glycine and 0.4 ml of 10 % (w/v) SDS. Purified protein was first separated by SDS-PAGE or two-dimensional electrophoresis. With great care, the gel was gently rinsed with distilled water and then equilibrated in transfer buffer for 15 minutes. The Polyvinylidene fluoride membrane (PVDF) was pre-wetted with 100 % methanol until translucent. The wetted membrane, filter paper and fiber pads were immersed in transfer buffer for 15 minutes. After 15 minutes, gel sandwich was prepared by placing the pre-wetted fiber pad on grey side of the cassette, a sheet of pre-wetted filter paper on top of fiber pad and the equilibrated gel on the filer paper then followed by a pre-wetted membrane, filter paper and fiber pad. The blot was run at 100 V for 45 minutes. After the blotting, the membrane was rinsed with distilled water and stained with 0.1% (w/v) coomasie brilliant blue G-250.

The stained membrane was rinsed three times with deionized water and destained with 50% (v/v) methanol/water. Protein on the stained membrane was cut into smaller pieces, loaded onto sequencer cartridge and run under standard conditions as per manufacturer instructions. Twenty pmol of standard solution (19 amino acids of known retention times) was injected per run. Pulsed Liquid PVDF was used as sequencing method. Automated Edman Degradation was carried out using an Applied Biosystems 494 Procise Protein Sequencing System.

N-terminal sequencing was carried out by service provider, Proteomics International Pty Ltd, Western Australia.

4.2.2 MALDI-TOF analysis

Protein bands were excised and cut into 1 $mm^3$ cubes on an acetone-wiped glass plate. The cubes were transferred to a sterilized micro-centrifuge tube. A total of 100 µl of 200 mM ammonium bicarbonate in 50 % (v/v) acetonitrile (ACN) was added into the micro-centrifuge tube. This step was repeated twice in order to completely remove the stain from the gel cubes. The gel cubes were dried for 10 minutes in dry bath incubator. Seven µl of trypsin solution (0.02 mg/mL) was added into the dehydrated gel cubes and incubated for an hour at room temperature. An additional 50 µl of 40 mM ammonium bicarbonate in 10 % (v/v) ACN was added and the mixture incubated for 16–18 hours at 37 ºC.

The extract was transferred into a new micro-centrifuge tube. Fifty µl of 0.1% (v/v) trifluoroacetic acid (TFA) was pippeted into the micro-centrifuge tube containing the gel cubes and incubated at 37 ºC for 45 minutes. This was to ensure complete extraction of any hydrophilic peptide remain in the gel cubes. The solution was separated from the gel cubes and combined with the first extract. The mixture was then dried completely in a dry bath incubator. The in gel-digestion method was used as described by Speicher *et al.* (2000).

α-cyano-4-hydroxycinnamic acid (CHCA) was prepared as saturated solution in 85 % (v/v) ACN/0.03% (v/v) TFA. One µl was pipetted and mixed with the dry extract. One µl of this solution was pipetted into a 192-well plate and air-dried.

Mass spectra were acquired on 4800 Plus Proteomics Analyzer (ABI). The peak intensity values were determined using Data Explorer using only fragment ions with S/N ratio higher than 10.

MALDI-TOF analysis was carried out by using the Proteomics facility, Medical biotechnology laboratory, University of Malaya.

4.2.3 Reactivity of purified putative GST isozymes towards pesticides by Thin Layer Chromatography (TLC) analysis

Three reactions mixtures were prepared for each of the pesticides: Propoxur, Isoproturon, Fenoxapop-ethyl and Clodinafop-propargyl. The composition of mixture was shown in Table 6. All the reactions were performed in a volume 3 ml at 25 ºC for 20 minutes. An aliquot of 4 ul of reaction products were loaded on a 0.2 mm thick TLC silica gel and developed using butan-ol/acetic acid/water (12:3:5, by volume) for 2 hours (Ben-Arie *et al.,* 1993). The air-dried plate was subsequently stained with ninhydrin (0.3 % (w/v), in acetone). Colored bands were observed with naked eyes after 15 minutes.

Table 6: Composition of mixture for TLC

| | **First reaction Mixture (X)** | **Second reaction mixture (Y)** | **Third reaction mixture (Z)** |
|---|---|---|---|
| **Buffer** | 0.1 M sodium phosphate buffer pH 6.5 | 0.1 M sodium phosphate buffer pH 6.5 | 0.1 M sodium phosphate buffer pH 6.5 |
| **Pesticide** | 0.2 mM | - | 0.2 mM |
| **GSH** | 1 mM | 1 mM | 1 mM |
| **Protein sample** | 100 μL | 100 μL | - |

### 4.2.4 Disc diffusion test

Single colony of bacteria was picked using a loop and dipped into a flask containing nutrient broth. Bacterial cells were allowed to grow overnight for 18 hours at 37 ºC. A sterile swab was dipped into the broth culture and pressed gently against the internal surface of the flask to remove excess fluid. Ten nutrient agar plates were streaked evenly by using the swab pre-wetted with bacteria culture. The nutrient agar plates were then allowed to dry for 5 minutes. On each of the nutrient agar plate, four sterile discs were dispensed at four different corners of the plates. Chlorpyrifos, Bromophos, Malathione, DDT, Propoxur, Permethin, Fenitrothion were prepared to a final concentration of 0.5 mg/ml and 1 mg/ml whereas hydrogen peroxide was prepared to a final concentration of 25% and 50%. Twenty µl from each of the concentration of the pesticides were pipetted on each of the pre-dispensed discs on the nutrient agar plates. The nutrient agar plates were inverted and incubated for 18 hours at 37 ºC.

# 5.0 Results

5.1.1 Bacteria identification from 16S rRNA gene sequence

In 16S rRNA partial species barcoding, V4-V6 hypervariable regions were targeted and resulting in a 690 bp PCR product. The electrophoretically determined nucleotide sequences were searched for homology against database by using the NCBI nucleotide blast. From the top 10 NCBI nucleotide blast results show in Figure 22, the DNA sequence had about 99% sequence identity to the genus *Acinetobacter*. Generally, a match with >99% homology rendered species-level identification if culture features were also compatible, 97% to <99% matches correspond to genus identification and 93% to<97% matches would be deemed either new genus or new species (Han, 2006). A phylogenetic tree (Figure 23) was built to further determine the species of the isolate which was subsequently recognized as *Acinetobacter calcoacetius* Y1.

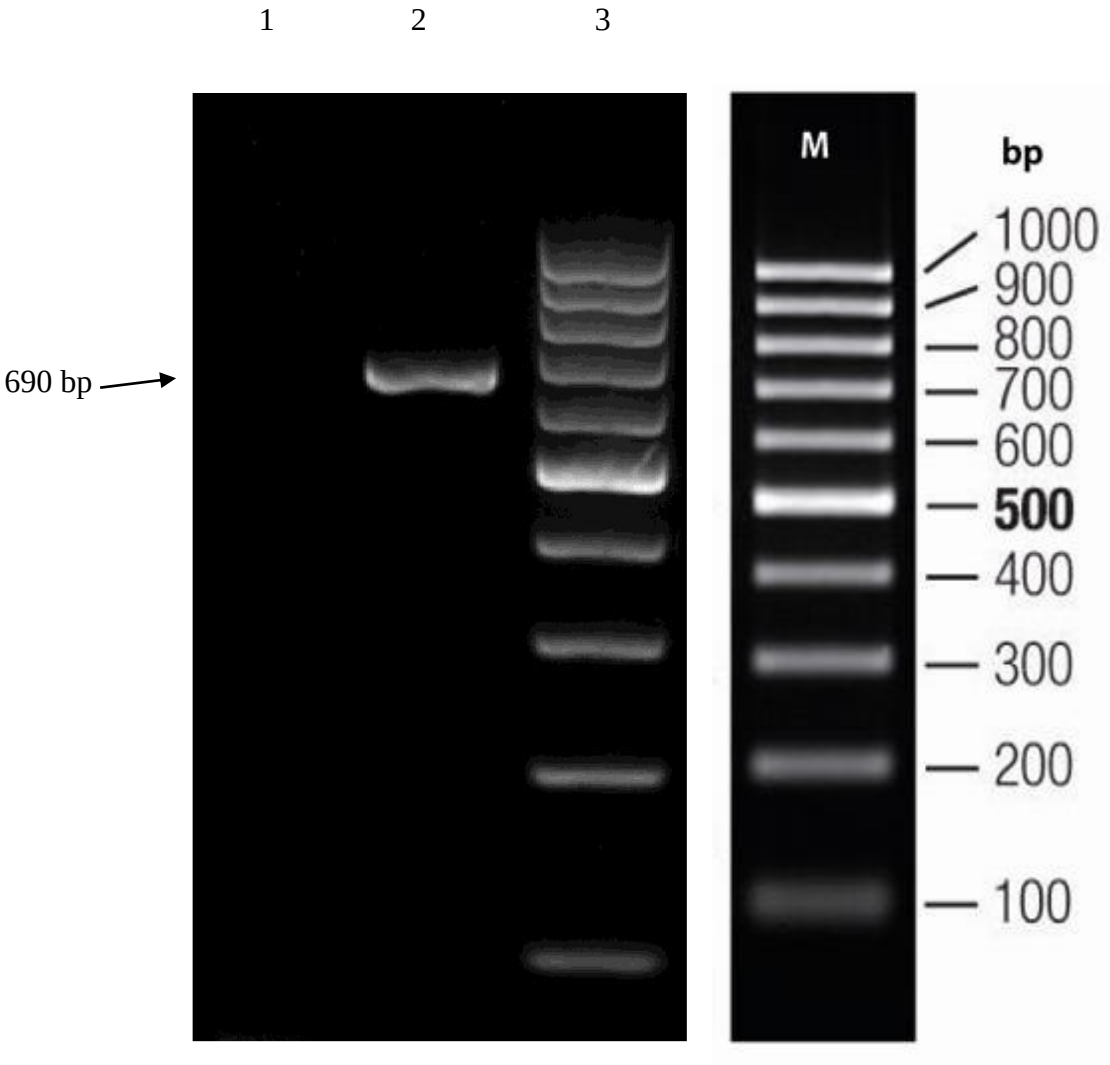


Figure 20: The amplicon of 16S rRNA targeted gene of *Acinetobacter calcoaceticus* Y1. Lane 1: Negative control; Lane 2: Amplicon (690 bp) of *A. calcoaceticus*; and Lane 3: Ladder of 100 bp.

GTAAAACGACGGCCAGGTGCCAGCAGCTGCGGTAATACAGAGGGTGCAAGCGTTA
ATCGGATTTACTGGGCGTAAAGCGCGCGTAGGCGGCTAATTAAGTCAAATGTGAA
ATCCCCGAGCTTAACTTGGAATTGCATTCGATACTGGTTAGCTAGAGTGTGGGAGA
GGATGGTAGAATTCCAGGTGTAGCGGTGAAATGCGTAGAGATCTGGAGGAATACC
GATGGCGAAGGCAGCCATCTGGCCTAACACTGAGCTGAGGTGCGAAAGCATGGGG
AGCAAACAGGATTAGATACCCTGGTAGTCCATGCCGTAAACGATGTCTACTAGCC
GTTGGGGCCTTTGAGGCTTTAGTGGCGCAGCTAACGCGATAAGTAGACCGCTGGG
GAGTACGGTCGCAAGACTAAAACTCAAATGAATTGACGGGGGCCCGCACAAGCG
GTGGAGCATGTGGTTTAATTCGATGCAACGCGAAGAACCTTACCTGGCCTTGACAT
AGTAAGAACTTTCAGAGATGGATTGGTGCCTTCGGGAACTTACATACAGGTGCTG
CATGGCTGTCGTCAGCTCGTGTCGTGAGATGGTGGGTTAAGTCCCGCAACGACCGC
AACCCGTCATAGCTGTTT

Figure 21: Partial sequence of 16S rRNA amplicon

**Sequences producing significant alignments:**

Select: All None Selected:0

Alignments Download GenBank Graphics Distance tree of results

| Description | Max score | Total score | Query cover | E value | Max ident | Accession |
|---|---|---|---|---|---|---|
| Acinetobacter sp. AHM1 16S ribosomal RNA gene, partial sequence | 1066 | 1066 | 95% | 0.0 | 99% | KC858868.1 |
| Acinetobacter calcoaceticus strain D06-95_JO 16S ribosomal RNA gene, partial sequence | 1066 | 1066 | 95% | 0.0 | 99% | KC900372.1 |
| Acinetobacter sp. YZT101 16S ribosomal RNA gene, partial sequence | 1066 | 1066 | 95% | 0.0 | 99% | KC833512.1 |
| Acinetobacter calcoaceticus PHEA-2 strain PHEA-2 16S ribosomal RNA, complete sequence | 1066 | 1066 | 95% | 0.0 | 99% | NR_102826.1 |
| Acinetobacter oleivorans DR1 strain DR1 16S ribosomal RNA, complete sequence | 1066 | 1066 | 95% | 0.0 | 99% | NR_102814.1 |
| Acinetobacter pittii strain H05-30 16S ribosomal RNA gene, partial sequence | 1066 | 1066 | 95% | 0.0 | 99% | KC847480.1 |
| Acinetobacter sp. enrichment culture clone LDC-18 16S ribosomal RNA gene, partial sequence >gb\|KF020733.1\| Acinetobacter sp. D-6 16S ribosomal RNA ge | 1066 | 1066 | 95% | 0.0 | 99% | KF020728.1 |
| Acinetobacter sp. W31 16S ribosomal RNA gene, partial sequence | 1066 | 1066 | 95% | 0.0 | 99% | KC853193.1 |
| Uncultured bacterium clone 34-2E 16S ribosomal RNA gene, partial sequence | 1066 | 1066 | 95% | 0.0 | 99% | KC777193.1 |
| Acinetobacter calcoaceticus strain K715 16S ribosomal RNA gene, partial sequence | 1066 | 1066 | 95% | 0.0 | 99% | KC758143.1 |

Figure 22: Top 10 hit using NCBI Nucleotide blast. (http://blast.ncbi.nlm.nih.gov/Blast.cgi)

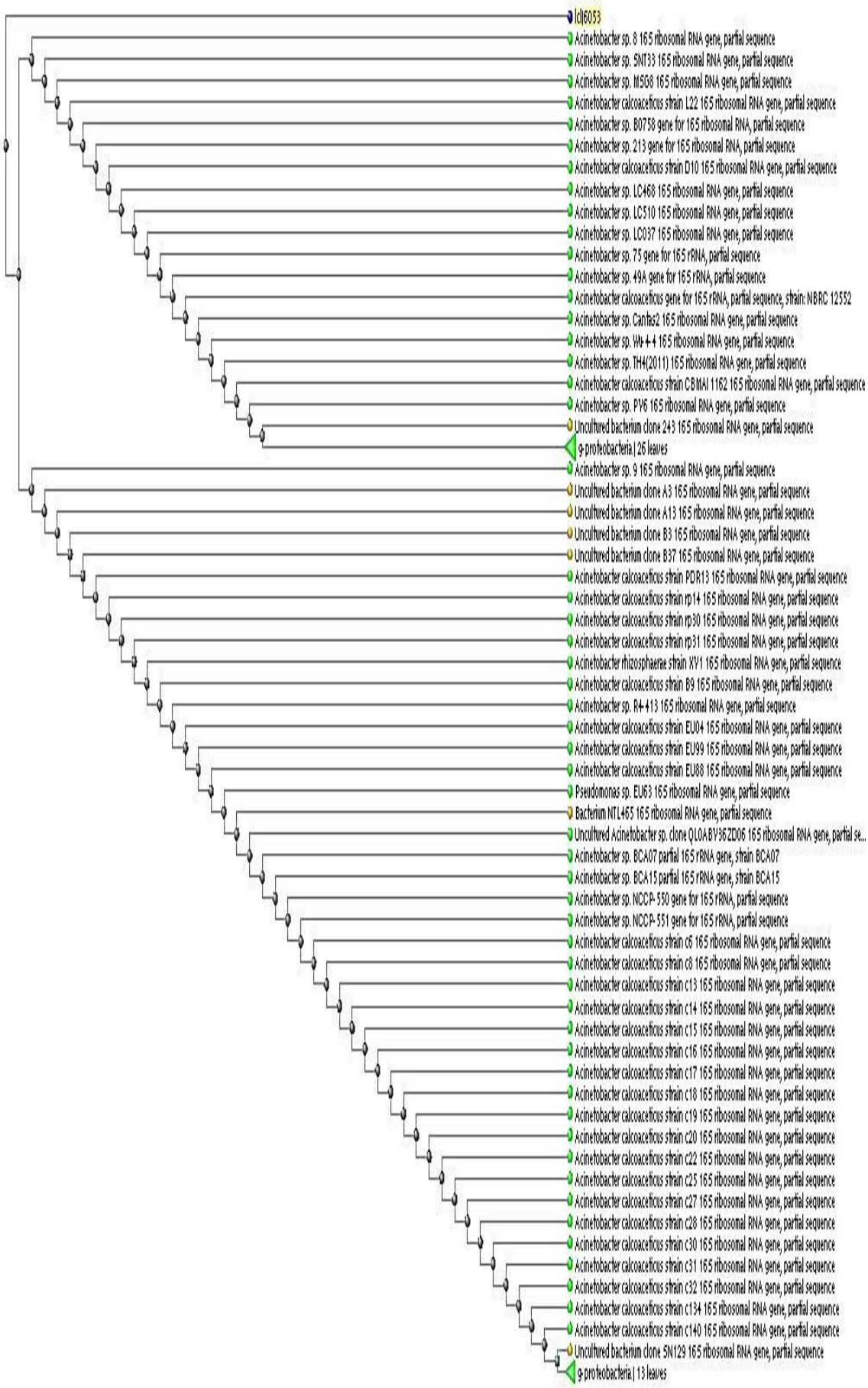


Figure 23: Phylogenetic tree-neighbour joining (unrooted tree)

5.1.2 Screening of bacteria GSTs by using monochlorobimane

Figure 24: No fluorescence colonies can be seen after spraying with monochlorobimane and view under 365 nm wavelength UV light for non-GSTs producing bacteria.

Figure 25: No fluorescence colonies can be seen without spraying any monochlorobimane after viewing under 365 nm wavelength UV light for *Acinetobacter calcoaceticus* Y1.

Figure 26: Fluorescence colonies can be seen after spraying with monochlorobimane and view under 365 nm wavelength UV light for *Acinetobacter calcoaceticus* Y1.

5.1.3 SDS-PAGE of purified putative cytosolic GSTs

Purified proteins ran on SDS-PAGE produced a single band at about 23 kDa which was within the range of GSTs molecular weights (Figure 27). Putative GSTs from *A. calcoaceticus* Y1 (AcGST) were a dimer made up of 23 kDa subunit. According to Sonoda *et al.* (2006), cytosolic GSTs were dimeric enzymes approximately 25 kDa in size.

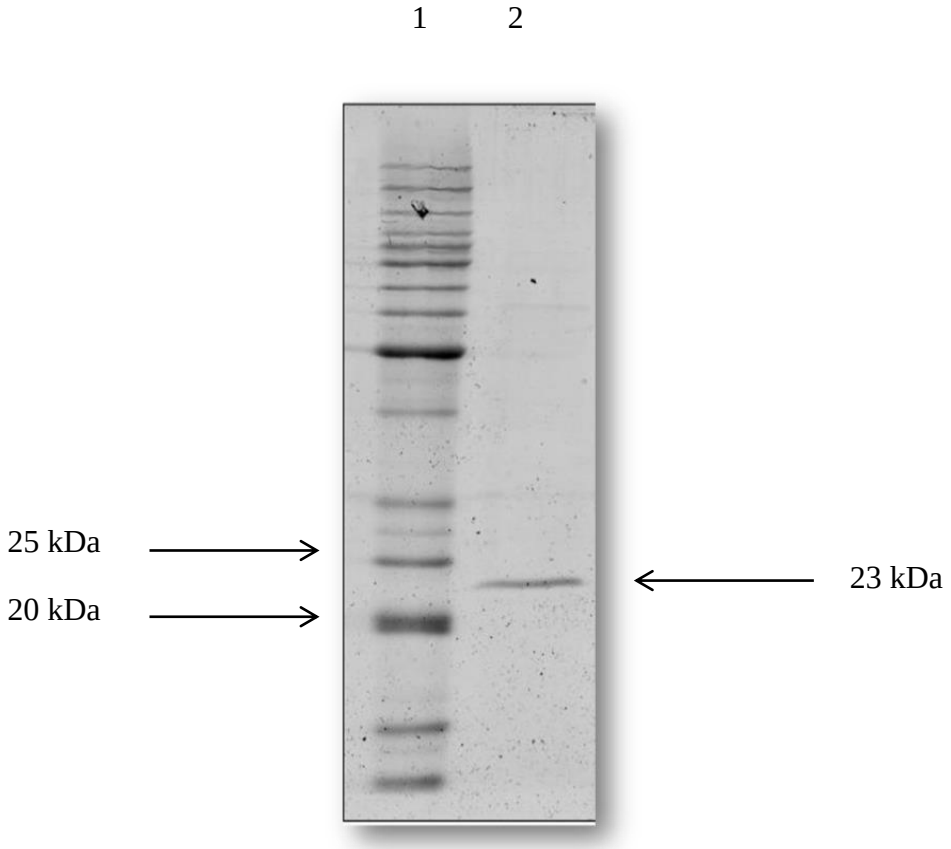


Figure 27: SDS-PAGE of purified putative GSTs from *Acinetobacter calcoaceticus* Y1. Lane 1 shows the Benchmark$^{TM}$ standard marker and Lane 2 shows the purified putative GSTs from *A. calcoaceticus* Y1.

5.1.4 Two-dimensional electrophoresis to determine number of putative GST isozymes

The purified putative GSTs were further analysed by using two-dimensional electrophoresis. Two-dimensional electrophoresis of purified protein produced two spots at about 23 kDa. These two putative GST isozymes were designated as AcGST-1 and AcGST-2. AcGST-1 appeared to be more acidic as compared to AcGST-2

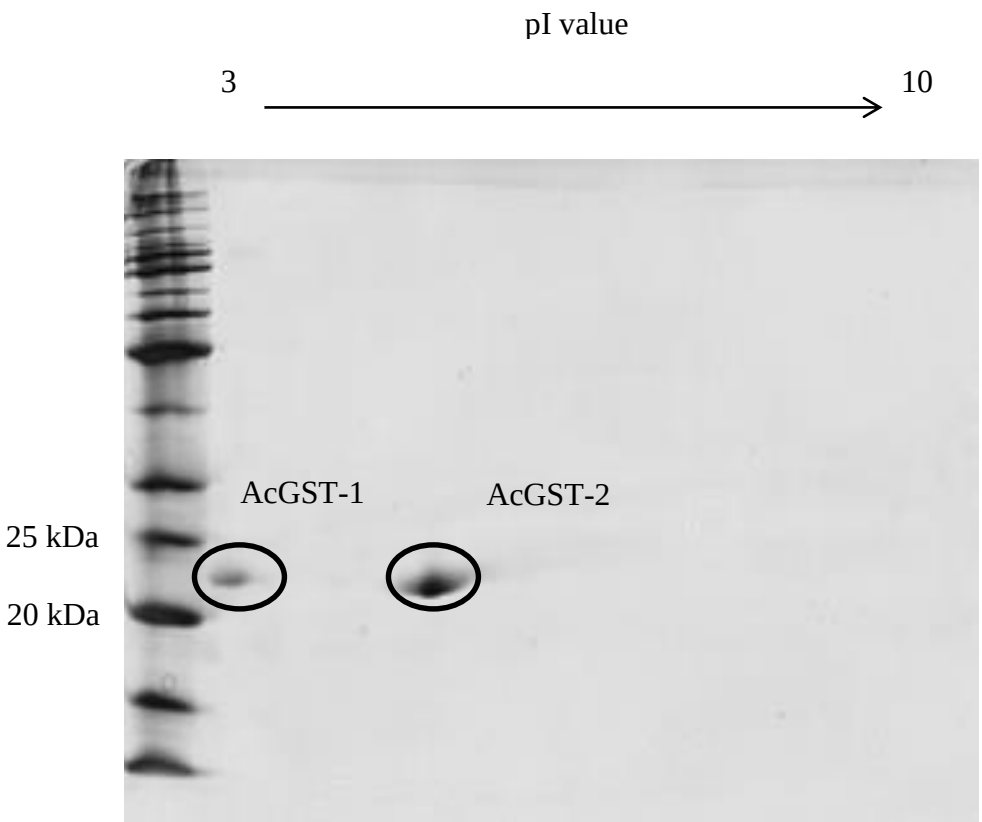


Figure 28: Two-dimensional electrophoresis of purified putative GSTs from *Acinetobacter calcoaceticus* Y1. Two putative GST isozymes designated as AcGST-1 and AcGST-2 were identified.

5.1.5 Isoelectric focusing (IEF) separates putative GST isozymes based on pI value

The two dimensional electrophoresis separated the two putative GST isozymes and gave the approximate pI value of the two GST isozymes. In order to determine the more precise pI value of AcGST-1 and AcGST-2, vertical IEF of the purified sample was performed as shown in Figure 29. IEF of the purified sample resulted in two bands at pI values of 4.5 and 6.2. The result was consistent with the result shows in Figure 28 where two spots were obtained. AcGST-1 and AcGST-2 appeared at pI values of 4.5 and 6.2 respectively.

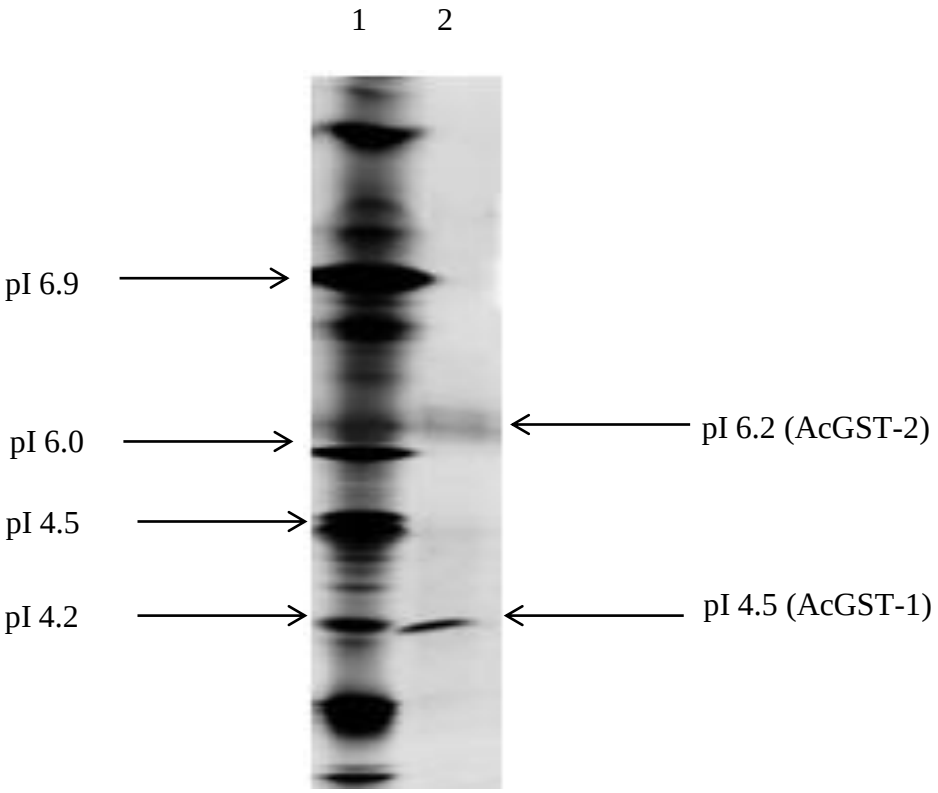


Figure 29: Isoelectric-focusing (IEF) of purified protein sample. Lane 1 shows the SERVA$^{TM}$ IEF marker (Invitrogen) and Lane 2 shows the pI value of AcGST-1 and AcGST-2 respectively.

5.1.6 Putative GST isozymes separation by using Ion-exchange chromatography

The AcGST-1 showed a single band on SDS-polyamide gel (Figure 30) which was consistent with result shown earlier in Figure 27 where a single band at 23 kDa was observed. AcGST-2 formed a single band at about 110 kDa (Figure 31) instead of at 23 kDa suggesting that AcGST-2 tend to form aggregation. Moreover, un-dissolvable white pellets were spotted during acetone precipiatation of AcGST-2. AcGST-2 was separated by 9% resolving gel (Bigger gel pore size) because no band spotted on 12% resolving gel (Smaller gel pore size) suggesting the formation of large protein aggregates. In Figure 30, when both AcGST-1 and AcGST-2 were presented together, no aggregation was observed.

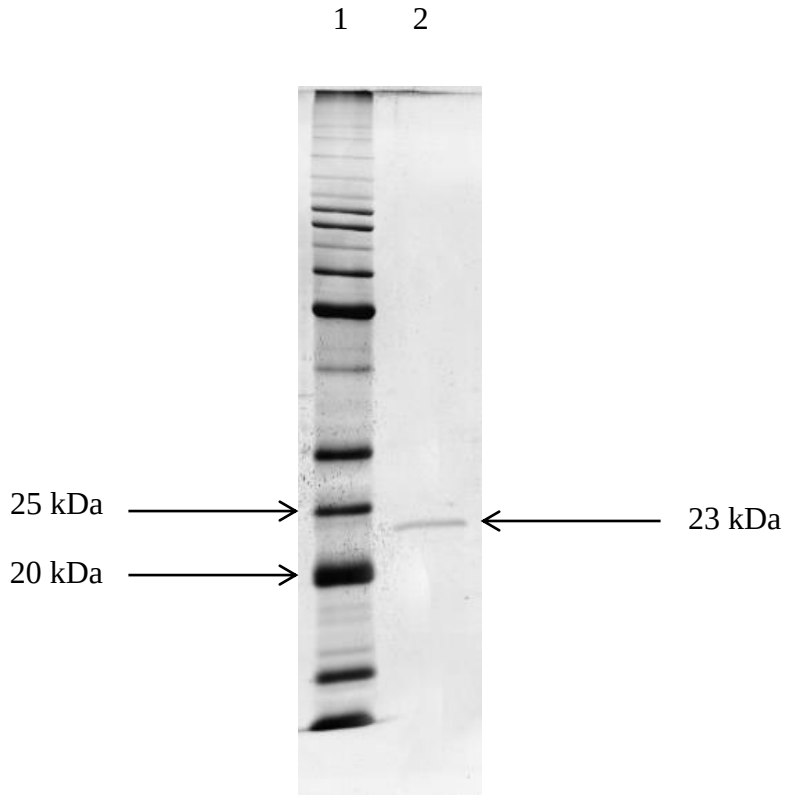


Figure 30: SDS-PAGE of AcGST-1 purified from CM Sepharose fast flow column. Lane 1 shows the Benchmark$^{TM}$ standard marker (Invitrogen) and Lane 2 shows the AcGST-1

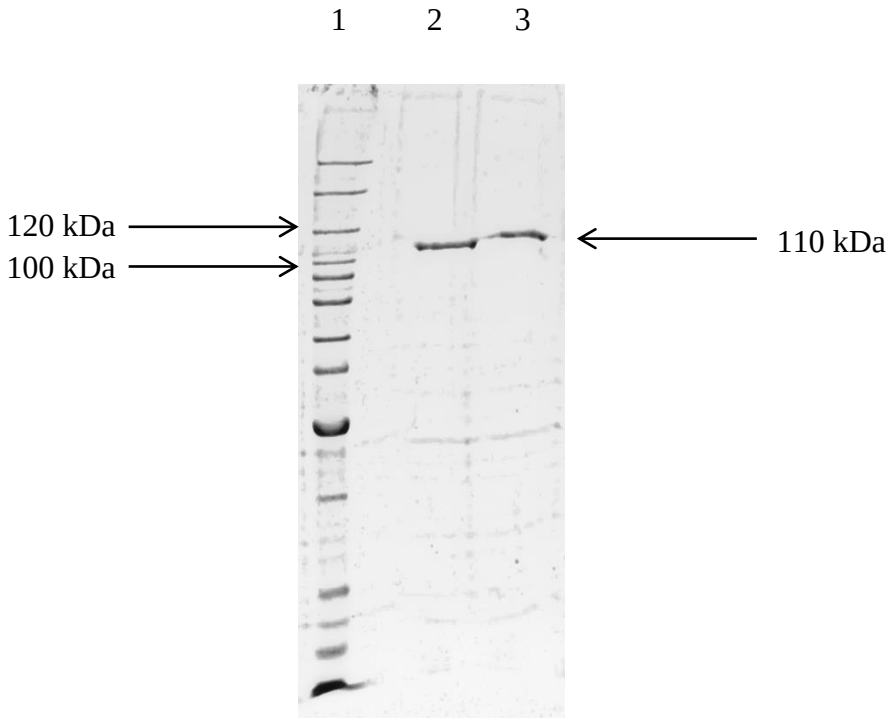


Figure 31: SDS-PAGE of AcGST-2 purified from DEAE Sepharose fast flow column. Lane 1 shows the Benchmark™ standard marker (Invitrogen). Lane 2 shows the aggregation of AcGST-2 purified from DEAE Sepharose fast flow column. Lane 3 shows the aggregation of AcGST-2 purified from chromatofocusing.

5.1.7 Substrate specificity test for AcGST-1 and AcGST-2

Table 7: Substrate specificity of AcGST-1 and AcGST-2 from *Acinetobacter calcoaceticus* Y1. ( n.d: not detected)

| **Substrate** | **AcGST-1 (µmol/min/mg)** | **AcGST-2 (µmol/min/mg)** |
|---|---|---|
| **Ethacrynic acid** | 24.99 ± 1.24 | 15.87 ± 2.54 |
| **Hydrogen peroxide** | 3.93 ± 0.32 | n.d |
| **1-Chloro-2,4-dinitrobenzene** | 0.61 ± 0.12 | 0.54 ± 0.13 |
| **2,4-heptadienal** | 0.11 ± 0.03 | 0.08 ± 0.01 |
| **Trans-2-octenal** | 0.08 ± 0.02 | 0.09 ± 0.01 |
| **Hexadienal** | 0.04 ± 0.003 | n.d |
| **1,2-dichloro-4-nitrobenzene** | n.d | n.d |
| **p-nitrophenyl chloride** | n.d | n.d |
| **Sulfobromophthalein** | n.d | n.d |
| **Trans-4-phenyl-3-butene-2-one** | n.d | n.d |
| **Cumene hydroperoxide** | n.d | n.d |
| **Dichloromethane** | n.d | n.d |

Tables 7 showed that AcGST-1 and AcGST-2 had highest affinity towards ethacrynic acid compared to the other tested substrates. Both putative GST isozymes also reacted with another GST common substrate: 1-chloro-2,4-dinitrobenzene. Conjugation of AcGST-1 towards hydrogen peroxide suggested the presence of glutathione peroxidase activity. The substrate specificities of both putative GST isozymes were different and thus it is believed that they were of two existing homodimers.

5.1.8 Kinetic properties of AcGST-1 and AcGST-2

Table 8: $V_{max}$ and $K_m$ of AcGST-1 and AcGST-2

| **GST** | **Substrate** | **$V_{max}$ (µmol/min)** | **$K_m$ (mM)** |
|---|---|---|---|
| **AcGST-1** | Ethacrynic acid | 3.74 ± 1.40 | 0.28 ± 0.02 |
| | Glutathione | 1.46 ± 0.02 | 0.01 ± 0.0003 |
| **AcGST-2** | Ethacrynic acid | 8.41 ± 1.08 | 0.28 ± 0.002 |
| | Glutathione | 1.35 ± 0.01 | 0.02 ± 0.003 |

Tables 8 shows that AcGST-2 had higher catalytic rate towards ethacrynic acid as compared to ACGST-1. This attributed to the high substrate conversion efficiency of AcGST-2. High affinity towards GSH was shown by AcGST-1 because its $K_m$ value was lower compared to AcGST-2 and required lesser concentration of GSH to achieve $V_{max}$.

5.1.9 N-terminal sequencing of AcGST-1 and AcGST-2

Ten amino acids were attempted to sequence for both of the putative GST isozymes, however, only 5 amino acids and 9 amino acids could be identified from AcGST-1 and AcGST-2 respectively. The result was not satisfactorily reliable due to inability to repeat similar sequence of amino acids and absence of identity at higher amino acids position. N-terminal sequencing was performed in total of three times, however it was still unable to get a consistent and reliable result and lead to MALDI-TOF analysis.

**Sample name**: AcGST1/pI4 (PI-2938A-5407)

| **Position** | **1st choice** | **2nd choice** |
|---|---|---|
| 1. | V | W,S,D,A,Y |
| 2. | G | |
| 3. | X | |
| 4. | X | S |
| 5. | X | |

Figure 32: N-terminal sequence of AcGST-1 until 5th amino acids. (X may imply the presence of cysteine)

**Sample name**: AcGST2/pI7 (PI-2938B-5408)

| **Position** | **1st choice** | **2nd choice** |
|---|---|---|
| 1. | A | E,W,N,D |
| 2. | G | L |
| 3. | X | F |
| 4. | X | |
| 5. | X | |
| 6. | X | |
| 7. | X | Q |
| 8. | X | A |
| 9. | X | L |

Figure 33: N-terminal sequence of AcGST-2 until 9th amino acids. (X may imply the presence of cysteine)

5.2.0 MALDI-TOF analysis of AcGST-1 and AcGST-2

From Figure 34, 35 and 36, AcGST-1 and AcGST-2 did not hit any classes of GST from *Acinetobacter calcoaceticus*. The m/z peak with intensity greater than 10% for AcGST-1 sample excised from ion-exchange chromatography (804.3740, 832.4032, 855.1490, 861.1654, 871.1266, 883.1443 and 1066.1933), AcGST-2 sample excised from two-dimensional electrophoresis (881.1007, 823.1623, 855.1118, 871.0887, 887.0635, 1012.6160, 1066.1527 and 1076.1155) and AcGST-2 sample excised from ion-exchange chromatography (881.1407, 805.1541, 823.1273, 1012.1706, 1034.1687, 1224.2103, 1283.8199, 2721.3808 and 3149.6310) were searched against NCBI protein database using UniProt seacrh engine. Due to lack of bacterial genome databases, we were unable to significantly identify each putative GST isozymes through MALDI-TOF mass spectrometry analysis

| | Accession | Mass | Score | Description |
|---|---|---|---|---|
| 1. | F195B_CHICK | 10779 | 36 | Protein FAM195B OS=Gallus gallus GN=FAM195B PE=3 SV=1 |
| 2. | RRF_CLOBM | 20642 | 32 | Ribosome-recycling factor OS=Clostridium botulinum (strain Loch Maree / Type A3) GN=frr PE=3 SV=1 |
| 3. | FTSH2_SYMTH | 64061 | 32 | ATP-dependent zinc metalloprotease FtsH 2 OS=Symbiobacterium thermophilum GN=ftsH2 PE=3 SV=1 |
| 4. | CVFB_STAES | 33835 | 32 | Conserved virulence factor B OS=Staphylococcus epidermidis (strain ATCC 12228) GN=cvfB PE=3 SV=1 |
| 5. | VIRE2_HELVI | 5059 | 28 | Viresin (Fragment) OS=Heliothis virescens PE=1 SV=1 |
| 6. | TRUB_TRIEI | 33292 | 27 | tRNA pseudouridine synthase B OS=Trichodesmium erythraeum (strain IMS101) GN=truB PE=3 SV=1 |
| 7. | RRF_CLOB6 | 20592 | 25 | Ribosome-recycling factor OS=Clostridium botulinum (strain 657 / Type Ba4) GN=frr PE=3 SV=1 |
| 8. | RRF_CLOBJ | 20592 | 25 | Ribosome-recycling factor OS=Clostridium botulinum (strain Kyoto / Type A2) GN=frr PE=3 SV=1 |
| 9. | RRF_CLOBK | 20592 | 25 | Ribosome-recycling factor OS=Clostridium botulinum (strain Okra / Type B1) GN=frr PE=3 SV=1 |
| 10. | RRF_CLOBL | 20606 | 25 | Ribosome-recycling factor OS=Clostridium botulinum (strain Langeland / NCTC 10281 / Type F) GN=frr |

Figure 34: Top 10 hits of AcGST-1 excised from ion-exchange chromatography

| | Accession | Mass | Score | Description |
|---|---|---|---|---|
| 1. | Y2174_PARDP | 8667 | 13 | UPF0235 protein Pden_2174 OS=Paracoccus denitrificans (strain Pd 1222) GN=Pden_2174 PE=3 SV=1 |
| 2. | MINE_PROM4 | 11497 | 13 | Cell division topological specificity factor OS=Prochlorococcus marinus (strain MIT 9211) GN=minE P |
| 3. | RIP21_CRIRI | 1653 | 12 | Riparin-2.1 OS=Crinia riparia PE=1 SV=1 |
| 4. | RL21_FERNB | 11894 | 12 | 50S ribosomal protein L21 OS=Fervidobacterium nodosum (strain ATCC 35602 / DSM 5306 / Rt17-B1) GN=r |
| 5. | TATD3_MOUSE | 32416 | 12 | Putative deoxyribonuclease TATDN3 OS=Mus musculus GN=Tatdn3 PE=2 SV=1 |
| 6. | NUSB_PEDPA | 15089 | 11 | N utilization substance protein B homolog OS=Pediococcus pentosaceus (strain ATCC 25745 / 183-1w) G |
| 7. | CUTI2_COLGL | 2132 | 11 | Cutinase 2 (Fragment) OS=Colletotrichum gloeosporioides PE=1 SV=1 |
| 8. | PTRD1_MOUSE | 16027 | 11 | Putative peptidyl-tRNA hydrolase PTRHD1 OS=Mus musculus GN=Ptrhd1 PE=3 SV=1 |
| 9. | FCA1_CANAX | 16489 | 11 | Cytosine deaminase OS=Candida albicans GN=FCA1 PE=3 SV=1 |
| 10. | CS010_MOUSE | 17971 | 10 | UPF0556 protein C19orf10 homolog OS=Mus musculus GN=D17Wsu104e PE=2 SV=1 |

Figure 35: Top 10 hits of AcGST-2 excised from two-dimensional electrophoresis.

| | Accession | Mass | Score | Description |
|---|---|---|---|---|
| 1. | S115A_MOUSE | 12861 | 37 | Protein S100-A15A OS=Mus musculus GN=S100a15a PE=2 SV=1 |
| 2. | PYRF_JANMA | 29427 | 33 | Orotidine 5'-phosphate decarboxylase OS=Janthinobacterium sp. (strain Marseille) GN=pyrF PE=3 SV=1 |
| 3. | VPS36_MOUSE | 43708 | 32 | Vacuolar protein-sorting-associated protein 36 OS=Mus musculus GN=Vps36 PE=1 SV=1 |
| 4. | ARTJ_CHLTR | 28611 | 31 | Probable ABC transporter arginine-binding protein ArtJ OS=Chlamydia trachomatis (strain D/UW-3/Cx) |
| 5. | ATG7_PICAN | 69960 | 30 | Ubiquitin-like modifier-activating enzyme ATG7 OS=Pichia angusta GN=ATG7 PE=3 SV=1 |
| 6. | UBE2S_NEMVE | 22606 | 30 | Ubiquitin-conjugating enzyme E2 S OS=Nematostella vectensis GN=v1g237158 PE=3 SV=1 |
| 7. | ACDH_BACC1 | 32402 | 29 | Acetaldehyde dehydrogenase OS=Bacillus cereus (strain ATCC 10987) GN=BCE_2156 PE=3 SV=1 |
| 8. | RNE_BUCBP | 47282 | 29 | Putative truncated ribonuclease E OS=Buchnera aphidicola subsp. Baizongia pistaciae (strain Bp) GN= |
| 9. | RL27_CLOAB | 10797 | 29 | 50S ribosomal protein L27 OS=Clostridium acetobutylicum GN=rpmA PE=3 SV=1 |
| 0. | RL7_DESVM | 13336 | 29 | 50S ribosomal protein L7/L12 OS=Desulfovibrio vulgaris (strain Miyazaki F / DSM 19637) GN=rplL PE=1 |

Figure 36: Top 10 hits of AcGST-2 excised from ion-exchange chromatography.

5.2.1 Reactivity of purified putative GST isozymes towards pesticides by Thin Layer Chromatography (TLC) analysis

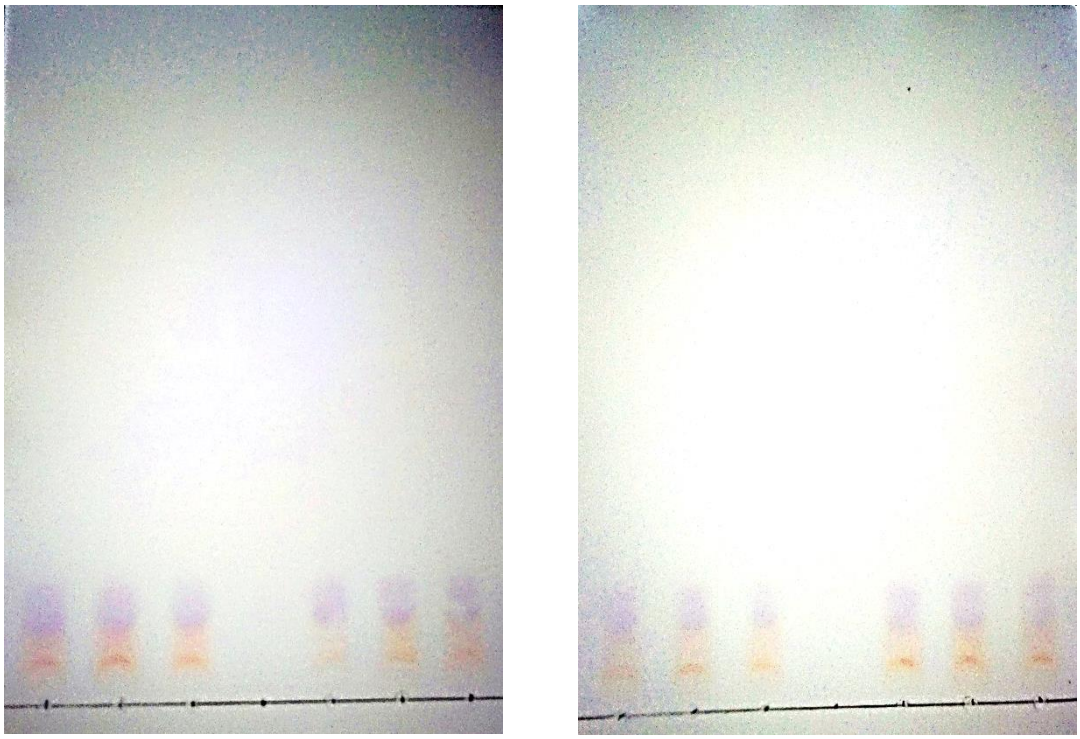

**X Y Z X Y Z X Y Z X Y Z**

**Isoproturon** **Fenoxaprop-ethly** **Propoxur** **Clodinafop-propargyl**

Figure 37

Figure 37: No conjugation can be viewed between AcGST-1 towards Isoproturon, Fenoxaprop-ethyl, Prospoxur and Clodinafop-propargyl. (X) represents GST reaction is carried out with addition of purified protein sample and pesticide while (Y) and (Z) represents GST reactions are carried out without addition of pesticide and protein sample respectively.

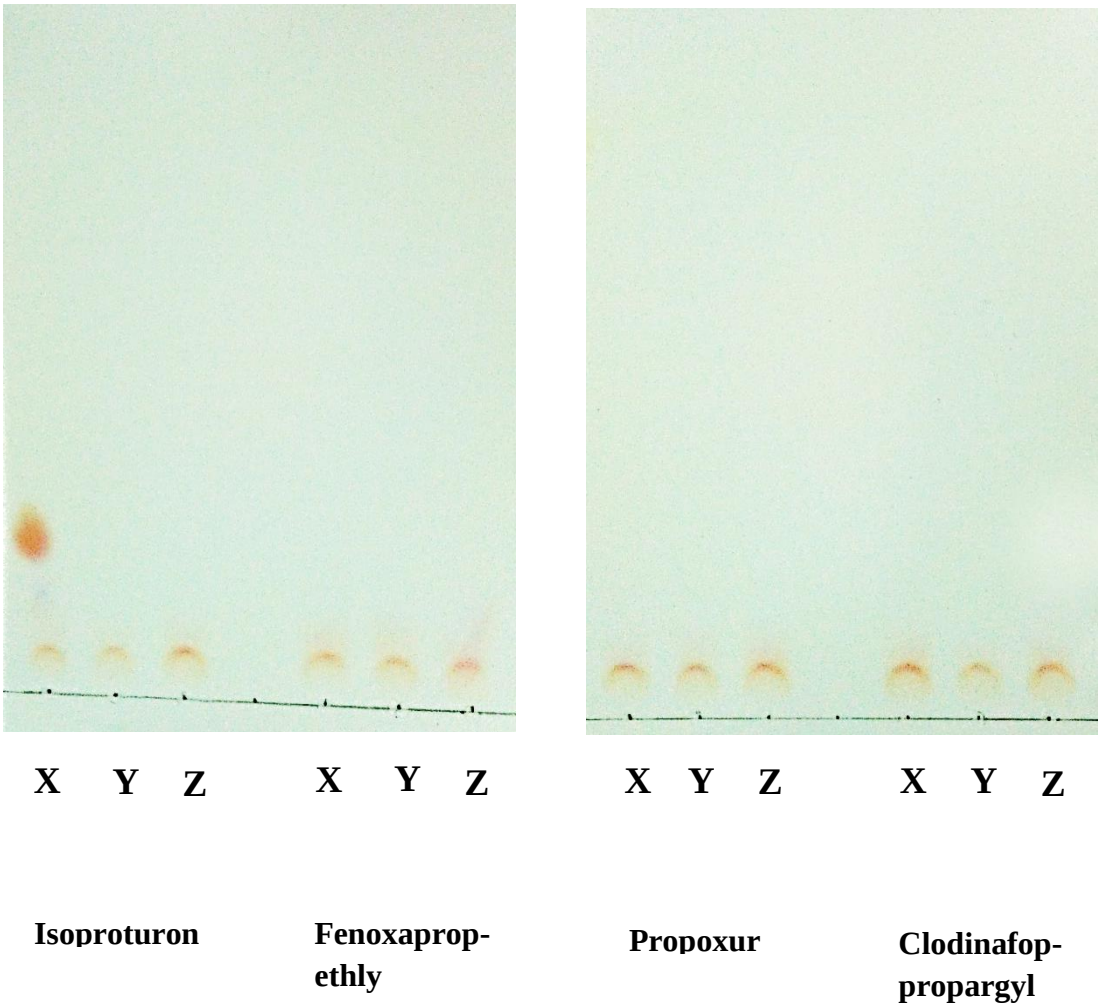


Figure 38

Figure 38: Conjugation happened between AcGST-2 with Isoproturon while AcGST-2 did not conjugate with Fenaxaprop-ethyl, Propoxur and Cladinafop-propargyl. (X) represents GST reaction is carried out with addition of purified protein sample and pesticide while (Y) and (Z) represents GST reactions are carried out without addition of pesticide and protein sample respectively.

5.2.2 Disc diffusion test towards pesticides and hydrogen peroxide

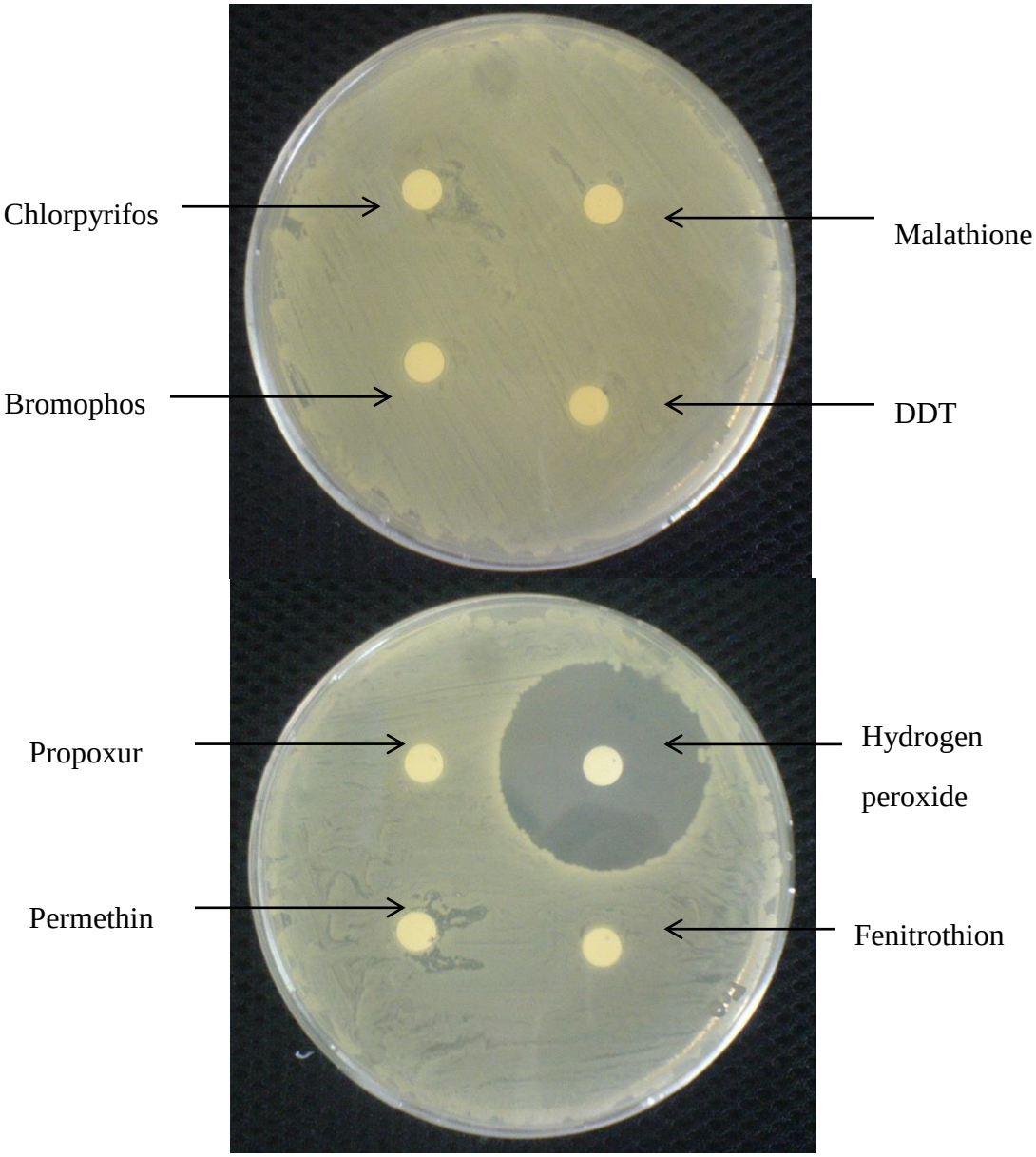


Figure 39

Figure 39 shows the susceptibility of *Acinetobacter calcoaceticus* Y1 towards 1 mg/ml pesticides and 50 % of hydrogen peroxide.

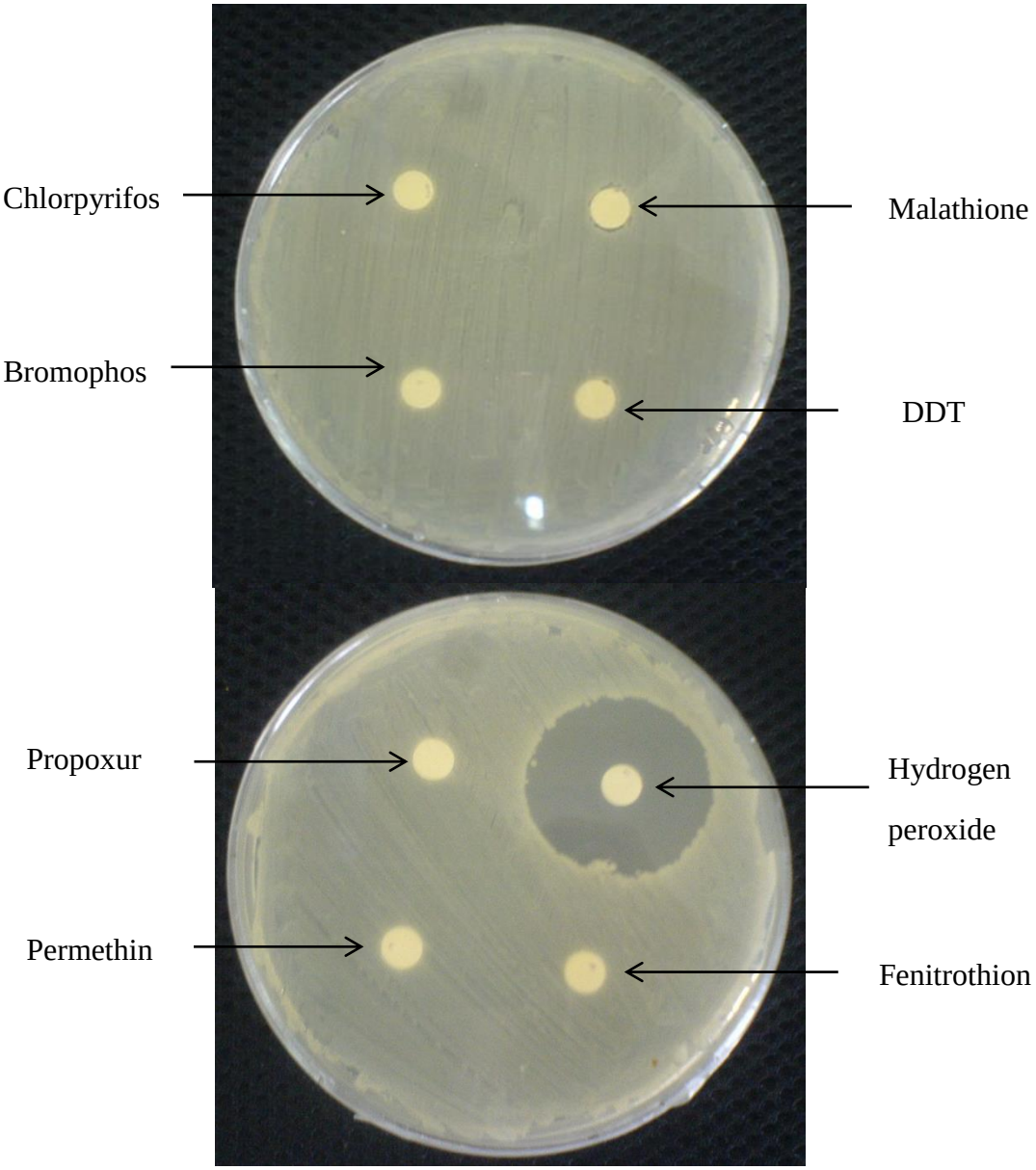


Figure 41

Figure 40 shows the susceptibility of *Acinetobacter calcoaceticus* Y1 towards 0.5 mg/ml pesticides and 25 % of hydrogen peroxide.

At 0.5 mg/ml and 1 mg/ml, all tested pesticides except from hydrogen peroxide did not affect the growth of *A. calcoaceticus* Y1. Zone of inhibition at 25% of hydrogen peroxide was smaller compared with 50% of hydrogen peroxide. This suggests the tolerance of *A. calcoaceticus Y1* towards hydrogen peroxide.

# 6.0 Discussion

In this project, bacteria were isolated from a chemical-contaminated site and the isolates were screened for GST production. Ten bacteria isolates were obtained, but out of these, only three bacteria isolates could form fluorescent colonies after spraying with monochlorobimane (MCB) under 365 nm wavelength light. Chloro derivative MCB was used instead of bromo derivative MBrB due to its lower reactivity, which provide higher selectively with glutathione in whole cells (Eklund *et al.*, 2002). To detect the bacteria isolate with the most prominent GST activity, the three bacteria isolates were further analysed using spectrophotometer. 1-Chloro-2,4-dinitrobenzene (CDNB) was chosen as a model substrate in the activity assay. CDNB conjugated with one molecule of GSH to give S-(2,4-dinitrophenyl) glutathione and changes of absorbance was recorded at 340 nm (Arca *et al.*, 1990). The bacteria isolate showed the highest GST activity towards CDNB was then identified from its 16S rRNA gene sequence. CDNB was chosen as model substrate for GST activity examination because most of the characterized GSTs reacted with CDNB and was a "universal" substrate for most GSTs. From the partial 16S rRNA gene sequence obtained, this bacteria isolate was identified as *Acinetobacter calcoaceticus* Y1, from the order Pseudomonadales.

The use of 16S rRNA gene sequence to study bacterial phylogeny and taxonomy was an ordinary and extensive used method for number of reasons. These reasons included (i) the 16S rRNA gene existed in almost all bacteria, often existing as a multigene family, or operons; (ii) the function of the 16S rRNA gene over time had not changed, suggesting that random sequence changes were a more accurate measure of time (evolution); and (iii) the 16S rRNA gene (1,500 bp) was large enough for informatics purposes (Janda & Abbott, 2007).

*A. calcoaceticus* was reported as an opportunistic pathogen with high degree of virulence (Henriksen, 1973). *A. calcoaceticus* had been reported to be a nosocomial pathogen in 1372 cases by the Centres for Disease Control (Spino & Geldreich, 1981) and was associated with ventilator associated pneumonias, urinary tract infections, surgical wound infections, and bloodstream infections (Blossom & Srinivasan, 2008). Three factors contributed to the emergence and recognition of *Acinetobacter* sp. as nosocomial pathogens: microbiological factors, host's factor and patient condition, and environmental factor (Towner, 1997).

*A. calcoaceticus* infections were quite difficult to cure by antibiotics due to antibiotics-resistance of the bacterial. Some *Acinetobacter* sp. had shown high resistance to beta-lactams, aminoglycosides, quinolones, and carbapenems (Reguero *et al.*, 2012). *Acinetobacter* sp. were chosen as environmental bacterial indicators due to their remarkable ability to develop resistance to antimicrobial agents, which made these microorganisms particularly suitable for monitoring antibiotic resistant in the environment (Guardabassi *et al.*, 1998). *A. calcoaceticus* had been reported to develop resistance towards gentamicin, minocycline, nalidixic acid, ampicillin, carbenicillin, cephalosporins, fluoroquinolones, semi synthetic aminoglycosides, and carbapenems (Manchanda *et al.*, 2010). Hence, it would be interesting to find out whether GSTs contributed to the antibiotics-resistance of *A. calcoaceticus*.

Purification of *A. calcoaceticus* Y1 putative GST (AcGST) from cells lysate produced a single band on SDS-PAGE gel at about 23 kDa. AcGST was purified by using the GSH-agarose column. GSH-agarose consisted of glutathione attached through the sulfur to epoxy activated 4% cross-linked beaded agarose resulting in a 12 atom (10 carbons) spacer. The binding capacity of GSH-agarose was about 5–10 mg GSTs per ml resin. AcGST had highest specific activity towards ethacrynic acid (EA) instead of CDNB.

The EA specific activity in *A. calcoaceticus* Y1 was lower as compared with catfish GSTs and rat pi class GST (Gardagbui & James, 2000).

In order to determine the number of putative GST isozymes in *A. calcoaceticus* Y1, the purified protein was analysed by using two-dimensional electrophoresis. Two putative GST isozymes, designated as AcGST-1 and AcGST-2, were identified at pI 4.5 and pI 6.2 respectively. To characterize these two putative GST isozymes independently, these two putative GST isozymes were separated on ion-exchange chromatography from the affinity eluate. Carboxymethyl (CM) Sepharose fast flow column was used to purify AcGST-1 (pI 4.5) while diethylaminoethyl (DEAE) Sepharose fast flow column was used to purify AcGST-2 (pI 6.2). CM Sepharose fast flow column, a weak cation exchanger with negatively charged carboxymethyl functional group in a mobile phase (pH 6) would bind to AcGST-2 (pI 6.2) while AcGST-1 (pI 4.5) come out in eluate (Note: When a protein is in a solution with a pH value above its pI its net charge is negative); DEAE Sepharose fast flow column, a weak anion exchanger with positively charged diethylaminoethyl group functional group in a mobile phase (pH 6) would bind to AcGST-1 (pI 4.5) while AcGST-2 (pI 6.2) come out in eluate (Note: When a protein is in a solution with a pH value below its pI its net charge is positive). Only “flow-through” fraction was collected and the eluates fraction containing salt (NaCl) were discarded from both of the columns. The eluates fraction containing NaCI were discarded because the eluates fraction from both of the columns did not show any conjugation activity towards EA and produced no band on SDS-PAGE gel. Protein in the eluates fraction believed to experience denaturation or distortion of the ionic interaction due to presence of sodium chloride (NaCl). There were basically two ways in affecting the protein stability with increasing salt concentration. The first way was through electrostatic influences on self-polarization energy and cross-polarization energy, or screening of electrostatic interactions and the second way was through the surface tension defined at the solute-

solvent interface with an increase in the salt concentration (Date & Dominy, 2013). The ions from the salt bound to ionic "R" groups and disrupted the ionic salt bridges or electrostatic interactions that stabilizing the tertiary and quaternary structures. The salts were thought to associate with oppositely charge groups in the protein. This combination of charged groups had higher tendency to bind water molecules rather than the charged groups and protein hydration was increased. Most of the proteins seldom experience changes in solubility until more salt was added to certain degree of salt concentration. At very high salt concentration, proteins preferred to bind ions instead of water molecules causing proteins dehydration and structure disruption.

From Figure 31, AcGST-2 form aggregate where a single band at 110 kDa was observed instead of at 23 kDa. This putative GST isozyme tended to form aggregate when it presented in single subunits and had about 5× molecular weight as compared with AcGST-1. The result contrasted with the two dimensional gel where AcGST-1 and AcGST-2 were at 23 kDa when these two putative GST isozymes were resolved at the same time (Figure 28). AcGST-2 was acetone precipitated instead of using concentrator because attempt to concentrate the sample using concentrator was futile in which no band was observed on SDS-PAGE albeit the molecular weight cut-off of the concentrator is way below the molecular weight of AcGST-2. Un-dissolvable white pellets were observed after acetone precipitation of AcGST-2. Intracellular aggregation of GSTs were reported from human pi class GST (hGSTP) (Ranganathan *et al.,* 2005) and *Onchocerca volvulus* GST (OvGST) (Liebau *et al.,* 1994). However, extracellular aggregation of GSTs had not been reported so far. There were typically five mechanisms of proteins aggregation: reversible association of native monomer, aggregation of conformationally-altered monomer, aggregation of chemically-modified product, nucleation-controlled aggregation and surface-induced aggregation (Philo & Arakawa, 2009). Our finding attributed the extracellular aggregation of AcGST-2 to the reversible association of the

native monomer mechanism (Figure 41). Protein monomers had tendency to form reversible associate. The surface of protein monomers were self-complimentary that led to self-associate of the monomers to form a reversible small oligomer. Size of oligomer was proportional to the concentration of the proteins and over time, these larger aggregates often became irreversible through the formation of covalent bonds such as disulphide bonds. Acetone precipitation of AcGST-2 resulted in white pellet formation that was visible to the naked eye. The aqueous layer around the protein monomers diminished as large amount of organic solvent was added to the proteins. This organic solvent continuously withdrew water from the protein monomer surface and bound as an aqueous layer around the organic solvent molecules. With this conformational change, the proteins aggregated through the electrostatic interaction.

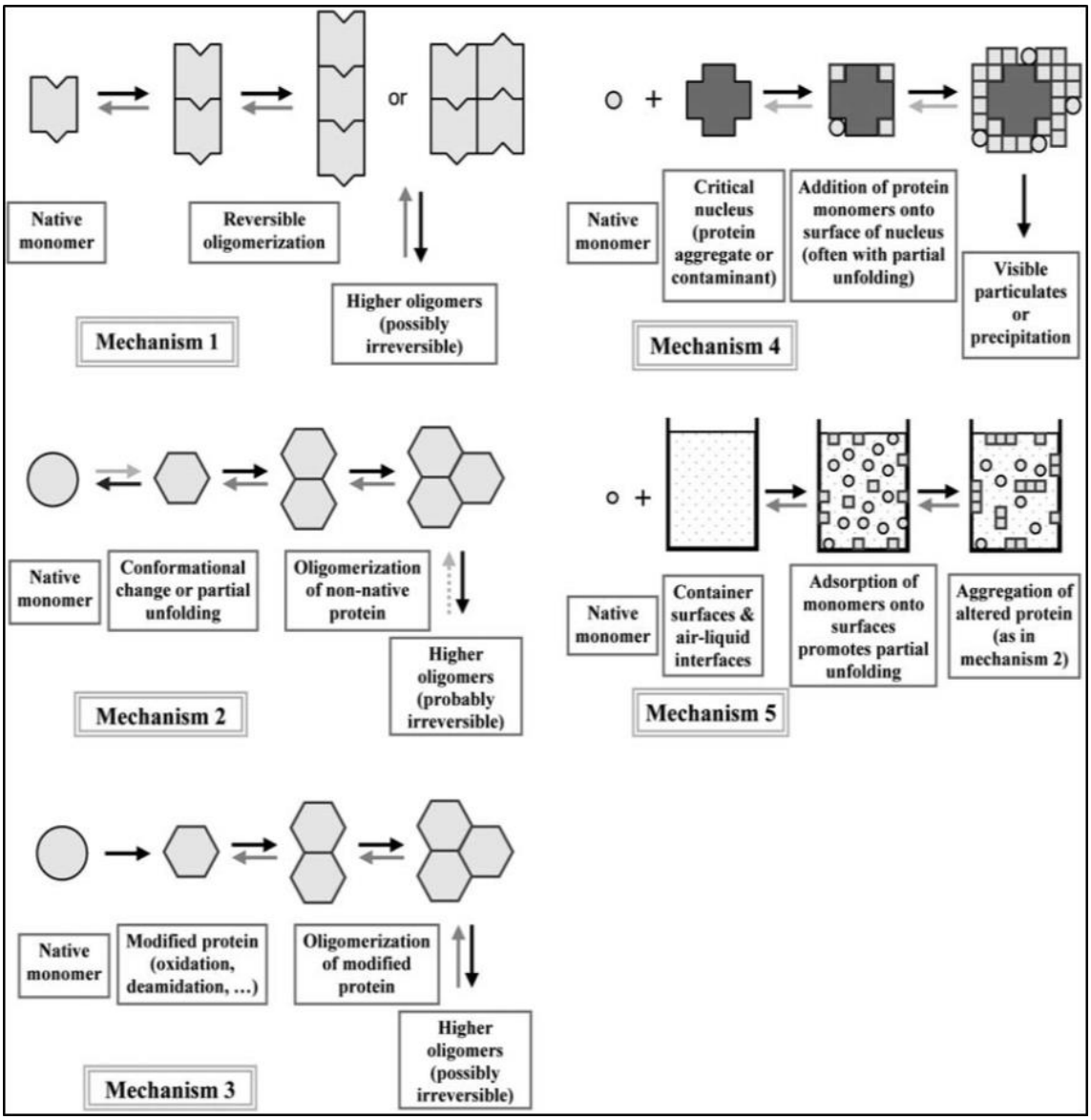


Figure 41: Schematic illustrations of five common aggregation mechanisms.

(Source: Philo & Arakawa, 2009)\

Substrate specificity test was performed to distinguish AcGST-1 and AcGST-2. The substrate specificities of both putative GST isozymes were different suggesting that they were of two different existing homodimers. Both putative GST isozymes were found to have highest conjugation activity towards EA which was 24.99 ± 1.24 µmol/min/mg and 15.87 ± 2.54 µmol/min/mg for AcGST-1 and AcGST-2 respectively. AcGST-1 and AcGST-2 were likely Pi class GST due to its high conjugation activity towards EA. Pi-class GST was characterized by its specific activity with EA (Kazemnejad *et al.*, 2006). Pi class GST three dimensional structure illustrated why Pi class GST had remarkable EA

conjugation activity. EA was bound to the ligand binding site (H site) while GSH was bound to the glutathione binding site (G-site). Figure 42 showed that Y108 (and possible N204) formed a hydrogen bond either directly or indirectly with the EA ketone oxygen, increasing the electrophilicity of the EA b-alkene carbon (Wu and Dong, 2012). The structure suggested bound glutathione was required for EA to dock into the H site in a productive binding mode (Oakley *et al.*, 1997). Pi class GST H site had been found to be comparatively open and explained the specificity towards the lesser hydrophobic substrates (Kazemnejad *et al.*, 2006).

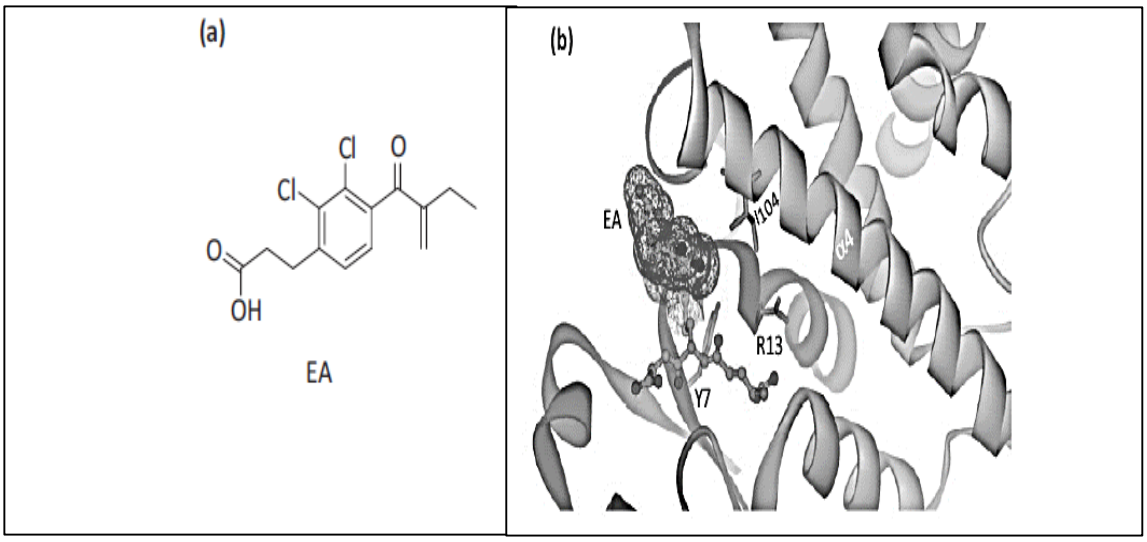


Figure 42: Crystal structure of Pi class GST during EA binding. (a) Chemical structure of EA (b) Binding of EA to the GST P1-1 active site

(Source: Wu and Dong, 2012)

The two putative GST isozymes from *A. calcoacticus* Y1 were active towards α:β-unsaturated carbonyl compounds. AcGST-1 conjugated towards 2,4-heptadienal (0.11 ± 0.03 µmol/min/mg), trans-2-octenal (0.08 ± 0.02 µmol/min/mg), and hexadienal (0.04 ± 0.003 µmol/min/mg) while AcGST-2 conjugated with towards 2,4-heptadienal (0.08 ± 0.01 µmol/min/mg), and trans-2-octenal (0.09 ± 0.01 µmol/min/mg). Free radical attack on polyunsaturated fatty acids initiated lipid peroxidation (LPO) chain reactions that

usually happened in the membrane lipid bilayer, leading to the production of highly reactive radical intermediates including alkanes, alkenes, aldehydes, ketones, and hydroxy-acids. Occurrences of aliphatic saturated and unsaturated aldehydes were mostly from the degradation of the hydroperoxides of arachidonic acid (20:4), linoleic acid (18:2) and docosahexaeneic acid (22:6). High concentration of aldehyde inside the cells implied greater oxidative stress. Conjugation of two putative GST isozymes towards α:β-unsaturated carbonyl compounds suggested that GSTs played a vital role in protecting the membrane lipid bilayer of *A. calcoaceticus* Y1 against oxidative stress.

Surprisingly, only AcGST-1 showed glutathione peroxidase activity towards hydrogen peroxide but not cumene hydrogen peroxide, and AcGST-2 did not react with both of the peroxides. AcGST-1 was likely a selenium-dependent glutathione peroxidase due to the specific activity of selenium-dependent glutathione peroxidase towards hydrogen peroxide (Doroshow *et al.,* 1980). This selenoprotein might contain one selenium per subunit which bound to cysteine named selenocysteine. However, according to Arthur (2000), only non-selenium dependent glutathione peroxidase activity was reported in GSTs but not selenium-dependent glutathione peroxidase activity. Non-selenium dependent glutathione peroxidase in GSTs mostly had highest conjugation activity towards organic peroxide but very little or no conjugation activity towards hydrogen peroxide. Our results suggesting that AcGST-1 was an antioxidant enzyme. According to Mugesh *et al.* (2002), the enzyme catalytic site had a selenocysteine residue in which the selenium involved in a redox cycle where the selenol (ESeH) as the active form to reduce hydrogen peroxides and organic peroxides. The selenol was oxidized to selenenic acid (ESeOH), which reacted with reduced glutathione (GSH) to form selenenyl sulfide adduct (ESeSG). A second glutathione then regenerated the active form of the enzyme by attacking the ESeSG to form the oxidized glutathione (GSSG) Thus, in overall

process, two equivalent of GSH were oxidized to the disulfide and water, while the hydroperoxide was reduced to the corresponding alcohol (Mugesh *et al.,* 2002)

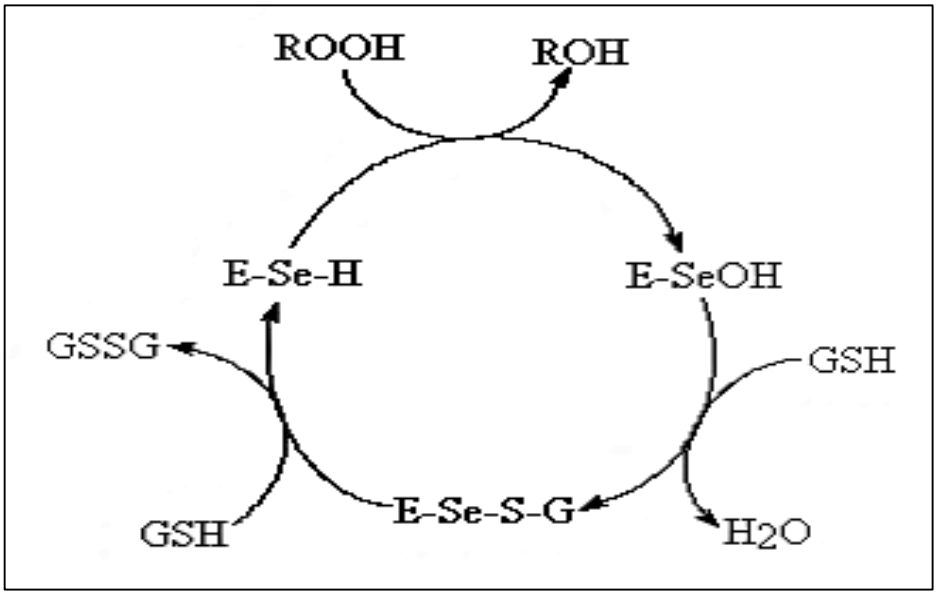


Figure 43: Proposed catalytic mechanism of glutathione peroxidase.

(Source: Mugesh *et al.,* 2002)

In order to gain insight into the kinetic mechanism, as well as to obtain the true $K_m$ and $V_{max}$ values for both GSH and ethacrynic acid (EA), steady-state kinetics were developed for AcGST-1 and AcGST-2. The way to do this was to experimentally determine the rate of reaction [V] over different concentration of substrates [S]. A number of plots were drawn to determine the true value of $V_{max}$ and $K_m$. Lineweaver-Burke plot, 1/[V] versus 1/[S] produced a straight line with a y-intercept = $1/V_{max}$ and a slope $=K_m/V_{max}$.

$$\frac{1}{V} = \frac{1}{Vmax} + \frac{Km}{Vmax}\frac{1}{[S]} \qquad (1)$$

From Lineweaver-Burke plot, Michaelis-Menten Equation (1) was able to obtain where V is the rate of reaction, $K_m$, is the Michaelis-Menten constant, $V_{max}$ is maximum velocity

and [S] is substrate concentration. According to Equation 1, when [S]=$K_m$ and V=$V_{max}$/2, $K_m$ was equal to substrate concentration at half of the maximum reaction rate. Hanes-Woolf plot, [S]/V versus [S] produced a straight line with a y-intercept= [S]/V and a slope=1/$V_{max}$

$$\frac{[S]}{V} = \frac{[S]}{Vmax} + \frac{Km}{Vmax} \quad (2)$$

From Equation 2, it yielded a perfect data where the slope of the line was 1/$V_{max}$ and x-intercept –$K_m$. Eadie-Hofstee plot, V versus V/[S] produced a negative slope with a y-intercept= V and a slope= -$K_m$.

$$V = -Km\frac{V}{[S]} + Vmax \quad (3)$$

From Equation 3, it yielded $V_{max}$ as y-intersect and –$K_m$ as the negative slope. For AcGST-1, the $V_{max}$ for EA and GSH were estimated as 3.74 ± 1.40 µmol/min and 1.46 ± 0.02 µmol/min, $K_m$ for EA and GSH were estimated as 0.28 ± 0.02 mM and 0.01 ± 0.0003 mM. Whereas for AcGST-2, the $V_{max}$ for EA and GSH were estimated as 8.41 ± 1.08 µmol/min and 1.35 ± 0.01 µmol/min, $K_m$ for EA and GSH were estimated as 0.28 ± 0.002 mM and 0.02 ± 0.003 mM. EA was chosen as a substrate to determine the kinetic properties of AcGST-1 and AcGST-2 due to their significant reactivity towards EA. $V_{max}$ and $K_m$ value for AcGST-1 and AcGST-2 towards EA and GSH were extremely low. It is suggested that EA was a GST inhibitor at certain concentration of GSH in the system. According to Awasthi *et al.* (1993), EA-GSH conjugate was a more potent inhibitor of GSTs than EA itself. Based on the $K_m$ value obtained for AcGST-1 and AcGST-2 towards GSH, the $K_m$ value was directly proportional to the amount of EA-GSH conjugate. High affinity towards GSH promoted the formation of EA-GSH conjugate as the $K_m$ value decreased

and thus promoted the inhibition of GSTs in the system. This explained the reason why the $V_{max}$ and $K_m$ value obtained for AcGST-1 and AcGST-2 were relatively low.

N-terminal sequencing was unable to produce a satisfactorily reliable result and generated inconsistent results on every replicates. Sequencing was achieved by repeated cycles of chemical reaction, and an amino acid (residue) was detected or called by its increase in signal during a particular cycle. However, strong valine and glycine peak present in all cycle during AcGST-1 analysis and strong methionine and glycine peak present in all cycle during AcGST-2 analysis. In each amino acid position there could be more than one residue apparent. This reflected inherent background effects such as the internal cleavage of the full protein during the sequencing procedure which created a second, third, and following N-terminus. Since the first and second positions were subjected to higher background signal and difficult to analyse, thus the present of possible contaminants was suggested.

MALDI-TOF analysis was unable to identify AcGST-1 and AcGST-2 as a family of GSTs from *A. calcoacticus*. According to Zhan *et al.* (2012), there were 10 putative GST protein had been reported from complete genome analysis of *A. calcoaceticus* PHEA-2 (Table 9). Of these expressed proteins, two proteins were closely resemble to AcGST-1 and AcGST-2 purified from our research. As shown in Table 9, The UniProt identifiers of F0KLY9 (putative glutathione transferase) and F0KKB0 (Glutathione S-transferase III) are similar in MW and pI values to AcGST-1 and AcGST-2, respectively. Nervertheless, more comfirmative evaluation was needed for the identification of these two GST isozymes, such as targeted proteomics using Triple quadrupole mass spectrometry.

Table 9: List of putative glutathione transferases of *Acinetobacter calcoaceticus* (strain PHEA-2) retrieved from http://www.uniprot.org/uniprot/.

| UniProt identifiers | Protein name | Gene name | Amino acid length | pI/MW |
|---|---|---|---|---|
| **F0KLY9** | **Putative glutathione transferase** | **Erd13 BDGL_0033315** | **201** | **4.85/22385.40** |
| **F0KKB0** | **Glutathione transferase III** | **gst3 BDGL_000699** | **214** | **5.97/24579.78** |
| F0K199 | Putative glutathione transferase | gstB BDGL_000451 | 203 | 4.91/22987.64 |
| F0KI95 | Putative glutathione transferase | yliJ BDGL_000447 | 208 | 5.19/24435.28 |
| FOKGP1 | Glutathione transferase FosA | fosA BDGL_002726 | 135 | 5.34/15740.79 |
| FOKH55 | Putative glutathione transferase | BDGL_001572 | 228 | 6.01/26244.78 |
| F0KL12 | Glutathione transferase-like protein | yghU BDGL_000797 | 282 | 5.62/31834.09 |
| F0KLP2 | Glutathione transferase | BDGL_000872 | 246 | 5.52/28865.77 |
| FOKND6 | Putative glutathione transferase | yfcG BDGL_003500 | 206 | 5.13/23912.28 |
| FOKJF2 | Glutathione transferase | gst3 BDGL_003061 | 222 | 6.79/26004.25 |

To determine the reactivity of both putative GST isozymes towards Isoproturon, Fenoxaprop-ethyl, Propoxur and Clodinafop-propargyl, a colorimetric method using thin layer chromatography was developed. Our results showed that AcGST-1 did not react with all the tested pesticides, but AcGST-2 conjugated with Isoproturon. After scrutinizing the chemical structure of Isoproturon, there was a presence of an amide bond. Hence, it was suggested that AcGST-2 broke down the amide bond in Isoproturon during conjugation and formed an enzyme-substrate complex.

For disc diffusion test, 0.5 mg/ml and 1 mg/ml of Bromophos, Malathione, DDT, Propoxur, Permethin, Chlorpyrifos and Fenitrothion were prepared. These pesticides did not inhibit the propagation of *A. calcoaceticus* Y1 but on the other hand, hydrogen peroxide inhibited the propagation of *A. calcoaceticus* Y1. Zone of inhibition at 25% of hydrogen peroxide was smaller compared with 50% of hydrogen peroxide. Thus, it was suggested that there was a mild resistance of *A. calcoaceticus* Y1 towards hydrogen peroxide and that it could tolerate lower concentration of hydrogen peroxide. Reactivity of AcGST-1 towards hydrogen peroxide might contribute to the mild tolerance of *A. calcoaceticus* Y1 to hydrogen peroxide. Hydrogen peroxide had been proven to cause severe damages to cells; hence, it was eminent for *A. calcoaceticus* Y1 to produce an antioxidant enzyme to cope with this oxidative stress.

# 7.0 Conclusion

Ten bacteria isolates obtained from chemically-contaminated soil were sprayed with monochlorobimane. Three GST-expressing bacteria isolates produced fluorescent colonies when viewed under 365 nm UV light. These 3 bacteria isolates were measured to determine their GSTs activity. The bacteria isolate with the most promising GST activity was identified as *Acinetobacter calcoaceticus* Y1 based on its 16S rRNA gene sequence. Putative GST from *A. calcoaceticus* Y1 (AcGST) was successfully purified by using GSH agarose affinity chromatography and suggesting it was a dimer made up of 23kDa subunit. These subunits were then resolved into two different putative GST isozymes designated as AcGST-1 and AcGST-2 which had pl a value of 4.5 and 6.2 respectively. AcGST-1 and AcGST-2 were isolated separately by using carboxymethyl (CM) and diethylaminoethyl (DEAE) ion exchange chromatography.

Based on the substrate specificity test, AcGST-1 and AcGST-2 were completely two different putative GST isozymes and thus it is believed that they were of two existing homodimers. AcGST-1 conjugated towards ethacrynic acid (EA) (24.99 ± 1.24 µmol/min/mg), hydrogen peroxide (3.93 ± 0.32 µmol/min/mg), 1-Chloro-2,4-dinitrobenzene (CDNB) (0.61 ± 0.12 µmol/min/mg), 2,4-heptadienal (0.11 ± 0.03 µmol/min/mg), trans-2-octenal (0.08 ± 0.02 µmol/min/mg), and hexadienal (0.04 ± 0.003 µmol/min/mg) while AcGST-2 conjugated with EA (15.87 ± 2.54 µmol/min/mg ), CDNB (0.54 ± 0.13 µmol/min/mg), 2,4-heptadienal (0.08 ± 0.01 µmol/min/mg), and trans-2-octenal (0.09 ± 0.01 µmol/min/mg). AcGST-2 showed no conjugation activity towards hexadienal and hydrogen peroxide, on the other hands, AcGST-1 conjugated with both of the mentioned substrates. High conjugation activity of AcGST-1 and AcGST-2 towards EA suggesting they were belonging to pi class GST as EA is a specific substrate for pi class GST. AcGST-1 had selenium dependent glutathione peroxidase activity

because hydrogen peroxide was a specific substrate to selenium dependent glutathione peroxidase. AcGST-1 and AcGST-2 appeared to be an antioxidant enzymes since they conjugated with products of lipid peroxidation and hydrogen peroxide. This was imperative for *A. calcoaceticus* to cope with intracellular oxidative stress.

For AcGST-1, the $V_{max}$ for EA and GSH were estimated as 3.74 ± 1.40 μmol/min and 1.46 ± 0.02 μmol/min, $K_m$ for EA and GSH were estimated as 0.28 ± 0.02 mM and 0.01 ± 0.0003 mM. Whereas for AcGST-2, the $V_{max}$ for EA and GSH were estimated as 8.41 ± 1.08 μmol/min and 1.35 ± 0.01 μmol/min, $K_m$ for EA and GSH were estimated as 0.28 ± 0.002 mM and 0.02 ± 0.003 mM. $V_{max}$ value of AcGST-2 towards EA was higher as compared with $V_{max}$ value of AcGST-1 towards EA. This indicated the higher catalytic efficiency of AcGST-2 compared with AcGST-1. The $K_m$ value of AcGST-1 and AcGST-2 towards GSH were extremely low and both of the GST isozymes only required very tiny concentration of GSH for maximal enzymatic activity. AcGST-2 had higher affinity towards GSH as compared to AcGST-1.

An attempt to identify AcGST-1 and AcGST-2 by N-terminal sequencing and MALDI-TOF analysis were futile. Both methods were unable to produce satisfactorily reliable results and generated inconsistent results on every replicates. Although the application of N-terminal sequencing and MALDI-TOF analysis were not successful in identifying AcGST-1 and AcGST-2 as GSTs, however our studies provided supportive evidences suggesting that AcGST-1 and AcGST-2 were GSTs. The utmost evidence was the binding of AcGST-1 and AcGST-2 to GSH agarose matrix during purification from cell lysate. Only specific enzymes with GSH binding site would conjugate with GSH and they were GSTs. The following proof was that AcGST-1 and AcGST-2 conjugated with GST common substrates such as CDNB and EA. A more concrete evidence appeared with the recent developed method by spraying monochlorobimane on *Acinetobacter calcoaceticus* Y1 colonies and fluorescent colonies were observed. Moreover, based on

our finding, AcGST-1 and AcGST-2 possessed hydroperoxidase activity. The UniProt identifiers of F0KLY9 (putative glutathione transferase) and F0KKB0 (Glutathione S-transferase III) closely resembled to AcGST-1 and AcGST-1 on the basis of molecular weight and pI.

In order to determine the reactivity of both putative GST isozymes towards Isoproturon, Fenoxaprop-ethyl, Propoxur and Clodinafop-propargyl, thin layer chromatography was performed. From the results obtained, AcGST-1 did not conjugate with all the tested pesticides while AcGST-2 conjugated with Isoproturon.

In disc diffusion test, *A. calcoaceticus* Y1 was tested against two different concentrations (0.5 mg/ml and 1 mg/ml) of Bromophos, Malathione, DDT, Propoxur, Permethin, Chlorpyrifus, Fenitrothion and (25% and 50%) hydrogen peroxide. Only hydrogen peroxide alone inhibited the growth of *A. calcoaceticus* Y1, and the zone of inhibition at 25% of hydrogen peroxide was smaller compared with 50% of hydrogen peroxide. This suggested a certain tolerance level of *A. calcoaceticus* Y1 towards hydrogen peroxide.

In conclusion, two putative GST isozymes which were designated as AcGST-1 (pI 4.5) and AcGST-2 (pI 6.2) were successfully isolated from *A. calcoaceticus* Y1, a bacteria strain isolated from a chemically-contaminated site. Both putative GST isozymes conjugated with GST common substrates CDNB and EA. AcGST-1 reacted with hexadienal, trans-2-octenal, 2,4-heptadienal and hydrogen peroxide while AcGST-2 reacted with trans-2-octenal and 2,4-heptadienal. The substrate specificities of both putative GST isozymes were different and therefore suggesting they were of two existing homodimers. AcGST-2 was found to conjugate with a pesticide named Isoproturon. Lastly, more comfirmative evalution was required in order to validate these two putative GST isozymes, such as targeted proteomics using Triple quadrupole mass spectrometry.

# 8.0 References


Alias, Z., and Clark, A, G. (2007). Studies on the glutathione S-transferase proteome of adult *Drosophila melanogaster*: Responsiveness to chemical challenge. *Proteomics.* 7: 3618–3628.

Allocati, N., Federici, L., Masuli, M., and Di Ilio, C. (2008). Glutathione transferases in bacteria. *FEBS J*. 276:58-76.

Anandarajah, K. Kiefer, P. M., Jr., Donoboe, B. S., and Copley, S. D. (2000). Recruitment of a double bond isomerase to serve as a reductive dehalogenase during biodegradation of pentachlorophenol. *Biochemistry.* 39: 5303-5311.

Anuradha, D., Reddy, K. V., Kumar, C., Neeraja, S., Reddy P. R. K., and Reddnna P. (2000). Purification and characterization of rat testicular glutathione S-transferases: role in the synthesis of eicosanoids. *Asian J. Androl.* 2: 277-282.

Arca, P. Rico, M., Brana, A. F., Villar, C. J., Hardisson, C., and Suzrez, J. E. (1988). Formation of an adduct between fosfomycin and glutathione: a new mechanism of antibiotic resistance in bacteria**.** *Antimicrob. Agents. Chemother.* 32(10):1552.

Arca, P., Hardisson, C., and Suarez, J. E. (1990). Purification of a glutathione S-transferase that mediates fosfomycin resistance in bacteria. *Antimicrob. Agents. Chemother*. 34(5): 844-848.

Arca, P., Garcia, P., Hardisson, C., and Suarez, J. E. (1990). Purification and study of a bacterial glutathione S-transferase. *FEBS Lett*. 263(1): 77-79.

Arthur, J. R. (2000). The glutathione peroxidases. *Cell. Mol. Life Sci.* 57: 1825-1835.

Awasthi, S., Srivastava, S. K., Ahmad, F., Ahmad, H., and Ansari, G. A. S. (1993). Interactions of glutathione S-transferase-π with ethacrynic acid and its glutathione conjugate. *Biochem. Biophys. Acta.* 1164(2): 173-178.

Bader, R., and Leisinger, T. (1994). Isolation and characterization of the *Methylophilus* sp. strain DM11 gene encoding dichloromethane dehalogenase/glutathione S-transferase. *J. Bacteriol.* 176(12): 3466.

Bartels, F., Backhaus, S., Moore, E. R., Timmis, K. N. and Hofer, B. (1999) Occurrence and expression of glutathione S-transferase-encoding bphK genes in *Burkholderia* sp. strain LB400 and other biphenyl-utilizing bacteria. *Microbiology* 145: 2821–2834.

Ben-Arie, N., Khen, M. and Lancet, D. (1993). Glutathione S transferase in rat olfactory epithelium: Purification, molecular properties and odorant biotransformation. *Biochem. J.* 292: 379–384.

Bernat, B. A., Laughlin, L. T., and Armstrong, R. N. (1997). Fosfomycin resistance protein (FosA) is a manganese metalloglutathione transferase related to glyoxalase I and the extradiol dioxygenases. *Biochemistry.* 36: 3050-3055.

Blossom, D. B., and Srinivasan, A. (2008). Drug Resistant *Acinetobacter baumannii calcoaceticus* complex an emerging nosocomial pathogen with few treatment options. *Infect. Dis. Clin. Prac.* 16(1): 1-3.

Board, P. G., Anders M. W., and Blackburn, A. C. (2005). Catalytic function and expression of glutathione transferase Zeta. *Methods in Pharmacology and Toxicology, Drug Metabolism and Transport: Molecular Methods and Mechanisms.* New Jersey: Totowa.

Bradford, M. (1976). A rapid and sensitive method for the quantitation of microgram quantities of protein utilizing the principle of protein-dye binding. *Anal. Biochem*. 72:248-254.

Brophy, P. M., Southan, C., and Barrett, J. (1989). Glutathione transferases in the tapeworm *Moniezia expansa*. *Biochem. J.* 262: 939-946.

Bryan, M. C., Bernat, A., Wang, Z. P., Armstrong, R. N., and Helmann, J. D. (2001). FosB, a cysteine-dependent fosfomycin resistance protein under the control of $\sigma^w$, an extracytoplasmic-function σ factor in *Bacillus subtilis. J. Bacteriol.* 183(7): 2380-2383.

Brune, B. (2003). Nitric oxide: NO apoptosis or turning it ON? *Cell. Death. Differ.* 10: 864–869.

Copley, S. D.( 1998). Microbial dehalogenase: enzymes recruited to convert xenobiotic substrates. *Curr. Opin. Chem. Biol.* 2: 613-617.

Dainelli, B., Paludi, D., Drahani, B., Cocco, R., Principe, D. R., Petrucci, M., Mucilli, F., Faraone, A., and Aceto, A. (2002). A novel glutathione transferase from *Haemophilus influenza* which has high affinity towards antibiotics. *Int. J. Biochem. Cell. B.* 34: 916-920.

Date, M. S. and Dominy, B. N. (2013). Modelling the influence of salt on the hydrophobic effect and protein fold stability. *Commun. Comput. Phys.* 13(1): 90-106.

Dhar, K., Dhar, A., and Rosazza, J. P. N. (2003). Glutathione S-transferase isozymes from *Streptomyces griseus. Appl. Environ. Microbiol.* 69(1):707.

Di Ilio, C., Aceto, A., Piccolomini, R., Allocati, N., Faraone, A., Cellini, L., Ravagnan, G., and Federici, G. (1988). Purification and characterization of three forms of glutathione transferase from *Proteus mirabilis*. *Biochem. J.* 255: 971-975.

Dixon, D. P., Lapthorn, A., and Edwards, R. (2002). Plant glutathione transferases. *Genome Biol.* 3(3): 1-10.

Doroshow, J. H., Locker, G. Y., and Myers, C. E. (1980). Enzymatic defences of the mouse heart against reactive oxygen metabolites. *J. Clin. Invest.* 65: 128-135

Dulce, R. A., Schulman, I. H., and Hare, J. M. (2010). S-glutathionylation: A redox-sensitive switch participating in nitroso-redox balance. *Nature*. 468:1115–1118.

Dwivedi, S., Sharma, A., Patrick, B., Sharma, R., and Awasthi, Y. C. (2007). Role of 4-hydroxynonenal and its metabolites in signalling, *Redox Rep*. 12(1): 4-10.

Edwards, R., and Cixon, D. P. (2005). Plant glutathione transferase. *Meth. Enzymol*. 401: 169-186.

Eklund, B, I., Edalat, M., Stenberg, G., and Mannervik, B. (2002). Screening for recombinant glutathione transferase active with monochlorobimane. *Anal. Biochem.* 309: 102-108.

Emanuelsson, M. A., and Osuna, M. B. (2009). Isolation of a *Xanthobacter* sp. degrading dichloromethane and characterization of the gene involved in the degradation. *Biodegr.* 20: 235–244.

Fahey, R. C., Buschbacher, R. M., and Newton, G. L. (1987). The evolution of glutathione metabolism in phototrophic microorganisms. *J. Mol. Evol.* 25: 81-88.

Fang, T., Li, D. F., and Zhou, N. Y. (2011). Identification and clarification of the role of key active site residues in bacterial glutathione S-transferase zeta/maleylpyruvate isomerase. *Biochem. Biophys. Res. Commun.* 410: 452-456.

Fahey, R. C., Brown, W. C., Adams, W. B., and Worsham, M. B. (1978). Occurrence of glutathione in bacteria. *J. Bacteriol.* 133(3): 1126-1129.

Favaloro, B., Melino, S., Petruzzelli, R., Di Illio, C., and Rotilio, D. (1998). Purification and characterization of a novel glutathione transferase from *Ochrobactrum anthropic*. *FEMS Microbiol. Lett.* 160: 81-86.

Fetzner, S. (1998). Bacterial dehalogenation. *Appl. Microbiol. Biotechnol.* 50: 633-657

Fillgrove K. L., Pakhomova, S., Newcomer, M. E., and Armstrong, R. N. (2003). Mechanistic diversity of fosfomycin resistance in pathogenic microorganisms. *J. Am. Chem. Soc.* 125: 15730- 15731.

Guardabassi, L., Peterson, A., Olsen, J. E., and Dalsgaad, A. (1998). Antibiotic resistance in *Acinetobacter* sp. isolated from sewers receiving waste effluent from a hospital and a pharmaceutical plant. *Appl. Environ. Microbiol.* 64(9):3499.

Harris, J. M., Meyer, D. J., Coles, B., and Ketterer, B. (1991). A novel glutathione transferase (13-13) isolated from the matrix of rat liver mitochondria having structural similarity to class Theta enzymes. *Biochem. J.* 278: 137-141.

Garcia, P., Arca, P., and Suarez, J. E. (1995). Product of FosC, a gene from *Pseudomonas syringae*, mediates fosfomycin resistance by using ATP as cosubstrate. *Antimicrob. Agents Chemother.* 39(7): 1569-1573.

Gardagbui, B. K. M. and James, M. O. (2000). Activities of affinity-isolated glutathione S-transferase (GST) from channel catfish whole intestine. *Aquat. Toxicol.* 49: 27-37.

Habig, W. H., Pabst, M. J., and Jakoby, W. B. (1974) Glutathione S-transferase: the first enzymatic step in mercapturic acid formation. *J. Biol. Chem*. 249: 7130-7139.

Han, X. Y. (2006). Advanced Techniques in Diagnostic Microbiology: *Bacterial Identification Based on 16S Ribosomal RNA Gene Sequence Analysis*. United States: Springer.

Henriksen, S. D. (1973). *Moraxella, Acinetobacter*, and the *Mimeae. Bacteriol Rev.* 34(4): 522-561.

Jakobsson, P. J., Mancini, J. A., Riendeau, D., and Ford-Hutchinson, A. (1997). Characterization of a novel microsomal enzyme with glutathione-dependent transferase and peroxidase activities. *J. Biol. Chem.* 272(36): 22934-22939.

Jakobsson, P. J., Morgenstern, R., Mancini, J., Ford-Hutchinson, A., and Persson, B. (2000). Membrane-associated proteins in eicosanoid and glutathione metabolism (MAPEG). *Am. J. Respir. Crit. Care. Med.* 161: 20-24.

Janda, J. M. and Abbott, S. L. (2007). 16S rRNA gene sequencing for bacterial identification in the diagnostic laboratory: Pluses, Perils, and Pitfalls. *J. Clin. Microbiol*. 45(9): 2761-2764.

Jung, U., Cho, Y. S., Seong, H. M., Kim, S. J., Kim Y. C., and Chung, A. S. (1996). Characterization of novel glutathione S-transferase from *Pseudomonas* sp. DJ77. *J. Biochem. Mol. Biol.* 29(2): 111-115.

Kayser, M. F., and Vuilleumier, S. (2001). Dehalogenation of dichloromethane by dichloromethane dehalogenase/glutathione S-transferase leads to formation of DNA adducts. *J. Bacteriol.* 183(17): 5209-5212.

Kazemnejad, S., Rasmi, Y., Sharifi, R. and Allameh, A. (2006). Class-Pi of glutathione S-transferase. *Iranian J. Biotech.* 4(1): 1-16.

Laemmli U. K. (1970). Cleavage of structural proteins during assembly of the head of bacteriophage T4. Nature. 227: 680-685.

Liu, M. L., Zhou, L. J., Xu, A. M., Lam, K. S. L., Wetzel, M. D., Xiang, R. H., Zhang, J. J., Xin, X. B., Dong, L. Q., and Liu. F. (2008). A disulfide-bond A oxidoreductase-like protein (DsbA-L) regulates adiponectin multimerization. *Proc. Natl. Acad. Sci*. 18302-18307.

Laborde, E., (2010). Glutathione transferases as mediators of signalling pathways involved in cell proliferation and cell death. *Cell. Death. Differ.* 17: 1373-1380.

Lizuka, M., Inoue, Y., Murata, K., and Kimura, A. (1989). Purification and some properties of glutathione S-transferase from *Escherichia coli* B. *J. Bacteriol.* 171(11):6039.

Manchanda, V., Sanchaita, S., and Singh, N. P. (2010). Symposium of infections agents in a multidrug resistance globe. *J. Global. Infect. Dis.* 2(3): 291-304.

Marsh, M., Shoemark, D. K., Jacob, A., Robinson, C., Cahill, B., Zhou, N. Y., Williams, P. A., and Hadfield, A. T. (2008). Structure of bacterial glutathione S-transferase maleyl pyruvate isomerase and implications for mechanism of isomerisation. *J. Mol. Biol.* 284: 165-177.

Mattson, M. P. (2009). Roles of the lipid peroxidation product 4-hydroxynonenal in obesity, the metabolic syndrome, and associated vascular and neurodegenerative disorders. *Exp. Gerontol.* 44(10): 625–633.

McCarthy, D. L., Navarrete, S., Willett, W. S., Babbitt, P. C., and Copley, S. D. (1996). Exploration of the relationship between tetrachlorohydroquinone dehalogenase and the glutathione S-transferase superfamily. *Biochemistry.* 35: 14634-14642.

McCharthy, D. L., Claude, A. A., and Copley, S. D. (1997). In Vivo levels of chlorinated hydroquinones in a pentachlorophenol-degrading bacterium. *Appl. Microbiol.* 63(5): 1883-1888.

Mendoza, C., Garcia, J. M., Llaneza, J., Mendez, F. J., Hardisson, C., and Ortiz, J. M. (1980). Plasmid-determined resistance to fosfomycin in *Serratia marcescens. Antimicrob. Agents Chemother.* 18(2) 215-219.

Mignogna, G., Allocati, N., Aceto, A., Piccolomini, R., Di Ilio, C., Barra, D., and Martini, F. (1993). The amino acid sequence of glutathione transferase from *Proteus mirabilis*, a prototype of a new class of enzymes. *Eur. J. Biochem.* 211: 421-425.

Mohsenzadeh, S., Esmaeili, M., Moosavi, F., Shahrtash, M., Saffari, B., and Mohabatkar, H. (2011) Plant glutathione S-transferase classification, structure and evolution. *Afr. J. Biotechnol.* 10(42).

Molina, D. M., Eshagi, S., and Nordlund, P. (2008). Catalysis within the lipid bilayer structure and mechanism of the MAPEG family of integral membrane proteins. *Curr. Opin. Struc. Biol.* 18: 442–449.

Mortz, E., Krogh, T. N., Vorum, H., and Görg, A. (2001) Improved silver staining protocols for high sensitivity protein identification using matrix-assisted laser desorption/ionization-time of flight analysis, *Proteomics*, 1: 1359-1363.

Morgenstern, R., and DePierre, J. W. (1983). Microsomal glutathione transferase: purification in inactivated form and further characterization of the activation process, substrate specificity and amino acid composition. *Eur. J. Biochem.* 134: 591 – 597.

Motoyama, N., and Dauterman, W.C. (1977) Purification and properties of housefly glutathione S-transferase. *Insect Biochem*. 7: 361–269.

Mugesh, G., Panda, A., Apte, S. D., Singh, H. B., and Butcher. R. J (2002). Intramolecularly coordinated diorganyl ditellurides: Thiol peroxidase-like antioxidants. *Organometallics.* 21: 884-892.

Neuhoff V., Stamm R., and Eibl H. (1985). Clear background and highly sensitive protein staining with Coomassie Blue dyes in polyacrylamide gels: A systematic analysis. *Electrophoresis*. 6(9): 427-448.

Nicholson, D. W., Ali, A., Klembat, M. W., Munday, N. A., Zamboni, R. J., and Ford-Hutchinson, A. W. (1992). Human leukotriene $C_4$ synthase expression in dimethylsulfoxide-differentiated U937 cells. *J. Biol. Chem.* 267(25): 17849-1785.

Oakley, A. J., Rossjohn, J., Lo Bello, M., Caccuri, A. M., Federici, G., and Parker, M. W. (1997). The three-dimensional structure of the human Pi class glutathione transferase P1-1 in complex with the inhibitor ethacrynic acid and its glutathione conjugate. *Biochem.* 36(3): 576-585.

Pajaud, J., Kumar, S., Rauch, C., Morel, F., and Aninat, C. (2012). Regulation of signal transduction by glutathione transferases. *Int. J. Hepatol*. 2012: 1-11.

Petit, E., Michelet, X., Rauch, C., Bertrand-Michel, J., Terce, F., Legouis, R., and Morel, F. (2009). Glutathione transferases kappa 1 and kappa 2 localize in peroxisomes and mitochondria, respectively, and are involved in lipid metabolism and respiration in *Caenorhabditis elegans*. *FEBS J.* 276: 5030-5040.

Pemble, S. E., Wardle, A. F., and Taylor, J. B. (1996). Glutathione S-transferase class Kappa: characterization by the cloning of rat mitochondrial GST and identification of a human homologue. *Biochem. J.* 319: 749-754.

Piccolomini, R., Di Ilio, C., Aceto, A., Allocati, N., Faraone, A., Cellini, L., Ravagnan, G., and Federici, G. (1989). Glutathione transferase in bacteria: subunit composition and antigenic characterization. *J. Gen. Microbiol.* 135:3119-3125.

Philo, J. S., and Arakawa, T. (2009). Mechanisms of protein aggregation. *Curr. Phar. Biotech.* 10: 348-351.

Raza. H., Robin, M. A., Fang, J. K., and Avadhani, N. G. (2002). Multiple isoforms of mitochondrial glutathione S-transferases and their differential induction under oxidative stress. *Biochem. J.* 366: 45-55.

Reguero, M. T., Medina, O. E., Hernandez, M. A., Florez, D. V., Valenzuela, E. M. and Mantila, J. R. (2012). Antibiotic resistance patterns of *Acinetobacter calcoaceticus– A. baumannii* complex species from Colombian hospitals. *Enferm. Infect. Microbiol. Clin.* S0213-005X (12)00264-9.

Rinaldi, R., Aniya, Y., Svensson, R., Eliasson, Swedmark, S., Shimoji, M., and Morgenstern, R. (2004). NADPH dependent activation of microsomal glutathione transferase 1. *Chem. Biol. Interact.* 147: 163-172.

Robinson, A., Huttley, G. A., Booth, H. S., and Board, P. G. (2004). Modelling and bioinformatics studies of the human Kappa-class glutathione transferase predict a novel third glutathione transferase family with similarity to prokaryotic 2-hydroxychromene-2-carboxylate isomerases. *Biochem. J.* 379: 541–552.

Rossjohn, J., Polekhina, G., Feil, S. C., Allocati, N., Masuli, M., Di Ilio, C., and Parker, M. W. (1998). A mixed disulfide bond in bacterial glutathione transferase: functional and evolutionary implications. *Structure.* 6(6):721-34.

Samuelsson, B., and Funk, C. D. (1989). Enzymes involved in the biosynthesis of leukotriene $B_4$. *J. Biol. Chem.* 264(33): 19469-19472.

Scholtz, R., Wackett, L. P., Cook, A. M., and Leisinger, T. (1988). Dichloromethane dehalogenase with improve catalytic activity isolated from a fast growing dichloromethane-utilizing bacterium. *J. Bacteriol.* 170(12): 5698.

Sheehan, D., Meade, G., Foley, V. M., and Dowd, C. (2001). Structure, function and evolution of glutathione transferases: implications for classification of non-mammalian members of an ancient enzyme superfamily. *Biochem. J.* 360: 1-16.

Sherratt, P. J., Pulford, D. J., Harrison, D. J., Green, T., and Hayes, J. D. (1997) Evidence that human class theta glutathione S-transferase T1-1 can catalyse the activation of dichloromethane, a liver and lung carcinogen in the mouse. *Biochem. J.* 326: 837-846.

Sherratt, P. J., and Hayes J. D. (2001). Glutathione S-transferase. *Enzyme systems that metabolise drugs and other xenobiotics.* UK: Unversity of Dundae.

Skipsey, M., Andrews, C. J., Townson, J. K., Jepson, I., and Edwards, R. (1997). Substrate and thiol specificity of a stress-inducible glutathione transferase from soybean. *FEBS Lett.* 409: 370-374.

Skopelitou, K., Muleta, A., Pavli, O., Skarakis, G. N., and Flemetakis E. (2012). Overlapping protective roles for glutathione transferase gene family members in chemical and oxidative stress response in *Agrobacterium tumefaciens*. *Funct. & Integr. Genom*. 12: 157–172.

Sonoda, S., Ashfaq, M, and Tsumuki, H. (2006). Genomic organization and developmental expression of glutathione S-transferase genes of the diamondback moth, *Plutella xylostella*. *J. Insect Sci.* 6(35): 1-9.

Speicher, K. D., Kolbas, O., Harper, S. and Speicher, D. W. (2000). Systematic analysis of peptide recoveries from in-gel digestions for protein identification in proteomic studies. *J. Biomol. Tech.* 11: 74-86.

Spino, D. F., and Geldreich, E. E. (1981). *Acinetobacter* spp.: distinct morphology on eosin methylene blue agar as an aid to identification in drinking water. *Appl. Environ. Microbiol.* 41(4):1063.

Sun, H. D., Ru, Y. W., Zhang, D. J., Yin, S. Y., Yin, L., Xie, Y. Y., Guan, Y. F., and Liu, S. Q. (2012). Proteomic analysis of glutathione S-transferase isoforms in mouse liver mitochondria. *World J. Gastroenterol*. 18(26): 3435-3442.

Tong, Z., Board, P. G., and Anders, M. W. (1998). Glutathione transferase Zeta catalyses the oxygenation of the carcinogen dichloroacetic acid to glyoxylic acid. *Biochem. J.* 331: 371-374.

Towner, K. J. (1997). Clinical importance and antibiotic resistance of *Acinetobacter* spp. *J. Med. Microbiol.* 46: 721-746.

Townsend, D. M., Manevich, Y., He, L. Hutchens, S., Pazoles, J. C., and Tew, K. D. (2008). Novel role for glutathione S-tranferase π: regulator of protein S-Glutathionylation following oxidative and nitrosative stress. *J. Biol. Chem.* 284: 436-445.

Townsend, D., M., and Tew, K. D. (2003). The role of glutathione-S-transferase in anti-cancer drug resistance. *Oncogene.* 22: 7369-7375.

Udomsinprasert, R., Bogoyevitch, M. A. and Ketterman, A. J. (2004). Reciprocal regulation of glutathione S-transferase spliceform and the *Drosophila* c-Jun N-terminal kinase pathway components. *Biochem. J.*, 383, 483-490.

Venkateswaran, P. S., and Wu, H. C. (1972). Isolation and characterization of a phosphonomycin-resistant mutant of *Escherichia coli* K-12. *J. Bacteriol.* 110(3): 935-944.

Vuilleumier, S. (1997). Bacterial Glutathione S-transferases: what are they good for*? J. Bacteriol.* 179(5): 1431-1441.

Vuilleumier, S., Sorribas, H., and Leisinger. T. (1997a). Identification of novel determinant of glutathione affinity in dichloromethane dehalogenase/glutathione S-transferase. *Biochem. Biophys. Res. Commun.* 238: 452-456.

Vuilleumier, S., and Pagni, M. (2002). The elusive roles of bacterial glutathione S-transferase: new lesson from genomes. *Appl. Microbiol. Biotechnol.* 58: 138-146.

Wang, W., and Ballatori, N. (1998). Endogenous glutathione conjugates: occurrence and biological functions. *J. Pharmacol. Exp. Ther.* 50(3): 335-355.

Welsch, D. J., Creely, D. P., Hauser, S. D., Mathis, K. J., Krivi, G. G., and Isakson, P. C. (1994). Molecular cloning and expression of human leukotriene-$C_4$ synthase. *Proc. Natl. Acad. Sci.* 91: 9745-9749.

Wendel, A. (1981). Glutathione peroxidase. *Methods Enzymol*. 77: 325-333.

Whalen, K. E., Lane, A. L., Kubanek, J., and Hahn M. E.( 2010). Biochemical warfare on the reef: the role of glutathione transferases in consumer tolerance of dietary prostaglandins. *PLOS ONE*. 5(1): 1-11.

Wiktelius, E., and Stenberg, G. (2007). Novel class of glutathione transferases from cyanobacteria exhibit high catalytic activities towards naturally occurring isothiocyanates. *Biochem. J.* 406: 115–123.

Wu, B. J. and Dong, D. (2012). Human cytosolic glutathionetransferases: structure, function, and drug discovery. *Trends Pharmacol. Sci.* 33(12): 656-668.

Zablotowicz, R. M., Hoagland, R. E., Locke, M.m A., and Hickey, W. J. (1995). Glutathione S-transferase activity and metabolism of glutathione conjugates by rhizosphere bacteria. *Appl. Environ. Microbiol.* 61(3):1054.

Zhan, Y. H., Yan, Y. L., Zhang. W., Chen, M., Lu, W., Ping, S. Z., and Lin, M. (2012). Comparative analysis of the complete genome of an *Acinetobacter calcoaceticus* strain adapted to a phenol-polluted environment. *Res. Microbiol.* 163(1): 36-43.

# 9.0 Appendices

Appendix A- Buffer solution preparation

1) Homogenising buffer (0.1 mM PMSF, 1 mM EDTA, 0.1 mM DTT, 0.1 mM PTU in eluting buffer)

To prepare 50 ml of homogenising buffer, 0.5 ml of 10 mM PMSF, 0.02 g of EDTA, 0.2 g of GSH and half a spatula of PTU were added in a beaker and dissolved in 50 ml of eluting buffer. 10 mM of PMSF was prepared by dissolving 0.01 g in acetone.

2) Eluting buffer-25 mM sodium phosphate buffer, pH 7.4

3 g of sodium phosphate was dissolved in approximately 900 ml of distilled water. The pH of the solution was adjusted to 7.4 at 20 ºC and the volume was made up to 1000 ml.

3) Buffer A- 25 mM sodium phosphate buffer, pH 6

3 g of sodium phosphate was dissolved in approximately 900 ml of distilled water. The pH of the solution was adjusted to 6 at 20 ºC and the volume was made up to 1000 ml.

4) Buffer B-0.025 M bis Tris uffer, pH 7.1

5.2 g of bis Tris was dissolved in approximately 900 ml of distilled water. The pH of the solution was adjusted to 7.1 with iminodiacetic acid at 20 ºC and the volume was made up to 1000 ml.

5) Buffer C- polybuffer 74, pH 4

10 ml of polybuffer 74 was mixed with 80 ml of distilled water. The pH of the solution was adjusted to 7.1 with iminodiacetic acid at 20 ºC and the volume was made up to 100 ml.

4) Buffer D-0.1 M sodium phosphate buffer, pH 6.5

12 g of sodium phosphate was dissolved in approximately 900 ml of distilled water. The pH was adjusted to 6.5 at 20 ºC. The volume was then made up to 1000 ml.

5) Buffer E-0.1 M Tris buffer, pH 9

12.1 g Tris base was dissolved in approximately 900 ml of distilled water and the pH was adjusted to 9 at 20 ºC. The volume was then made up to 1000 ml.

6) Buffer F-0.1 M sodium phosphate buffer, pH 7.5

12 g of sodium phosphate was dissolved in approximately 900 ml of distilled water. The pH was adjusted to 7.5 at 20 ºC. The volume was then made up to 1000 ml.

7) Buffer G-0.25 M sodium phosphate buffer, pH 7

30 g of sodium phosphate was dissolved in approximately 900 ml of distilled water. The pH was adjusted to 7 at 20 ºC. The volume was then made up to 1000 ml.

8) Buffer H-0.1 M Tris HCl, pH 8

12.1 g Tris base was dissolved in approximately 900 ml of distilled water and the pH was adjusted to 8 at 20 ºC. The volume was then made up to 1000 ml.

Appendix B- Sodium dodecyl phosphate polyacrylamide gel electrophoresis

1) 10 % (w/v) SDS

10 g of SDS was dissolved in 50 ml distilled water with gentle shaking. Then the volume was made up to 100 ml.

2) SDS sample buffer

The buffer consisted of 62.5 mM Tris-HCl, pH 6.8, 20 % (v/v) glycerol, 2 % (w/v) SDS and 5 % (v/v) β-mercaptoethanol. To prepare a buffer solution of 2 ml, 0.3 ml of 0.5 M Tris-HCl, pH 6.8, 0.4 ml of glycerol, 0.4 ml of 10 % (w/v) SDS, 0.1 ml of β-mercaptoethanol, 0.1 ml of 0.5% (w/v) bromophenol blue and 0.8 ml of distilled water were mixed.

3) Electrophoresis (running) buffer

15.1 g of Tris, 5 g of SDS and 72.1g of glycine were dissolved in 5 L of distilled water.

4) Stacking gel

To prepare 10 ml of 4 % gel: 1.3ml 30 % acrylamide/Bis, 2.5 ml 0.5 M Tris-HCl, pH 6.8, 0.1 ml 10 % (w/v) SDS, 6.1 ml of distilled water, 0.01 ml TEMED and 0.05 ml 10 % (w/v) APS were mixed. All ingredients except TEMED and APS were combined and degassed for 15 minutes. The polymerisation was initiated by addition of TEMED and APS followed by gentle mixing.

5) Separating gel

To prepare 10 ml of 4 % gel: 4 ml 30 % acrylamide/Bis, 2.5 ml 1.5 M Tris-HCl, pH 6.8, 0.1 ml 10 % (w/v) SDS, 3.4ml of distilled water, 0.01ml TEMED and 0.05ml 10 % (w/v) APS were mixed. All ingredients except TEMED and APS were combined and degassed for 15 minutes. The polymerisation was initiated by addition of TEMED and APS followed by gentle mixing.

## Appendix C- Reagents for proteomic analysis

### 1) IPG strip rehydration buffer

The solution consisted of 8 M urea, 2 % (w/v) CHAPS, 15 mM DDT and 2 % (v/v) ampholyte, pH 3-10. To prepare 1 ml of the solution, 0.5 g of urea was dissolved in 0.3 ml of double distilled water completely. Then 0.02 ml of ampholyte, 0.02 g of CHAPS, 0.02 g of DDT and 0.0017 g of thiourea were added and topped up to 1 ml with double distilled water. The rehydration buffer was prepared freshly once needed.

### 2) Equilibration buffer

The buffer solution consisted of 50 mM Tris-HCl, pH 8, 6 M urea, 30 % (v/v) glycerol, 2 % (w/v) SDS and traces of bromophenol blue. To prepare 10 ml of the buffer, 0.3 ml of urea was dissolved in 5 ml of double distilled water. Then 0.3 ml of 1.5 M Tris-HCl, 3.5 ml and 0.2g of SDS were added and topped up to 10 ml.

### 3) Agarose sealing solution

0.5 g agarose and traces of bromphenol blue were added into 100 ml of SDS electrophoresis running buffer. The mixture was heated with microwave until agarose was completely melted.

## Appendix D- Coomasie brillian blue G-250 reagent

100 mg Coomasie Brilliant Blue G-250 was dissolved in 50 ml 95 % (v/v) ethanol. To this solution, 100 ml 85 % (v/v) phosphoric acid was added. The solution was diluted to a final volume of 1 L with distilled water. The solution was filtered with filter paper.

Appendix E- Substrate preparation and enzyme assay conditions

1) 1-Chloro-2,4-dinitrobenzene (CDNB)

2.9 ml of Buffer D, 0.05 ml of purified protein sample, 0.05 ml of 60 mM (0.06 g in 3 ml Buffer D) GSH and 0.05 ml of 60 mM (0.2 g in 30 ml ethanol) CDNB were mixed. Change of absorbance at 340 nm was recorded for 10 minutes. Molar absorption coefficient of CDNB is 9600 $M^{-1}$ $cm^{-1}$.

2) 1,2-Dichloro-4-nitrobenzene (DCNB)

2.8 ml of buffer E, 0.1 ml of purified protein sample, 0.05 ml of 24 mM (0.22 g in 3 ml Buffer D) GSH and 0.05 ml of 24 mM (0.1 g in 20 ml ethanol) DCNB were mixed. Change of absorbance at 344 nm was recorded at 10 minutes. Molar absorption coefficient of DCNB is 8400 $M^{-1}$ $cm^{-1}$.

3) p-Nitrophenyl chloride (NBC)

2.6 ml of Buffer D, 0.1 ml of purified protein sample, 0.3 ml of 60 mM GSH and 0.05 ml of 60 mM (0.2 g in 20 ml ethanol) NBC were mixed. Change of absorbance at 310 nm was recorded for 10 minutes. Molar absorption coefficient of NBC is 1900 $M^{-1}$ $cm^{-1}$.

4) Sulfobromophthalein (BSP)

2.6 ml of Buffer G, 0.1 ml of purified protein sample, 0.3 ml of 60 mM GSH and 0.05 ml of 2 mM (0.03 g in 20 ml ethanol) BSP were mixed. Change of absorbance at 330 nm was recorded for 10 minutes. Molar absorption coefficient of BSP is 4500 $M^{-1}$ $cm^{-1}$.

5) Ethacrynic acid (EA)

2.8 ml of Buffer D, 0.1 ml of purified protein sample, 0.05 ml of 15 mM (0.01 in 3 ml Buffer D) GSH and 0.05 ml of 12 mM (0.07 g in 20 ml ethanol) EA were mixed. Change of absorbance at 270 nm was recorded for 10 minutes. Molar absorption coefficient of BSP is 5000 $M^{-1}$ $cm^{-1}$.

6) Trans-4-phenyl-3-butene-2-one (PBO)

2.8 ml of Buffer D, 0.1 ml of purified protein sample, 0.05 ml of 15 mM GSH and 0.05 ml of 3 mM (0.1 g in 20 ml ethanol) PBO were mixed. Change of absorbance at 290 nm was recorded for 10 minutes. Molar absorption coefficient of BSP is -24800 $M^{-1}$ $cm^{-1}$.

7) Trans-2-octenal

2.8 ml of Buffer D, 0.1 ml of purified protein sample, 0.05 ml of 60 mM GSH and 0.05 ml of 60 mM trans-2-octenal were mixed. Change of absorbance at 225 nm was recorded for 10 minutes. Molar absorption coefficient of trans-2-octenal is -22000 $M^{-1}$ $cm^{-1}$.

8) Hexadienal

2.8 ml of Buffer D, 0.1 ml of purified protein sample, 0.05 ml of 60 mM GSH and 0.05 ml of 3 mM hexadienal were mixed. Change of absorbance at 280 nm was recorded for 10 minutes. Molar absorption coefficient of trans-2-octenal is -34200 $M^{-1}$ $cm^{-1}$.

9) 2,4-Heptadienal

2.8 ml of Buffer D, 0.1 ml of purified protein sample, 0.05 ml of 60 mM GSH and 0.05 ml of 3 mM 2,4-heptadienal were mixed. Change of absorbance at 280 nm was recorded for 10 minutes. Molar absorption coefficient of 2,4-heptadienal is -30300 $M^{-1}$ $cm^{-1}$.

10) Dichloromethane (DCM)

2.8 ml of Buffer H, 0.1 ml of purified protein sample, 0.05 ml of 10 mM (0.01 g in 3 ml of distilled water) GSH and 0.05 ml of 5 mM DCM were mixed. 1.5 ml was removed from these mixtures after 5, 10, 15 and 20 minutes, and the reaction was stopped by adding 0.3 ml of trichloroacetic acid. 1.5 ml was withdrawn and mixed with 1.5 ml of solution containing 2 M ammonium acetate, 0.05 M acetic acid and 0.02 M acetylacetone. The Hantzsh reaction was allowed to go completion at 42 ºC for 30 minutes before measuring the absorbance at 412 nm. Molar absorption coefficient of formaldehyde is 65000 $M^{-1}$ $cm^{-1}$.

11) Glutathione peroxidase assay (Cumene hydroperoxide and hydrogen peroxide)

2.7 ml of Buffer G, 0.05 ml of purified protein sample, 0.05 ml of 10 mM GSH, 0.05 ml of glutathione reductase with activity 6 µmol/min per ml at 25 ºC., 0.05 ml of 25 mM NADPH (0.01 g in 3 ml of 10 % (w/v) sodium bicarbonate) and 0.05 ml of 12 mM hydrogen peroxide or cumene hyroperoxide. Change of absorbance at 366 nm was recorded for 10 minutes. Molar absorption coefficient of NADPH is -6220 $M^{-1}$ $cm^{-1}$.